Author's response:

Section 1 Point-to-point response (*blue*)

1.1 Point-to-point responses to reviewer 1:

general comments

This study by *Lu et al.* provides valuable new insights into the distribution of ammonia-oxidizing archaea (AOA) sublineages and AOA versus ammonia-oxidizing bacteria in the subtropical Pearl River estuary. The study shows a difference in the composition of AOA sublineages at the DNA and RNA level and correlation of nitrification rates with the relative abundance of only one AOA sublineage suggesting a niche partitioning between different AOA sublineages. Furthermore, the authors present data on the contribution of nitrification to oxygen consumption.

Response: *We thank the reviewer for the accurate summary of our study.*

Parts of the data set are only superficially mentioned in the manuscript (e.g. fig 8) although they contain valuable information. Especially the comparison between particle attached vs free-living AOA community composition deserves more attention.

Response: *While comparing the particle-attached and free-living communities, we did not observe significant difference correspondingly (ANOSIM: r=-0.02177, P=0.797, permutation=999). In contrast, we observed large variation of community along the steep environmental gradient in Pearl River estuary at both DNA and RNA levels (ANOSIM: r=0.7142, P=0.001, permutation=999). Here, we provide two heatmap plots for your reference by splitting Figure 6 (new figure 6 & new figure 7 below): New figure 6: Phylogenetic tree and relative abundance (heatmap)of particle-attached AOA. New figure 7: Phylogenetic tree and relative abundance (heatmap)of free-living AOA. Here, the revised figure 6 and new figure 7 show no significant difference. Therefore, we mainly focused on biogeography of different AOA sublineages and the disagreement between DNA and RNA communities.* Page 28-29 Line 629-637

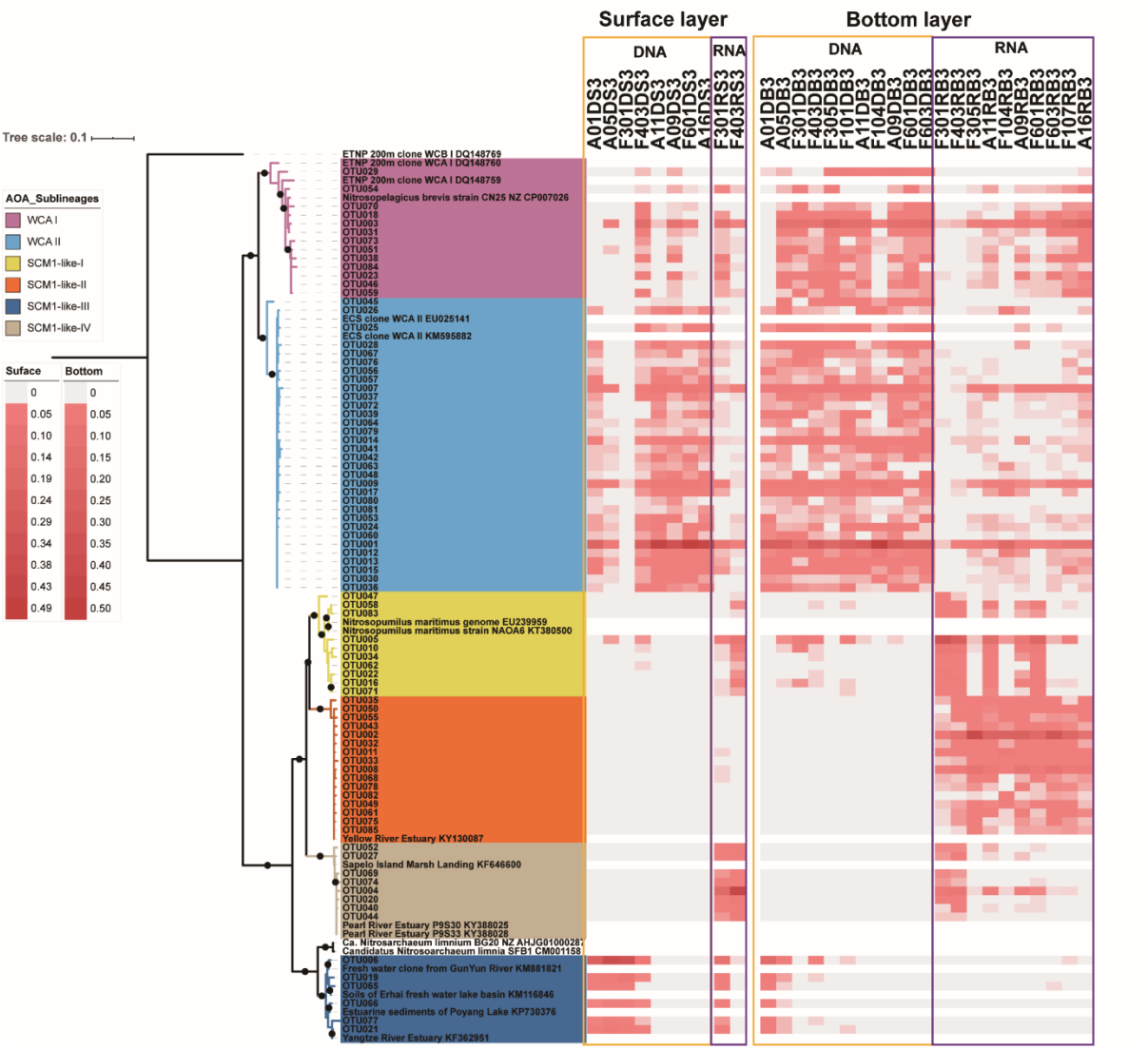

(Revised) Figure 6. Maximum likelihood phylogenetic tree of top 85 OTUs based on amoA gene sequences using T92+G+I model with 1000 bootstrap. The associated heat map is generated based on the relative abundance of top OTUs in the particle-attached samples. Samples are listed from left to right along the ascending salinity gradient.

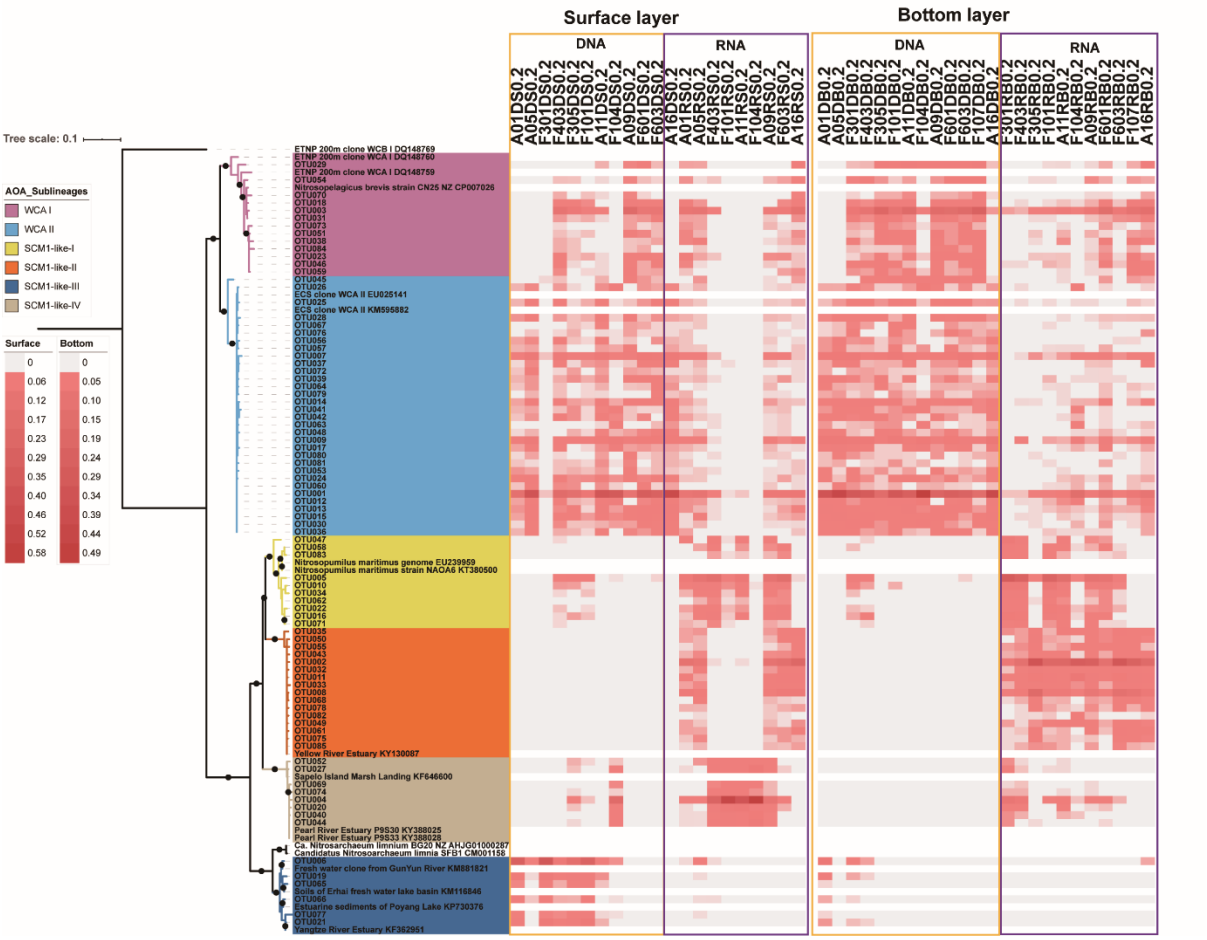

(Newly added) Figure 7. Maximum likelihood phylogenetic tree of top 85 OTUs based on amoA gene sequences using T92+G+I model with 1000 bootstrap. The associated heat map is generated based on the relative abundance of top OTUs in the free-living samples. Samples are listed from left to right along the ascending salinity gradient.

NOD/CRs ratios are a central focus of this manuscript. At the same time the NOD rates are part of different manuscript. In order to see the clear separation of focus and content, the other manuscript should be made accessible to the reviewers. This probably would also help to get important information on the method of NOD determination that are missing from this manuscript (e.g. how many time points were taken per rate measurement?).

Response: *We have elaborated the method of rates measurement (showed below) in the revised manuscript. We did not conduct rates measurement with multiple time points. The estimation of NOD is based on stoichiometric equation (NH_3 +1.5 O_2 →NO_2^- + H_2O + H^+ ”). This study (using qPCR, Ion-torrent sequencing, rates measurement, environmental data) provided a comprehensive view of two group of ammonia oxidizers and more importantly, new insight on distinct distribution patterns of AOA sublineages at DNA and RNA level in the estuarine*

environment in 2017 summer cruise. The other study, using two sets of dark ammonia assimilation rates and nitrification rates from 2015 and 2017 cruises, mainly focus on source and sink of riverine ammonium. We think these two studies contain different and separated contents since they only shared a small part of nitrification rates data in 2017 cruise. Here, we provide the title and abstract of Chen L's work for your reference.

"Title: Title: ***Dark ammonium transformations in the Pearl River Estuary during summer***

Abstract

Growing human activities in recent decades have collectively resulted in large amounts of nutrients export into coastal oceans. As the most reactive nitrogen species, ammonium (NH_4^+) plays the critical role in biogeochemical cycles in estuaries and the coastal ocean. In the highly polluted Pearl River Estuary (PRE), NH_4^+ predominates to be the energy source for nitrification, and to be the material source for bacteria and phytoplankton to grow. Both above processes are affected by light, yet in opposite ways. Nevertheless, rare studies paid attention to dual NH_4^+ transformation processes specifically during dark conditions. By using nitrogen isotope tracer technique, we quantitatively and simultaneously differentiated two distinctive NH_4^+ consumption pathways, i.e., NH_4^+ oxidation (AOD) and assimilation (AAD) rates, specially under dark conditions along the PRE during the 2015 and 2017 summer cruises when biological activities were the highest. We found the NH_4^+ transformations display a bilayer structure with AAD>AOD in almost all the surface waters and vice versa in all bottom waters, suggesting bacteria and phytoplankton (mainly bacteria) control NH_4^+ consumption in surface during the night while nitrifiers are the major NH_4^+ consumer in the bottom waters. Through redundancy analysis, we found that both processes are mainly driven by NH_4^+ in the PRE during summer."

Here is the elaborated method of the rates measurement in the revised manuscript: "Community respiration rates (CR) were measured in triplicate in 60ml BOD bottles without headspace through the dissolved oxygen variance before and after 24 h dark incubation submerged in seawater continuously pumped from sea surface. Nitrification were measured by incubating $^{15}NH_4^+$ amended (less than 10 % of ambient concentration) seawater in duplicated 200 ml HDPE bottles in dark for 6-12 h, with temperature controlled by running seawater. After incubation, filtrate (0.2 μm-syringe-filtered) was collected and stored in -20 ℃ for

downstream $^{15}NO_x^-$ ($^{15}NO_3^-$+ $^{15}NO_2^-$) analysis (Sigman et al. 2001).

The nitrification rates were calculated using the following equation:

$$AO_b = \frac{(R_t NO_x^- \times [NO_x^-]_t) - (R_{t0} NO_x^- \times [NO_x^-]_{t0})}{t\text{-}t0} \times \frac{[^{14}NH_4^+] + [^{15}NH_4^+]}{[^{15}NH_4^+]} \quad (1)$$

In equation 1, AO_b is the bulk nitrification rate. $R_{t0}\,NO_x^-$ and $R_t\,NO_x^-$ are the ratios (%) of ^{15}N in the NO_x^- pool measured at the initial (t_0) and termination (t) of the incubation. $[NO_x^-]_{t0}$ and $[NO_x^-]_t$ are the concentration of NO_x^- at the initial and termination of the incubation, respectively. $[^{14}NH_4^+]$ is the ambient NH_4^+ concentration. $[^{15}NH_4^+]$ is the final ammonium concentration after addition of the stable isotope tracer ($^{15}NH_4^+$). The NO_x^- was completely converted to N_2O by a single strain of denitrifying bacteria (Pseudomonas aureofaciens, ATCC#13985) which lack N_2O-reductase activity (Sigman et al. 2001). The converted N_2O was further analyzed using IRMS (Isotope Ration Mass Spectrometer, Thermo Scientific Delta V Plus) to calculate the isotopic composition of NO_x^- (Sigman et al. 2001; Casciotti et al. 2002; Knapp et al. 2005).We analyzed the correlation between nitrification rates and AOA sublineages. Equation 2 was generally considered as the oxidation of ammonia to nitrite. Inferred from the nitrification rates, we estimated the nitrification oxygen demand (NOD) based on equations 2. Inferred from the nitrification rates, we estimated the nitrification oxygen demand (NOD) based on equation 2. We used NOD/CR ratio (percentage) to evaluate potential the contribution of nitrification to total oxygen consumption in the field.

$$NH_3 + 1.5O_2 \rightarrow NO_2^- + H_2O + H^+ \quad (2)$$" Page 5 Line 92-107

A lot of emphasis is put on the relative importance of NOD in CR. It is stressed various times throughout the manuscript that NOD is high and at times amounts to more than 200%. However, at these stations NOD is not significantly higher compared to other stations, instead CR rates are VERY low. A critical discussion of the CR rates is absent and should be added to the discussion section. How can the observed patchiness of CR rates be explained?

Furthermore, this raises the question of how well constrained the CR data are. Are they based on two data points per rate measurement? How many replicates have been performed? No

standard deviation is reported for NOD or CR. I ask the authors to add this information to the respective tables in the supplementary information and would like them include the number of replicates performed in the material and method section. According to the material and method section, triplicates were performed for the qPCR data. However, standard deviations are also missing in the respective data tables in the supplementary information. I ask the authors to add this.

Response: *We have added the standard deviation information in Table S2, S3, S4. We also added information in the methodology section that we performed triplicate in community respiration rates measurement. Nitrification rates were measured in duplicates. Both rates were measured only at the end of incubation and we did not perform multi-time-point measurements. We have to admit that the high contribution ratios may be introduced by the underestimation of community respiration rates at low oxygen condition (Sampou and Kemp 1994). Nevertheless, the NOD/CR ratio in our study is to show the potential effect of active nitrification on oxygen consumption in the estuarine system. As the community respiration rates were inhibited but the nitrification rates were not limited at the DO concentrations observed in our survey, it is suggested that nitrification could potentially contribute a large proportion of oxygen consumption under low DO concentration. We have added discussion on community respiration rates in Section 4.1.* Page 11 288-309

Please see the attached and revised version of Table S2, S3 and S4 at the bottom of this file.

For the calculation of the inferred nitrification oxygen demand, the authors use improperly balanced equations. This strongly influences the outcome: e.g. for ammonia oxidation, when using

$NH_3 + 1.5\ O_2 \rightarrow NO_2^- + H_2O + H^+$

instead of equation (1), the oxygen demand changes by 33%. During carbon fixation, some electrons are used to reduce CO_2 and not oxygen. However, the assumption that for every NH_3 molecule 1.98 HCO_3 gets fixed is hardly realistic. Furthermore, the authors assume 1:1 coupling between ammonia oxidation and nitrite oxidation. However, no data on the abundance of nitrite oxidizers is provided and the rate measurements provided do not distinguish between nitrite or nitrate production. I suggest that the estimate of oxygen demand should focus on the

first step of nitrification only or at least a paragraph needs to be added to the discussion section. The grammar and language need to be revised. There are too many issues throughout the manuscript to list here, which at times makes it hard to follow the authors line of thought.

Response: *We have removed the equation 2 and 3 in the manuscript and changed our NOD calculation based on equation "NH_3 +1.5 O_2 →NO_2^- + H_2O + H^+" (which is now equation 2 in the revised manuscript). The nitrification rates measurement in this study were performed by adding ^{15}N labeled ammonium before dark incubation, then collected the filtrate containing $^{15}NO_x^-$. The $^{14/15}$Nitrite and $^{14/15}$Nitrate were converted to N_2O by denitrifer method (Sigman et al, 2001). We have elaborated the method of the nitrification rates measurement in the revised manuscript in section 2.2. We now assume each molecule of ammonia consumes 1.5 molecule of oxygen. The NOD and NOD/CR were recalculated based on equation 2 and listed in the revised version of Table S3, description in Section 3.2 and Section 4.1.* Page 2 Line 25; Page 8 Line 203-206; Page 11 Line 288-309 *We have improved the manuscript by reducing the grammar and syntax as well as following the important suggestions from the reviewer. We hope that the current version is much clearer.*

specific comments

l. 63 they would not have overlooked them, but rather underestimated their activity and relative contribution to ammonia oxidation.

Response: *We have changed "overlooked" into "underestimated the importance of some active groups in the natural environment"* Page 4 Line 59

ll. 86-87 microbial instead of bacterial.

Response: *We have changed "bacterial" into "microbial"* Page 4 Line 81

l. 96 clarify "running seawater"

Response: *We have changed it into "Community respiration rates (CR) were measured in triplicate in 60ml BOD bottles without headspace through the dissolved oxygen variance before and after 24 h dark incubation submerged in seawater continuously pumped from sea surface".* Page 4-5 Line 91-92

l. 158 please provide an overview over the 76 samples (which stations and depths are they from) and refer to table S5. The 2523 reads per file does not match the data reported in table S5. The sample categories provided in table S5 need further explanations.

Response: *We subsampled the sequencing reads based on the number of the sample that contains minimum number of reads before OTU clustering. We added abbreviations for sample categories under the Table S5. The sampling depth information have been added to Table S2. Here is revised Table S5:*

(Revised) Table S5. Basic sample information of sequencing samples and corresponding Shannon index, Margalef richness.

Station	Lon (E º)	Lat (W º)	Sample Cat.	Sequence No.	Shannon index	Margalef richness
			A01RS0.2	4469	4.26	42.06
			A01DB0.2	25484	3.70	39.66
A01	113.65	22.74	A01DB3	33527	3.73	37.25
			A01DS0.2	28147	3.64	37.09
			A01DS3	30179	3.68	39.3
			A05RS0.2	10504	4.21	43.33
			A05DB0.2	32747	3.25	33.3
A05	113.77	22.46	A05DB3	28121	4.00	40.49
			A05DS0.2	27297	3.33	35.85
			A05DS3	20389	3.42	33.75
			A09RB0.2	21803	3.78	39.07
			A09RB3	16585	3.87	41.38
			A09RS0.2	12693	4.14	43.61
A09	113.80	22.21	A09DB0.2	21927	4.04	37.99
			A09DB3	21343	3.71	33.55
			A09DS0.2	10794	4.07	29.95
			A09DS3	25603	3.53	37.12
			A11RB0.2	29345	4.12	43.19
			A11RB3	26206	3.78	39.4
			A11RS0.2	4080	3.26	28.6
A11	113.84	22.09	A11DB0.2	24215	3.82	37.84
			A11DB3	22422	3.72	36.47
			A11DS0.2	20568	3.62	38.78
			A11DS3	29216	3.18	34.89
			A16RB0.2	20644	4.12	40.51
			A16RB3	24676	4.01	41.43
A16	114.05	21.66	A16RS0.2	16931	3.88	39.06
			A16DB0.2	30526	3.31	35.74
			A16DS0.2	31112	3.02	31.63

			A16DS3	28739	3.25	35.5
			F101RB0.2	20949	3.67	38.37
			F101RS0.2	2523	2.61	23.22
F101	113.12	21.82	F101DB0.2	20840	3.61	30.87
			F101DB3	15602	3.96	36.95
			F101DS0.2	8348	3.90	35.38
			F104RB0.2	33200	3.60	32.74
			F104RB3	16037	3.69	31.77
F104	113.25	21.56	F104RS0.2	33670	2.22	17.82
			F104DB0.2	30782	2.84	28.32
			F104DB3	30769	2.69	26.59
			F104DS0.2	6990	3.01	30.22
			F107RB0.2	21167	3.89	40.88
F107	113.42	21.27	F107RB3	5633	3.89	38.1
			F107DB0.2	20909	3.90	35.52
			F301RB0.2	17778	3.76	34.19
			F301RB3	16657	3.48	34.53
			F301RS3	5653	4.03	37.6
F301	113.55	21.99	F301DB0.2	22088	3.82	38.42
			F301DB3	3436	4.19	31.49
			F301DS0.2	7823	3.40	27.44
			F301DS3	20310	3.51	26.54
			F305RB0.2	27580	3.35	36.05
			F305RB3	27095	3.20	33.45
F305	113.63	21.83	F305DB0.2	18856	3.96	33.86
			F305DB3	21410	3.78	35.12
			F305DS0.2	7007	4.20	42.21
			F403RB0.2	10000	3.86	37.69
			F403RB3	8858	3.69	38.31
			F403RS0.2	4431	3.57	31.38
F403	113.74	22.08	F403RS3	4166	3.04	28.24
			F403DB0.2	21959	3.91	40.19
			F403DB3	21744	3.85	38.99
			F403DS0.2	19571	4.26	43.7
			F403DS3	20370	3.83	36.83
			F601RB0.2	27041	4.12	43.22
			F601RB3	22320	3.75	38.81
F601	114.03	22.14	F601DB0.2	18421	3.82	34.78
			F601DB3	20092	3.80	33.59
			F601DS0.2	23411	3.70	37.44
			F601DS3	15932	2.94	33.22
			F603RB0.2	30619	3.55	37.54
F603	114.09	22.04	F603RB3	9410	3.55	38.81
			F603RS0.2	5859	3.90	39.93

F603DB0.2	16912	3.96	40.71
F603DB3	19693	3.81	35.48
F603DS0.2	18314	3.78	36.1

* Sample categories: Station ID + D/R (DNA/RNA) + S/B (Surface/Bottom) + 3/0.2 (Particle attached (>3 μm)/Free-living (3-0.2 μm)).

l. 162 Ion torrent is known for introducing homopolymers. Filtering reads with >8 homopolymers is quite a weak setting considering your aim of "performing fine-scale phylogenetic classification". Please comment.

Response: *The quality control standards resulted that the mean length of homopolymers is 3. The length of the maxhomopolymer in the top OTU sequences we used for phylogenetic analysis in our study is 4, so we think the quality control had excluded error from homopolymers introduced by the Ion torrent.*

ll. 170ff. What is the sampling depth of the samples you classified as "bottom".

Response: *The sampling depth information was added to the revised Table S2.*

l. 330 substrate requirement: do the authors mean substrate concentration?

Response: *Yes, we mean substrate concentration. We have added "concentration".* Page12 Line 325

l. 355 "questionable" How so? Such a statement needs to be accompanied with an explanation.

Response: *In line 361 to 363, the low-salinity adapted cluster were proposed by Mosier and Francis in 2008, however, a later study by Molin in 2009 observed these phylotypes in salt marsh with high salinity, which led to the low-salinity adaptation cluster questionable. This was summarized by Bernhard and Bollmann 2010. We think we had the explanation.*

Section 4.1 repeats results in great detail that are already described in the result section. Consider condensing this section.

Response: *We have removed the repeated results.* Page 11 Line 288-289

Fig. 2: figure 2 consists of a selection of graphs to show the most interesting pattern among the environmental parameters measured. This is alright, but the rest of the graphs needs to be provided as well (e.g. supplementary info). For example, surface nitrate concentrations and bottom nitrite concentrations are shown, but bottom nitrate concentrations and bottom salinity are missing.

Response: *We have moved all nutrient plots to the supplementary materials. The current version of figure 2 showed below contains the spatial pattern of salinity, chlorophyll-a and DO concentration at both surface and bottom layer. The nutrient plots of nitrate, nitrite and ammonia were moved to supplementary in Figure S3.* Page 24 Line 612-616; Supplementary Figure S3

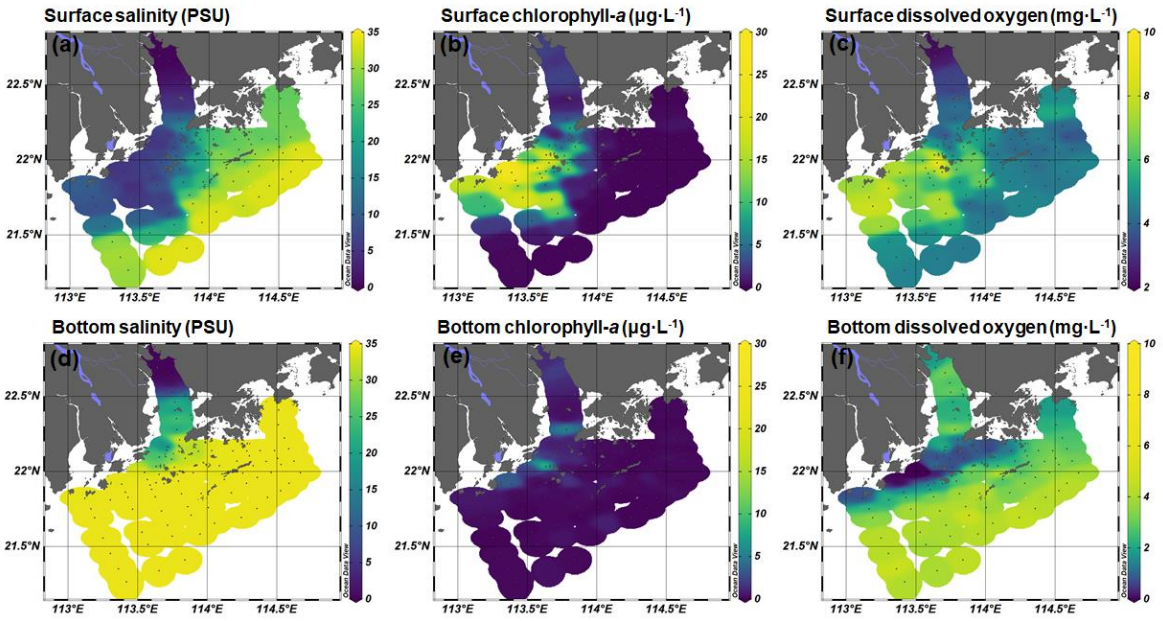

(Revised) Figure 2. Spatial distribution of (a & d) salinity, (b & e) chlorophyll-a, and (c & f) dissolved oxygen concentration at both surface and bottom layer during the 2017 summer cruise in Pearl River estuary. These figures were generated using Ocean Data View v. 5.0.0 (http://odv.awi.de).

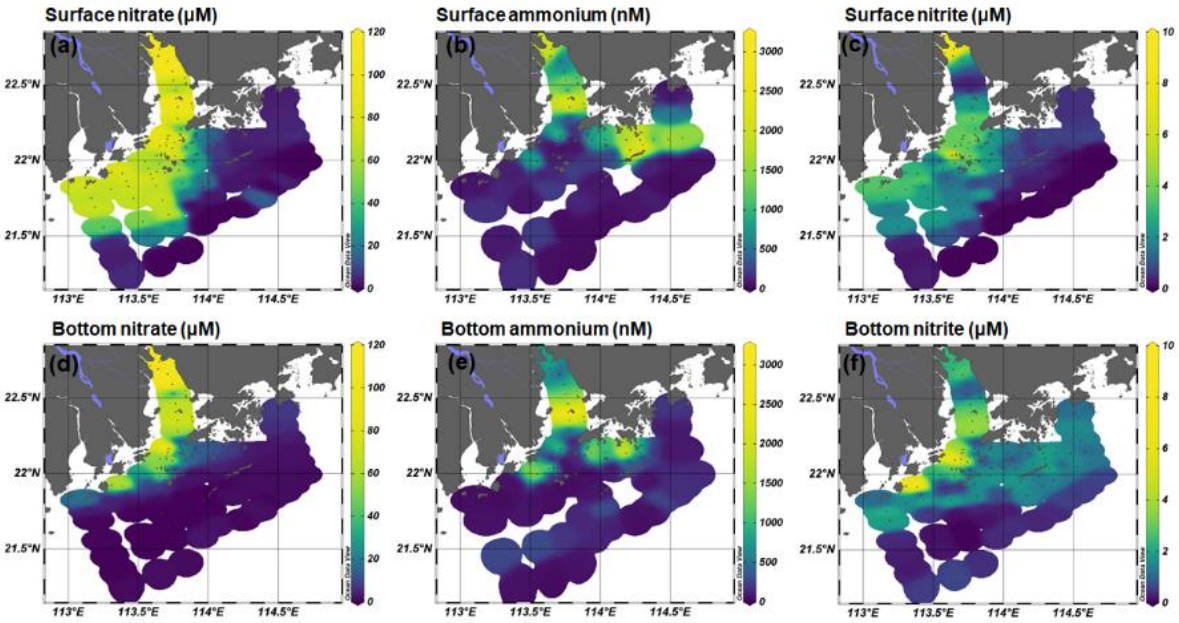

(Newly added) Figure S3. Spatial distribution of (a & d) nitrate, (b & e) ammonium, and (c & f) nitrite concentration at both surface and bottom layer during the 2017 summer cruise in Pearl River estuary. These figures were generated using Ocean Data View v. 5.0.0 (http://odv.awi.de).

Fig. 3c: Data are only plotted for a fraction of the stations compared to 3a and b. Why is a part of the data missing?

Response: *The comparisons were only performed for stations where community respiration rates were measured. We did not conduct the measurements of community respiration rates at many stations as we did for the nitrification rates. The spatial distribution of community respiration rates at the bottom layer was newly added as Figure S4 in supplementary. The citations of these figures were revised accordingly.*

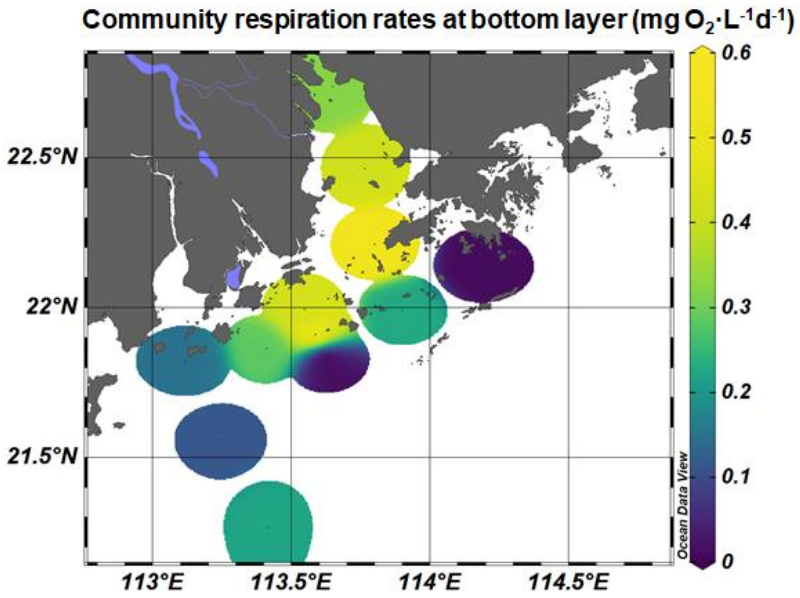

(Newly added) Figure S4. Spatial distribution of community respiration rates at the bottom layer (mg O_2·$L^{-1}d^{-1}$).

Fig. 4: please provide the scale in the same number format for AOA and AOB. In order to compare abundances between surface layer and bottom layer please use the same range for the scale for 4a and c and b and d respectively.

Response: *We have changed the number format and used same scale range for corresponding figures in Figure 4. (new version is attached below and Figure 4 in the main text had been replaced with this new version).* Page 26 Line 621-624

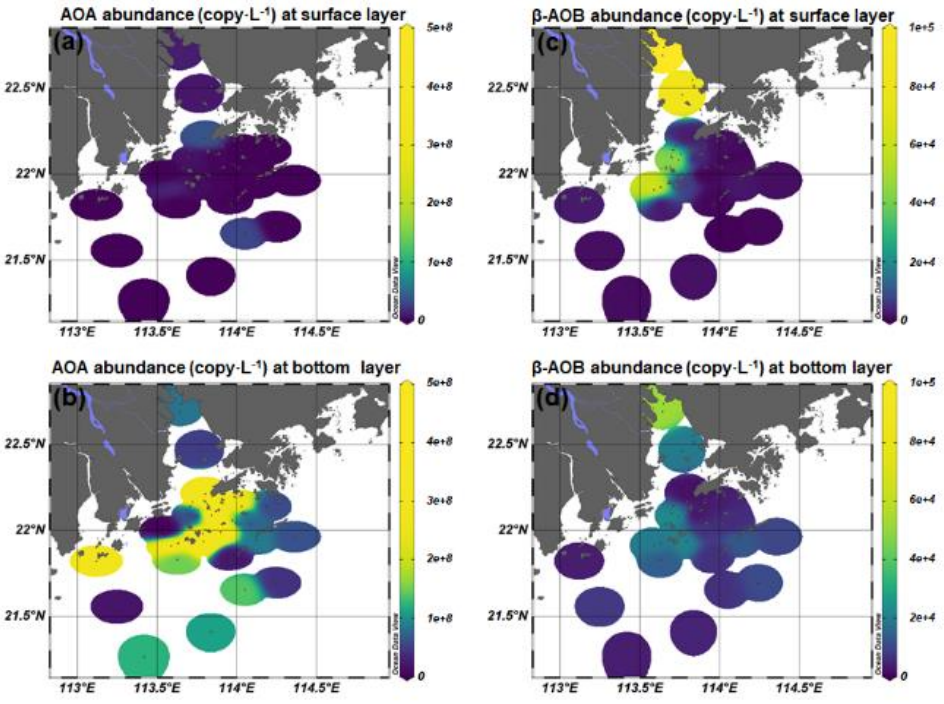

(Revised) Figure 4. Spatial distribution of AOA and β-AOB abundance at the surface and the bottom layer at DNA level.

Fig. 9: you include the temperature in the Spearman correlation in this table. Therefore, you should also provide the temperature data. Maybe add them to table S2.

Response: *We have added "Temperature" in table S2.* Supplementary information Table S2

Fig.9 and l. 391: How did you quantify heterotrophic bacteria? With the cell quantification method, you reported in the material and method section heterotrophic microbes cannot be distinguished from autotrophic non-phototrophic microbial cells (such as the nitrifiers that this study focuses on).

Response: *We admit that flow cytometry method cannot distinguish the autotrophic non-phototrophic microbial cells. We have changed the term in to "non-phototrophic prokaryotic cells" with abbreviation "NPC" in the figure legend in Figure 9.* Page 32 Line654; Page10 Line268; Page 14 Line 388-389

technical corrections

As pointed out above, there are too many issues throughout the manuscript to address here. Some selected comments:

l. 42 "Based on the" instead of "as revealed by"

Response: *We have revised "as revealed by" to "Based on the"* Page 3 Line 41

l. 47 The WCA, WCB, and SCM1-like groups correspond...

Response: *We have revised accordingly.* Page 3 Line 44-45

l. 102 introduce the abbreviation CR in line 93

Response: *We have added abbreviation "CR" in line 93.* Page 5 Line 89

Fig. 9: this is a table not a figure. Typos in the first column: Surface.

Response: *Sorry for the typo. We have corrected it. We considered this heatmap as a figure.*

Page 32 Line 650-654. *It is now figure 10.*

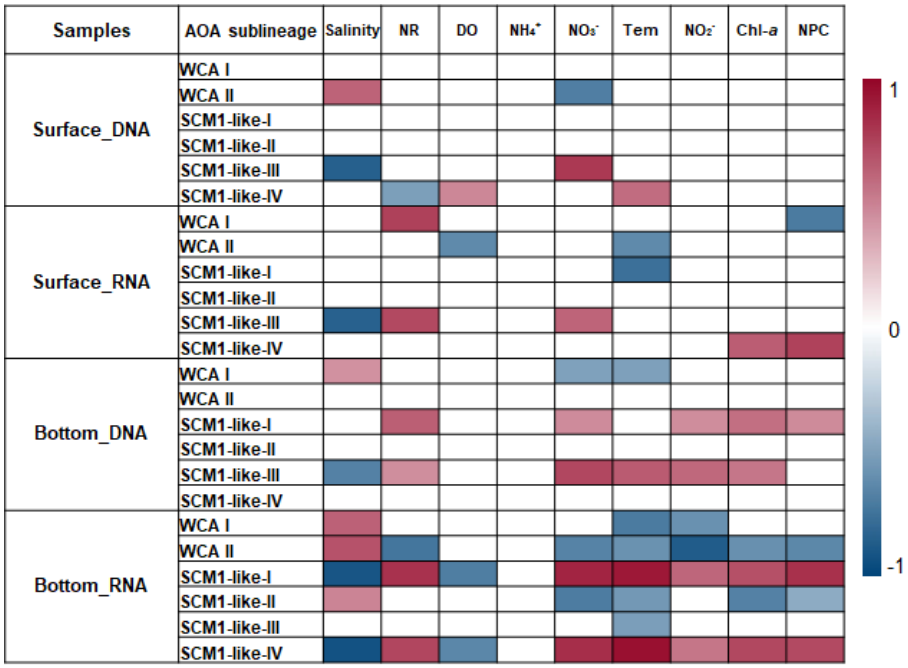

(Revised) Figure 10. Spearman correlation between AOA sublineages (relative abundance at DNA and RNA levels) and environmental factors in the surface and bottom layers of the water column in the Pearl River estuary during summer 2017. Only the significant correlations (P<0.05) are displayed (NR-nitrification rates; DO-dissolved oxygen; Tem-Temperature; NPC-non-phototrophic prokaryotic cells).

Reference

Casciotti, K. L., D. M. Sigman, M. G. Hastings, J. K. Bohlke, and Hilkert, A. : Measurement of the oxygen isotopic composition of nitrate in seawater and freshwater using the denitrifier method., Anal. Chem., 74, 4905–4912, https://doi.org/10.1021/ac020113w, 2002.

Knapp, A. N., D. M. Sigman, and Lipschultz, F. : N isotopic composition of dissolved organic nitrogen and nitrate at the Bermuda Atlantic time-series study site, Global Biogeochem. Cycle, 19, https://doi.org/10.1029/2004gb002320, 2005.

Sigman, D. M., K. L. Casciotti, M. Andreani, C. Barford, M. Galanter, and Bohlke, J. K. : A bacterial method for the nitrogen isotopic analysis of nitrate in seawater and freshwater, Anal. Chem., 73, 4145–4153, https://doi.org/10.1021/ac010088e, 2001.

(Revised) Table S2. Quantitative PCR results at DNA level of both AOA and β-AOB in 23 stations

Station	Lon (E °)	Lat (W °)	Layer	Salinity (PSU)	DO (mg·L^{-1})	Temperature (℃)	Ammonium (nmol·L^{-1})	Nitrification rate (nmol·L^{-1}·h^{-1})	AOA-PA (Copy·L^{-1})	AOA-FL (Copy·L^{-1})	AOB-PA (Copy·L^{-1})	AOB-FL (Copy·L^{-1})
			S-1m	32.30	4.53	29.07	155.70	0.21	1.54E+04 ± 1.35E+03	7.93E+04 ± 4.04E+03	1.81E+02 ±3.02E+01	8.05E+02 ±1.04E+02
F107	113.42	21.27										
			B-41m	34.51	4.09	22.77	48.64	0.96	3.31E+04 ±7.10E+03	1.22E+08 ±3.06E+06	7.77E+02 ±1.57E+02	3.03E+03 ±2.97E+02
			S-1m	16.69	6.80	31.01	ND	0.14	2.92E+04 ±8.54E+02	1.27E+05 ±1.27E+04	4.90E+02 ±1.11E+02	7.56E+02 ±1.60E+02
F104	113.25	21.56										
			B-28m	34.45	4.26	24.06	ND	0.33	1.09E+06 ±6.11E+04	1.76E+07 ±3.61E+05	5.17E+03 ±7.73E+02	2.83E+03 ±6.77E+02
			S-1m	10.20	6.38	29.29	67.03	1.18	4.20E+04 ±5.67E+03	1.19E+06 ±3.79E+04	1.11E+02 ±4.40E+01	2.57E+03 ±1.87E+02
F101	113.12	21.82										
			B-9m	33.73	0.54	24.18	34.78	36.62	2.61E+07 ±2.00E+05	3.95E+08 ±4.51E+06	1.67E+03 ±3.30E+02	2.00E+03 ±3.71E+02
			S-1m	33.91	4.47	29.74	32.41	ND	1.24E+03 ±6.11E+01	2.67E+05 ±1.08E+04	1.31E+02 ±4.05E+01	1.35E+03 ±4.02E+02
F309	113.84	21.41										
			B-43m	34.51	4.21	22.36	56.68	0.40	1.31E+05 ±2.48E+04	1.10E+08 ±4.61E+06	2.57E+03 ±7.72E+02	2.02E+03 ±4.51E+02
			S-1m	9.04	7.08	30.52	233.66	1.84	4.83E+04 ±9.26E+02	3.21E+05 ±2.04E+04	4.77E+02 ±5.88E+01	8.42E+02 ±1.01E+02
F305	113.63	21.83										
			B-26m	34.43	3.47	23.80	44.11	1.28	7.27E+07 ±2.47E+06	7.42E+07 ±4.36E+06	1.08E+04 ±9.10E+02	2.80E+03 ±2.97E+02
			S-1m	7.54	6.82	30.14	104.01	0.48	7.55E+06 ±2.29E+05	6.09E+06 ±1.17E+05	2.89E+04 ±1.95E+03	3.42E+04 ±3.47E+02
F303	113.59	21.91										
			B-18m	34.45	1.44	23.40	42.73	36.37	1.40E+08 ±1.25E+07	1.62E+08 ±3.61E+06	1.65E+04 ±3.31E+03	3.16E+03 ±5.28E+02
			S-1m	6.70	7.67	29.12	865.79	5.20	5.80E+04 ±2.19E+03	3.29E+04 ±3.53E+03	ND	ND
F301	113.55	21.99										
			B-6m	23.17	2.10	27.25	1423.19	41.94	5.04E+03 ±1.72E+03	3.54E+05 ±3.49E+04	ND	ND
			S-1m	12.29	6.53	29.05	250.81	1.48	2.48E+05 ±8.02E+03	2.65E+06 ±3.61E+04	9.73E+02 ±3.05E+02	6.54E+03 ±1.14E+03
F405	113.79	21.94										
			B-22m	34.43	2.61	23.65	34.19	1.04	5.88E+07 ±2.47E+06	4.39E+08 ±1.24E+07	1.10E+04 ±2.10E+03	1.08E+04 ±1.94E+03
			S-1m	7.56	4.11	28.85	24.08	3.07	2.02E+06 ±4.77E+04	3.63E+06 ±1.86E+05	9.57E+03 ±1.94E+03	3.62E+04 ±6.24E+02
F403	113.74	22.08										
			B-8m	22.46	1.31	26.19	24.16	9.91	1.42E+07 ±7.22E+05	3.11E+07 ±1.73E+05	7.75E+03 ±7.65E+02	1.59E+04 ±1.23E+03
			S-1m	33.67	4.73	29.77	35.32	ND	1.70E+07 ±6.61E+04	1.33E+07 ±6.36E+05	ND	ND
A16	114.05	21.66										
			B-45m	34.52	4.21	22.01	111.37	0.65	3.90E+07 ±2.03E+06	9.95E+07 ±1.32E+06	6.91E+03 ±9.79E+02	2.12E+01 ±7.46E+00
A14	113.96	21.85	S-1m	24.15	5.26	29.98	69.85	0.44	1.20E+05	1.16E+06	ND	4.77E+02

Station	Lon (E °)	Lat (W °)	Layer	Salinity (PSU)	DO (mg·L^{-1})	Temperature (℃)	Ammonium (nmol·L^{-1})	Nitrification rate (nmol·L^{-1}·h^{-1})	AOA-PA (Copy·L^{-1})	AOA-FL (Copy·L^{-1})	AOB-PA (Copy·L^{-1})	AOB-FL (Copy·L^{-1})
									±5.63E+03	±4.58E+04		±8.29E+01
			B-25m	34.39	4.00	24.21	355.19	0.06	5.12E+06 ±1.12E+05	1.50E+07 ±1.73E+05	4.68E+03 ±4.56E+02	1.85E+03 ±2.95E+02
			S-1m	19.56	6.68	29.82	278.65	0.80	9.21E+05 ±3.39E+04	2.73E+05 ±2.98E+04	1.80E+02 ±5.64E+01	2.25E+01 ±9.03E+00
A12	113.90	21.99										
			B-22m	34.41	2.62	26.63	56.18	1.13	6.00E+07 ±3.05E+06	2.61E+08 ±6.08E+06	3.69E+03 ±7.40E+02	3.37E+03 ±5.25E+02
			S-1m	13.88	6.37	28.72	47.10	1.13	1.24E+06 ±2.30E+04	6.56E+05 ±4.11E+04	2.69E+01 ±4.30E+00	2.83E+03 ±2.58E+01
A11	113.84	22.09										
			B-13m	32.15	0.97	24.56	120.77	2.64	1.02E+08 ±4.86E+06	2.58E+08 ±1.42E+07	1.49E+03 ±6.58E+01	6.81E+02 ±3.59E+01
			S-1m	17.52	5.39	27.93	161.39	2.58	1.36E+06 ±7.81E+04	3.50E+07 ±8.62E+05	2.56E+02 ±2.95E+01	2.60E+03 ±1.97E+01
A09	113.80	22.21										
			B-21m	33.36	1.15	24.18	91.45	22.43	4.73E+07 ±2.54E+06	3.85E+08 ±9.50E+06	1.10E+03 ±2.55E+02	8.10E+02 ±1.56E+02
			S-1m	2.28	3.27	28.68	865.84	1.90	5.07E+06 ±2.33E+05	3.77E+06 ±5.77E+04	6.03E+04 ±7.06E+03	3.52E+04 ±1.39E+03
A05	113.77	22.46										
			B-10m	14.96	2.45	26.79	1673.87	35.10	2.04E+07 ±1.92E+05	2.93E+07 ±3.61E+05	1.92E+04 ±5.36E+02	8.13E+01 ±5.26E+00
			S-1m	0.11	2.00	28.44	2043.89	94.78	9.76E+06 ±5.80E+05	1.74E+06 ±4.56E+05	8.79E+04 ±2.43E+03	1.92E+04 ±1.42E+03
A01	113.65	22.74										
			B-11m	0.11	1.93	27.46	786.73	17.32	5.08E+07 ±4.06E+06	3.26E+07 ±5.56E+06	4.18E+04 ±3.50E+03	1.04E+04 ±9.35E+02
			S-1m	32.74	4.88	28.74	61.84	ND	2.08E+03 ±3.57E+02	6.07E+04 ±3.75E+03	3.70E+01 ±7.50E+00	5.30E+02 ±1.88E+02
F607	114.24	21.69										
			B-45m	34.49	4.51	22.52	483.80	1.33	3.32E+05 ±9.85E+03	4.07E+07 ±4.93E+05	7.57E+03 ±5.13E+02	2.97E+03 ±4.89E+02
			S-1m	30.11	4.64	28.10	ND	1.91	4.98E+03 ±1.16E+03	1.29E+06 ±6.16E+04	1.11E+02 ±3.14E+01	2.07E+03 ±1.56E+02
F605	114.12	21.95										
			B-35m	34.39	2.75	23.90	ND	7.08	1.53E+07 ±3.31E+06	7.23E+07 ±3.15E+06	8.69E+03 ±2.22E+03	4.27E+03 ±2.48E+02
			S-1m	29.09	4.46	28.30	358.38	1.68	1.78E+03 ±4.75E+02	1.44E+06 ±4.94E+05	5.56E+01 ±1.38E+01	8.82E+02 ±4.80E+01
F603	114.09	22.04										
			B-27m	34.40	2.42	23.74	79.18	2.97	1.13E+07 ±8.58E+05	6.04E+07 ±2.25E+06	2.65E+03 ±9.33E+02	3.12E+03 ±5.23E+02
			S-1m	27.08	4.86	28.96	ND	0.33	6.10E+03 ±2.52E+03	4.69E+05 ±1.54E+05	6.18E+01 ±1.19E+01	2.17E+02 ±8.47E+01
F602	114.06	22.10										
			B-22	34.27	1.56	23.79	ND	4.36	2.68E+06 ±8.65E+05	6.48E+07 ±2.35E+06	4.47E+03 ±1.21E+03	2.32E+03 ±6.52E+02
F601	114.03	22.14	S-1m	25.32	5.09	28.38	983.39	16.09	3.58E+04 ±1.26E+03	7.92E+04 ±1.26E+04	4.85E+01 ±2.16E+01	1.29E+03 ±1.18E+02

Station	Lon (E °)	Lat (W °)	Layer	Salinity (PSU)	DO (mg·L^{-1})	Temperature (℃)	Ammonium (nmol·L^{-1})	Nitrification rate (nmol·L^{-1}·h^{-1})	AOA-PA (Copy·L^{-1})	AOA-FL (Copy·L^{-1})	AOB-PA (Copy·L^{-1})	AOB-FL (Copy·L^{-1})
F701	114.18	22.14	B-19m	32.98	0.53	24.49	372.06	7.22	1.68E+06 ±3.91E+05	3.04E+08 ±4.51E+06	1.03E+03 ±1.03E+02	2.22E+03 ±1.10E+03
			S-1m	26.57	4.63	28.54	1682.83	0.51	1.33E+03 ±5.22E+02	4.86E+05 ±6.24E+04	ND	ND
			B-22m	34.16	1.18	23.88	1993.45	19.13	7.90E+05 ±3.50E+04	5.41E+07 ±9.33E+06	ND	ND
F804	114.36	21.96	S-1m	31.78	4.47	28.70	121.59	0.05	2.43E+03 ±8.98E+02	7.00E+05 ±1.88E+04	1.14E+02 ±9.51E+01	1.14E+03 ±1.81E+02
			B-29m	34.47	3.46	22.91	55.20	2.86	1.47E+07 ±1.69E+06	4.71E+07 ±2.78E+06	6.91E+03 ±3.15E+02	3.16E+03 ±2.24E+03

* S-Surface; B-Bottom; PA-Particle attached (> 3 μm); FL-Free-living (3-0.2 μm); ND-Under detection limit.

(Revised) Table S3. Nitrification, community respiration rates and corresponding oxygen demand.

Station	Layer	Nitrification rate ($nmol \cdot L^{-1} \cdot h^{-1}$)	Nitrification oxygen Demand ($mg\ O_2 \cdot L^{-1} \cdot d^{-1}$)	Community respiration rate ($mg\ O_2 \cdot L^{-1} \cdot d^{-1}$)	NOD/CR%
F101	S	1.1770±0.0447	0.0014	1.4400±0.3024	0.094
F101	B	36.6152±0.1790	0.0422	0.1499±0.0021	28.137
F104	S	0.1443±0.0055	0.0002	1.6813±0.2433	0.010
F104	B	0.3277±0.0433	0.0004	0.1146±0.1568	0.330
F107	S	0.2057±0.0121	0.0002	0.2264±0.0722	0.105
F107	B	0.9596±0.0609	0.0011	0.2191±0.1756	0.505
F301	S	5.1961±0.0285	0.0060	1.1372±0.1240	0.526
F301	B	41.9434±0.4959	0.0483	0.4283±0.1175	11.282
F303	S	0.4847±0.0033	0.0006	1.0797±0.1843	0.052
F303	B	36.3678±1.0384	0.0419	0.5141±0.1635	8.150
F305	S	1.8411±0.2199	0.0021	0.6203±0.1090	0.342
F305	B	1.2795±0.3351	0.0015	0.0023±0.0017	64.894
F701	S	0.5144±0.1081	0.0006	0.9343±0.1157	0.063
F701	B	19.1291±1.0963	0.0220	0.0121±0.1519	181.913
A14	S	0.4443±0.058	0.0005	1.0191±0.1596	0.050
A14	B	0.0609±0.0059	0.0001	0.8222±0.2808	0.009
A12	S	0.8040±0.0692	0.0009	0.9928±0.4831	0.093
A12	B	1.1319±0.0479	0.0013	0.2256±0.0743	0.578
A09	S	2.5768±0.1457	0.0030	1.3144±0.2086	0.251
A09	B	22.4347±0.6230	0.0258	0.6340±0.1077	4.525
A05	S	1.9032±0.186	0.0022	0.2582±0.0848	0.849
A05	B	35.0975±2.5993	0.0404	0.4280±0.0347	9.446
A01	S	94.7793±12.3754	0.1092	0.6128±0.1521	17.819
A01	B	17.3175±0.3106	0.0199	0.3231±0.1861	6.175

* S-Surface; B-Bottom.

(Revised) Table S4. Quantitative PCR results of cDNA (template for RNA level) of AOA and β-AOB in 13 stations

Station	AOA-PA ($copy \cdot L^{-1}$)	AOA-FL ($copy \cdot L^{-1}$)	AOB-PA ($copy \cdot L^{-1}$)	AOB-FL ($copy \cdot L^{-1}$)
A01	3.10E+03 ±1.12E+01	3.08E+03 ±7.11E+02	ND	ND
A01	ND	1.16E+03 ±7.70E+02	ND	ND
A05	8.24E+02 ±4.30E+02	1.02E+04 ±1.84E+03	ND	ND
A05	1.30E+03 ±8.48E+02	6.03E+02 ±3.48E+02	ND	ND
A09	ND	1.18E+05	ND	ND

		±1.06E+04		
A09	1.77E+03 ±1.76E+03	1.47E+06 ±1.07E+05	ND	ND
A11	ND	2.56E+03 ±8.36E+02	ND	ND
A11	3.61E+04 ±3.64E+03	1.14E+05 ±1.30E+04	ND	ND
A16	ND	ND	ND	ND
A16	2.62E+04 ±6.64E+03	ND	ND	ND
F101	ND	1.82E+03 ±5.00E+02	ND	ND
F101	7.43E+03 ±1.46E+03	1.87E+04 ±2.70E+03	ND	ND
F104	ND	1.43E+03 ±4.38E+02	ND	ND
F104	1.21E+03 ±7.13E+01	8.26E+03 ±8.37E+02	ND	ND
F107	ND	ND	ND	ND
F107	ND	1.74E+06 ±5.89E+03	ND	ND
F301	2.99E+03 ±1.07E+03	ND	ND	ND
F301	5.09E+03 ±1.15E+02	1.85E+05 ±1.73E+04	ND	ND
F305	ND	8.07E+02 ±5.65E+02	ND	ND
F305	1.05E+04 ±1.44E+03	9.98E+03 ±1.62E+03	ND	ND
F403	6.46E+03 ±1.26E+03	1.18E+05 ±1.78E+04	ND	ND
F403	3.30E+03 ±1.14E+03	1.17E+05 ±9.54E+03	ND	ND
F601	ND	ND	ND	ND
F601	4.28E+03 ±5.20E+02	3.21E+06 ±1.67E+05	ND	ND
F603	ND	3.72E+03 ±3.08E+02	ND	ND
F603	1.03E+03 ±7.51E+01	2.50E+05 ±3.04E+04	ND	ND

* S-Surface; B-Bottom; PA-Particle attached (>3 μm); FL-Free-living (3-0.2 μm); ND-Under detection limit.

1.2 Point-to-point responses to reviewer 2:

Response to review 2:

I feel that this manuscript contains valuable information regarding ammonia oxidizing archaea in estuarine systems, particularly in that it focuses on processes occurring in the water column rather than the sediment, which, as the authors point out, is understudied. However, there are numerous issues with the manuscript in its current form.

Response: *We thank the reviewer for the comments.*

First and foremost, there are serious issues throughout the manuscript with grammar and syntax. Sometimes these issues are so severe that they obscure the meaning of the text. This made it difficult to grasp the authors' meaning and to review the manuscript effectively.

Response: *We thank the reviewer for the comments. We have improved the manuscript by reducing the grammar and syntax as well as following the important suggestions from the reviewer. We have also added detailed information into the method section. We hope that the current version is much clearer.*

In general, the description of the methods is unclear and lacking in detail.

For example: line 78: "the 10-50m by 10m interval" What does this mean?

Response: *We removed "by 10m interval" for the clarity of the station design. The current version is "In the first leg, 83 stations were designed within the 10-50m isobaths covering areas from the upper estuary to the continental shelf"* Page 4 Line 72-73

lines 87-89: "Sea water was prefiltered... analysis (Liu et al. 2014)." Which analysis was this performed for?

Response: *This sentence described flow cytometry (for microbial cell abundances) sample preparation. For clarity, the current version is "Seawater for microbial abundance quantification was prefiltered by a 20 μm mesh, fixed with final concentration of 0.5 % seawater-buffed paraformaldehyde in cryotubes, and stored in*

liquid nitrogen until flow cytometric analysis (Liu et al. 2014).” Page 4 Line 82-84

line 93: "Community respiration rates were measured" in what? Microcosms? Incubations are mentioned but no volume is given, whether a headspace was left in the bottle...

line 94: "running seawater" Outside the (unmentioned) bottle?

Response: *We have added the corresponding information of community respiration measurement. The running seawater was used to control incubation temperature. The current version is “Community respiration rates (CR) were measured in triplicate in 60ml BOD bottles without headspace through the dissolved oxygen variance before and after 24 h dark incubation submerged in seawater continuously pumped from sea surface”* Page 5 Line 99-102

line 95: "less 10%" Does this mean "less than 10%"?

Response: *Yes. It was revised to “less than 10%”.* Page 4 Line 91

line 96: "The del-15N in NO- x the product of nitrification" I have no idea what this means.

line 97: "denitrifier method" What is that? The authors provide citations but for methods but do not explain what they are or how they are performed. Similarly the measurement of the nitrification rate is not described, only cited in an unpublished manuscript.

Response: *We have added the detailed information of nitrification measurement in the revised manuscript. The current version is “Nitrification were measured by incubating* $^{15}NH_4^+$ *amended (less than 10 % of ambient concentration) seawater in duplicated 200 ml HDPE bottles in dark for 6-12 h, with temperature controlled by running seawater. After incubation, filtrate (0.2 μm-syringe-filtered) was collected and stored in -20 ℃ for downstream* $^{15}NO_x^-$ *(*$^{15}NO_3^- + {}^{15}NO_2^-$*) analysis (Sigman et al. 2001).*

The nitrification rates were calculated using the following equation:

$$AO_b = \frac{(R_t NO_x^- \times [NO_x^-]_t) - (R_{t0} NO_x^- \times [NO_x^-]_{t0})}{T} \times \frac{[^{14}NH_4^+] + [^{15}NH_4^+]}{[^{15}NH_4^+]} \quad (1)$$

In equation 1, AO_b is the bulk nitrification rate. $R_{t0} NO_x^-$ and $R_t NO_x^-$ are the ratios (%) of ^{15}N in the NO_x^- pool measured at the initial (t_0) and termination time (t) of the incubation. $[NO_x^-]_{t0}$ and $[NO_x^-]_t$ are the concentration of NO_x^- at the initial and termination of the incubation, respectively. T is the incubation time. $[^{14}NH_4^+]$ is the ambient NH_4^+ concentration. $[^{15}NH_4^+]$ is the final concentration after addition of the stable isotope tracer ($^{15}NH_4^+$). The NO_x^- was completely converted to N_2O by a single strain of denitrifying bacteria (Pseudomonas aureofaciens, ATCC#13985) which lack N_2O-reductase activity (Sigman et al. 2001). The converted N_2O was further analyzed using IRMS (Isotope Ration Mass Spectrometer, Thermo Scientific Delta V Plus) to calculate the isotopic composition of NO_x^-. (Sigman et al. 2001; Casciotti et al. 2002; Knapp et al. 2005)." Page 5 Line 89-102

lines 110-111: "Fast DNA SPIN Kit for Soil" Why would you use a soil kit for filter samples from seawater?

Response: *Our samples spanned from highly turbid riverine water to oceanic waters. For better purification and consistency of our DNA samples, we used the "Fast DNA SPIN kit for Soil". We have used this kit in previous studies, and it works well with plankton samples, so the name of the kit is a bit misleading.*

line 117: "transpired" I assume you mean "transferred"

Response: *Yes. We have revised it into "transferred".* Page 6 Line 118

line 136: "the DNA mixture" I don't know what is meant by this. DNA and cDNA?

Response: *The DNA mixture consisted of 28 DNA samples from 7 stations along A-transect (A01, A05, A09, A11, A12, A14, A16). The DNA mixture here used as a template for clone construction. We want an amoA clone generated from the local community to reduce the dissimilarity between our standard curve and samples.*

Because the methods were so unclear in general, it is difficult for me to assess whether the claims made in the results and discussion sections are to be believed. For example, AOA and AOB copy numbers are referred frequently as evidence of dominance of one group over the other. Is this a rational claim, particularly without 16S data to support it? How many copy numbers of the amoA gene do AOA have vs AOB? And if archaeal amoA transcripts are more abundant than bacterial amoA transcripts, does that mean the archaea are more abundant or simply more active? Is the difference is gene/transcript number statistically significant?

Response: *The amoA gene copies in AOA is one while it is 2-3 copies in AOB* (Norton, et al. 2002, Hallam et al. 2006). *At DNA level, as the amoA gene abundances of AOA in this study were orders of magnitude higher than AOB, we assumed that AOA should be the dominant ammonia oxidizers (Table S2). On the transcript (RNA use cDNA as template) level, we also performed qPCR. We found that AOA were detectable while AOB were under our detection limit (Table S4). Although we cannot rule out the nitrifying activities of AOB by our method, the current evidences supported that AOA is dominant and active in our study.*

As for the measurement of nitrification rates, so little detail is given regarding how these numbers were reached, as to render the data meaningless. The sections on spatial distribution were in general unclear and difficult to follow.

Response: *We have elaborated the nitrification method.* Page 5 Line 99-102

More specific comments:

line 223: "B-proteobacteria amoA were under detection limit" Not in all your samples though, judging by Figure 5?

Response: *It is not judged by figure 5. The figure 5 only displayed the size fractionated amoA gene abundance along the A-transect on DNA level. The "under detection limit" is specified for cDNA level in the original sentence. We performed qPCR for both AOA and β-proteobacterial amoA gene abundance using cDNA (represent the RNA level) as template. The data were listed in Supplementary Table S4. Using cDNA as template,*

we found β-proteobacterial amoA gene abundance were under the detection limit (Table S4).

line 257: "Besides" Besides what? What is meant by this?

Response: *We have removed "Besides" for clarity.* Page 11 Line 257

line 270: "heterotrophic bacteria abundance" How was this determined? It's not described in the methods.

Response: *We had used the term for all non-phototrophic (no-pigmented) microbial cells in flow cytometric analysis. We admit that flow cytometry method cannot distinguish autotrophic non-phototrophic microbial cells. We have changed "heterotrophic bacteria" into "non-phototrophic prokaryotic cells" with abbreviation "NPC" in the figure legend in Figure 10.* Page 32 Line 650-654; Page10 Line 286; Page 15 Line 388-389

lines 271-272: "Nutrient concentration showed an opposite pattern comparing with salinity" I have no idea what this means.

Response: *We intended to give a general description of the correlation between AOA sublineages and nutrients. Nutrients in PRE were associated with the freshwater discharge. To be clearer, we have revised the sentence as the follow: "In general, WCA sublineages were negatively correlated with nutrient concentration, while SCM1-like sublineages were positively correlated with nutrient concentration."* Page 10 Line 269-271

line 274: "which may be introduced by" Again, no idea.

Response: *We have revised the sentence to "Ammonium showed no significant correlation with AOA sublineages."* Page 10 Line271

lines 295-296: "Intensive nitrification... oxygen consumption (Pakulski et al. 1995)." Was that observed in this study or in the study cited?

Response: *It is observed in the cited study. The current version is "Intensive nitrification was observed at intermediate salinities, and it accounted for 20 to over 50 % of oxygen consumption in the Mississippi River plume (Pakulski et al. 1995)"* Page 11 Line 292

lines 300-301: "It is well known... organic matter degradation (respiration)." Be that as it may, you still have to cite it- and it's hardly proof that ammonia is supplied to nitrification by this process.

Response: *We added the citation of paper "Nitrification and ammonification in aquatic systems" (Ward 1996).* Page 11 Line 396

line 305: 229.21% oxygen consumption? How do you consume more than 100% of something in a closed microcosm?

Response: *This may be caused by the methodological difference in the two measurements. Nitrification oxygen consumption were estimated via equation 2 ($NH_3 + 1.5O_2 \rightarrow NO_2^- + H_2O + H^+$). Nitrification in this study are measured in HDPE bottle while community respiration rates were measure in BOD bottles without headspace. We only have one data point at station F701 that exceeding 100%. Similar situation was also observed in Nueces estuary (Yoon and Benner, 1992) and Chang Jiang estuary (Hsiao et al. 2014). Although the unreasonably high NOD/CR ratio might be caused by the underestimated community respiration rates under low oxygen condition (Sampou and Kemp 1994), it showed the potential effect of active nitrification on oxygen consumption in the estuarine system suffered by hypoxia. We have discussed the issue in section 4.1. The oxygen limitation was rather strong for community respiration than nitrification activities (in Section 4.1). Thus, we considered that oxygen consumption via nitrification may contribute to hypoxia formation in the bottom waters.*

lines 328-329: "Though size-fractionated... were observed." I don't understand what is meant here.

Response: *It was a typo, and we mean "Through". We performed qPCR of the size-*

fractionated (PA-Particle-attached (>3μm) and FL-Free-living (3-0.2μm)) samples. The amoA gene abundances were listed in table S2. Furthermore, figure 5 displayed the amoA gene abundances of the sized-fractionated samples along the A-transect with an increasing salinity gradient. Our result showed differential distribution of the two group of ammonia oxidizers with AOA more abundant in the free-living fraction while AOB more abundant in particle attached fraction and distributed near the upper estuary. We added the citation of figure 5 and Table S2. Page 12 Line 324-325

line 330: "higher substrate requirement" of what substrate?

Response: *The substate here means "ammonia". We have revised it. Current version is "..higher substrate (ammonia) concentration requirement…".* Page 12 Line 325

In multiple locations in the document the authors mention previous DNA-based studies of AOA and how such studies may overlook active AOA populations. To begin with, those populations would not be overlooked, but perhaps underrepresented in the data. Additionally, several culture-independent studies of AOA activity utilizing stable isotope probing (in particular, the use of urea as a substrate, and heterotrophy) have been performed in both salt marsh sediment (Seyler et al., 2014, ISME J) and the open ocean (Seyler et al., 2018, FEMS Microbiol Ecol; Seyler et al., 2019, Frontiers Mar Sci), and none of these studies are cited in the text. AOA activity has also been previously described in an estuarine water column using similar techniques to this manuscript (Horak et al., 2013, ISME J; Happel et al., 2018, Env Microbiol)- these should be cited in the text.

Response: *We thank the reviewer for these suggestions. We have revised the statement of "overlooked" or "neglected" into "underrepresented". We have added the citation of Seyler's and Happel's work in the revised manuscript. We have added the citation of Horak's and Happel's work in the revised Table S1.*

We have cited Seyler's work by adding "Using the stable isotope probing technology, the utilization of organic matter provided evidences of heterotrophy of AOA in the salt marsh sediment and oceanic environment (Seyler, et al. 2014; Seyler et al. 2018; Seyler

et al. 2019).” Page 14 Line 382-384.

We have cited Happel’s work by adding “In Baltic sea, a distinct AOA community were retrieved from RNA level and a few phylotypes related to Nitrosomarinus showed widespread expression in the coastal region (Happel et al. 2018).” Page 12 Line 336-338.

As for the figures:

Figure 6 is impossible to read. Could it be separated into two figures by size fraction? Otherwise there’s just too much going on.

Response: *The figure 6 displayed the phylogenetic relationship of top OTUs together with their distinct distribution among samples in the heatmap at both DNA and RNA level. As for the more specific information about the size-fractionated community, we have also displayed in figure 8 by two separated figures. Here, we make a new version for your reference (Figure 6 & 7 below): New Figure 6: Phylogenetic tree and relative abundance (heatmap) of particle attached AOA. New Figure 7: Phylogenetic tree and relative abundance (heatmap) of free-living AOA. Here, we have split original figure 6 into two figures: new figure 6 and new figure 7. The rest of figure legends in the main-text were revised correspondingly.*

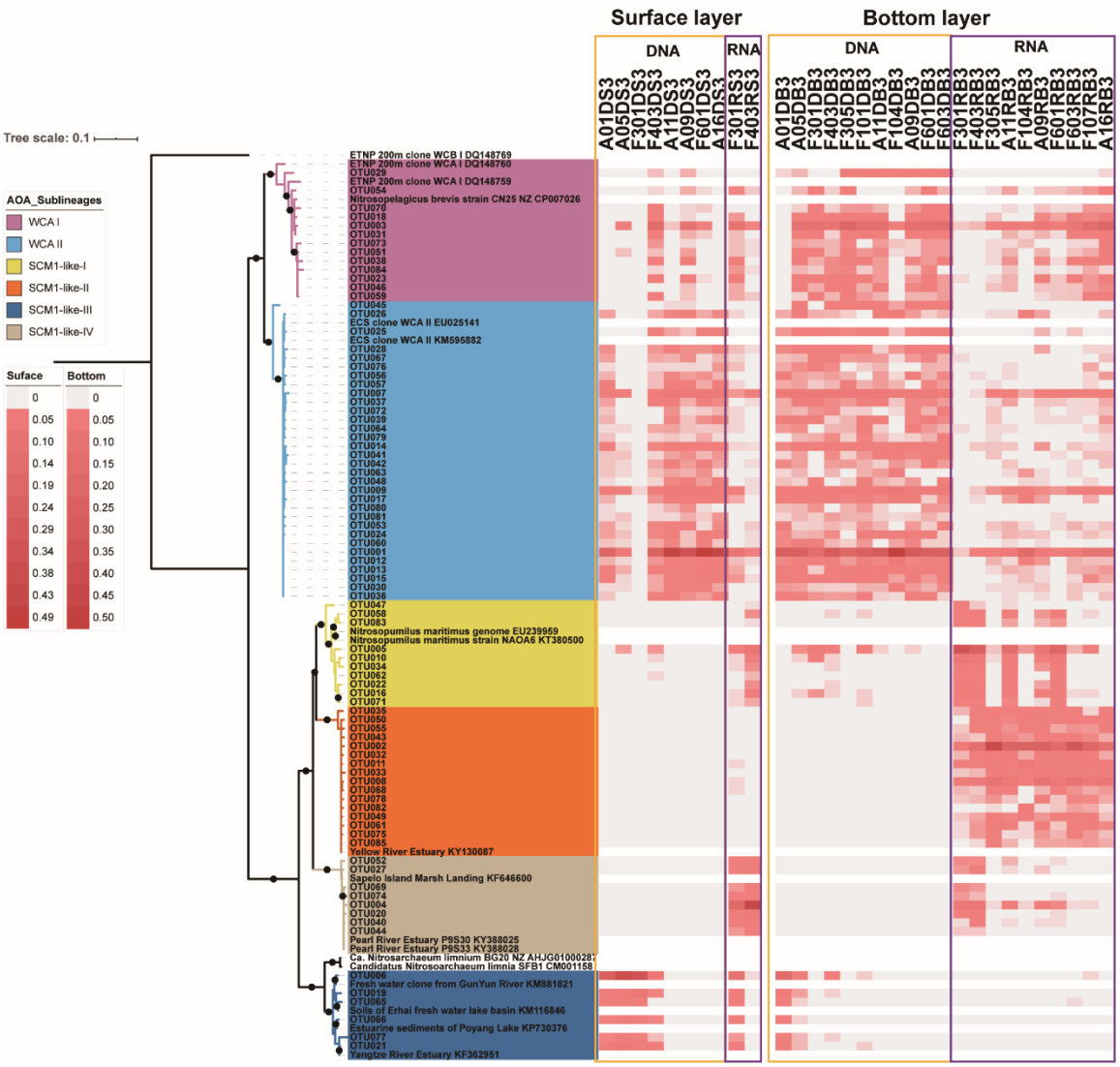

(Revised) Figure 6 Maximum likelihood phylogenetic tree of top 85 OTUs based on amoA gene sequences using T92+G+I model with 1000 bootstrap. The associated heat map is generated based on the relative abundance of top OTUs in the particle-attached samples. Samples are listed from left to right along the ascending salinity gradient.

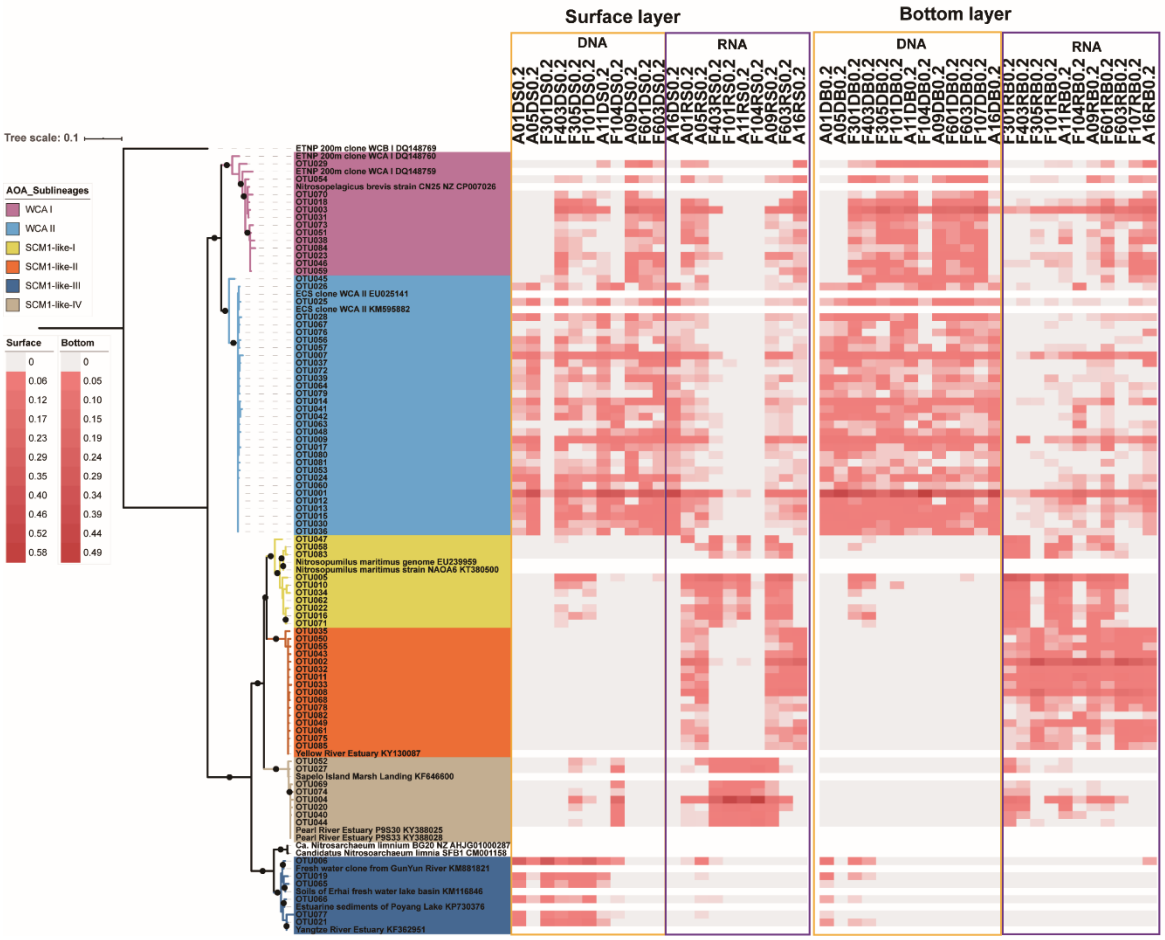

(Newly added) Figure 7. Maximum likelihood phylogenetic tree of top 85 OTUs based on amoA gene sequences using T92+G+I model with 1000 bootstrap. The associated heat map is generated based on the relative abundance of top OTUs in the free-living samples. Samples are listed from left to right along the ascending salinity gradient.

Figure 7 has me completely puzzled. Firstly because the figure has no axes or scale. Secondly because there's no description of how NDMS analysis was performed in the text. But most importantly, how is it possible that there is absolutely no overlap between the DNA and RNA sequences? I find this incredibly difficult to believe. Are the DNA and RNA sequence data even capturing the same community?

Response: *Figure 7 is NMDS plot generate using Primer 5 (Primer-E-Ltd, PML, UK). The input data was the community composition of 76 samples (OTU table, i.e. relative abundance). The community dissimilarities matrix was calculated using "Bray-Curtis dissimilarity". Thus, the dissimilarity between samples were introduced by compositional difference (different relative abundance of each OTU across all samples). As for the sequence data, for example, the heatmap in figures 6 and 7 has showed the*

relative abundance of WCA sublinseages presented in both DNA and RNA samples. So, there are shared OTUs in these samples. The archaeal amoA sequencing samples for DNA and RNA (using cDNA as template) were amplified using same primer pair under same conditions and thermal cycles (Francis et al., 2005). The highly dissimilar community composition retrieved from DNA and RNA as well as the differential distribution AOA sublineages is one of our key findings.

The previous version generated by Primer 5 cannot show axis information. The current version was generated by R via package "vegan" and "ggplot2" (Oksanen, et al. 2019; Wickham, 2016). The method of NMDS plot has been added into Page 7 Line 168-171. *This figure is now figure 8 in the revised main text after splitting figure 6 into new figure 6 and new figure 7 according to your suggestion.*

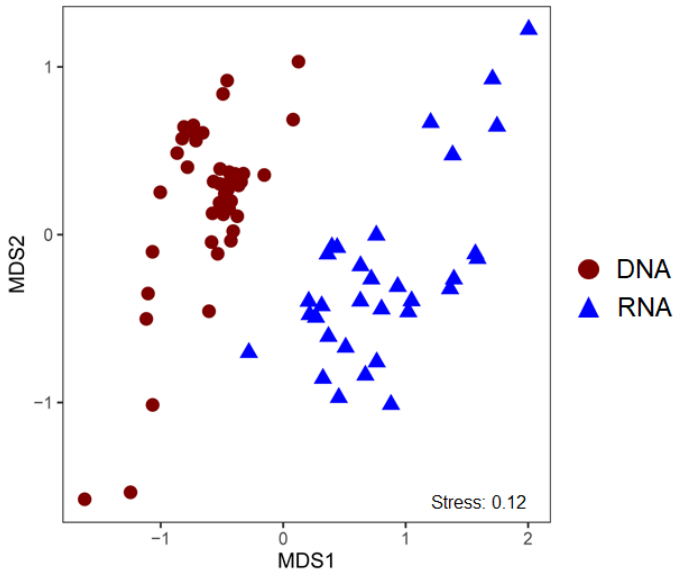

(Revised) Figure 8. Nonmetric multidimensional scaling (NMDS) plot of AOA community similarity at DNA and RNA level.

Figure 8 I think is very interesting, but some of the pie charts are so small as to be illegible.

Response: *The revised version is added into the revised manuscript and showed below. The pie charts are enlarged. This figure is now figure 9 after splitting figure 6.*

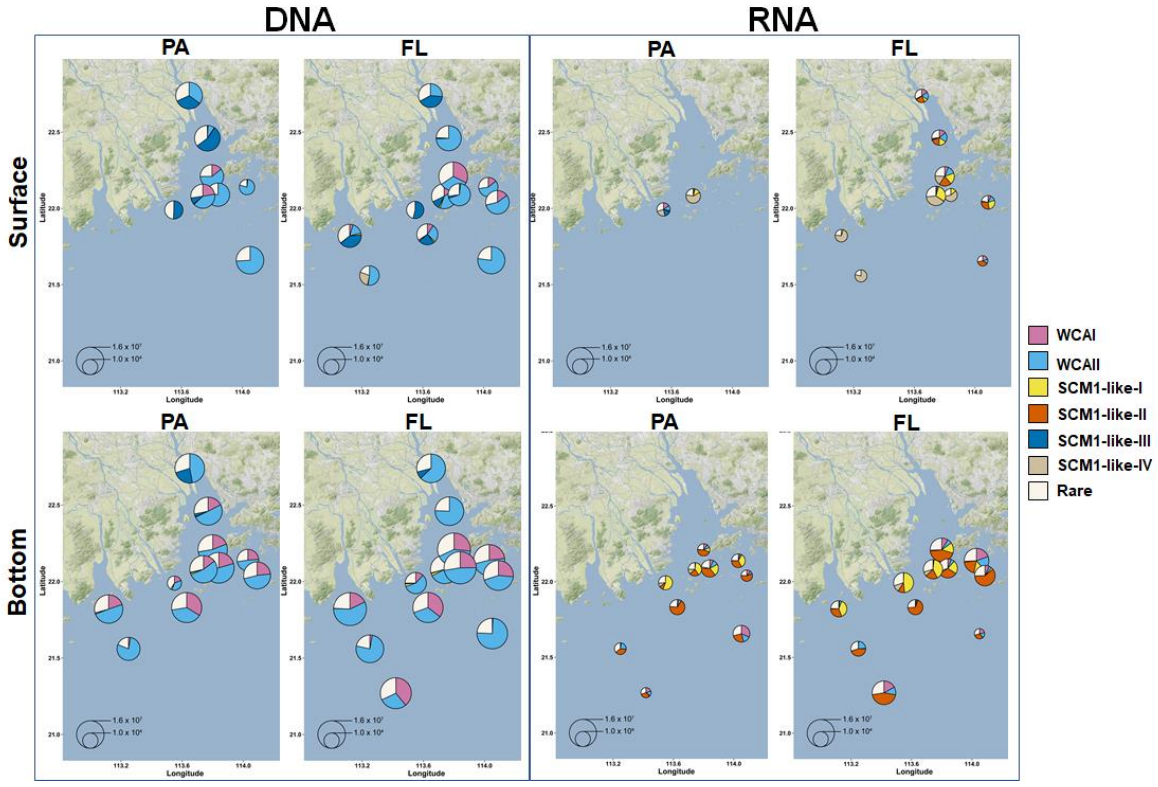

(Revised) Figure 9. Free-living and particle-attached AOA community composition and distribution in the Pearl River estuary. The size of the pie charts represents the archaeal amoA gene abundance quantified by qPCR. For a clear display of the AOA community composition, the minimum size of the pie charts is set as 500 copies·L^{-1}. The charts were overlaid on Google Maps (© Google Maps) images using "ggmap" with "ggplot" in R (D. Kahle and H. Wickham, 2013)

Figure 9 contains some of the most interesting data in the paper, but the figure needs improvement. I think you could combine this heatmap with your phylogenetic tree, and move Figure 6 to supplemental.

Response: *We have followed the suggestions for figure 6 and the figure 9 were replaced with corrected one. Figure 9 is now figure 10 in the revised main text after splitting figure 6.*

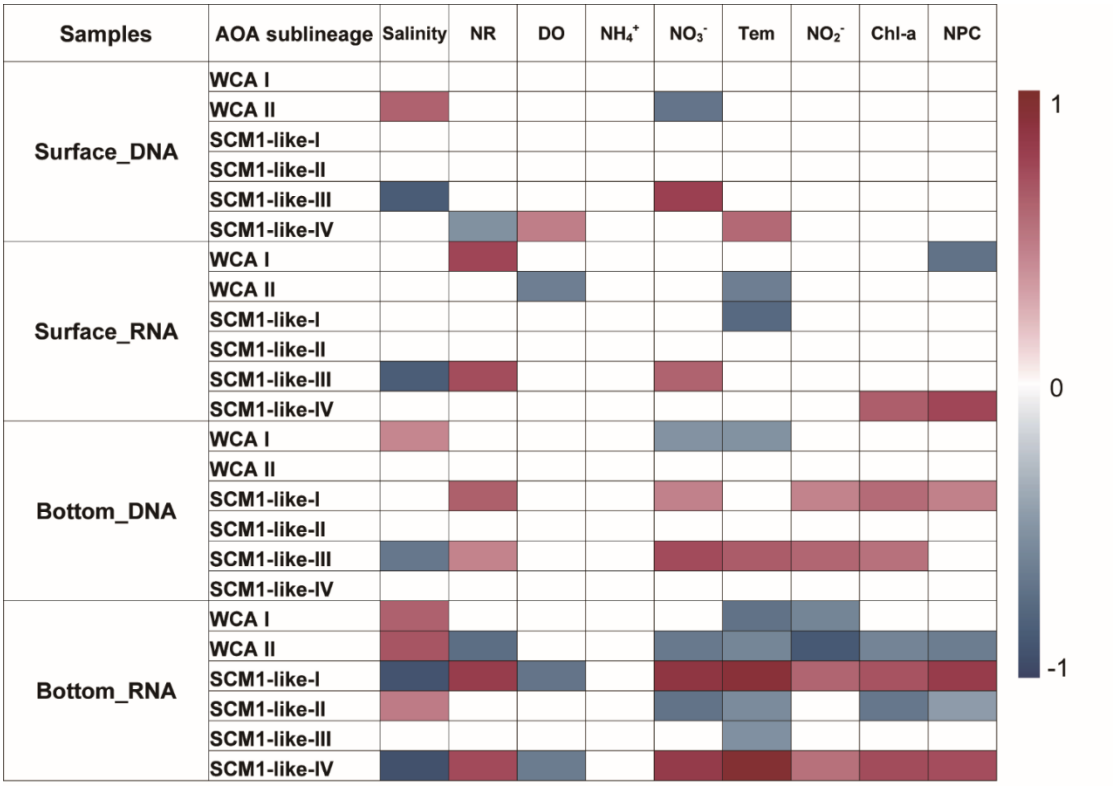

(Revised) Figure 10. Spearman correlation between AOA sublineages (relative abundance at DNA and RNA levels) and environmental factors in the surface and bottom layers of the water column in the Pearl River estuary during summer 2017. Only the significant correlations (P<0.05) are displayed (NR-nitrification rates; DO-dissolved oxygen; Tem-Temperature; NPC-non-phototrophic prokaryotic cells).

Overall I believe the findings presented in this manuscript are likely of interest to the community. The correlations of various AOA lineages to geochemical data and sampling location are very interesting, if difficult to parse in the manuscript's current format. But the issues with the methods in particular and the text in general made it difficult to understand the findings, and some of the claims lack sufficient evidence. I would very much like to see this manuscript again, after significant revisions.

Response: *We thank the reviewer for all insightful and helpful comments. We hope the revised manuscript can meet the standard for publication in Biogeosciences.*

Reference:

Casciotti, K. L., D. M. Sigman, M. G. Hastings, J. K. Bohlke, and Hilkert, A. : Measurement of the oxygen isotopic composition of nitrate in seawater and freshwater using the denitrifier method., Anal. Chem., 74, 4905–4912, https://doi.org/10.1021/ac020113w, 2002.

Hallam, S. J. Konstantinidis, K. T. Putnam, N. Schleper, C. Watanabe, Y. Sugahara, J. Preston, C. de la Torre, J. Richardson, P. M. and DeLong, E. F. : Genomic analysis of the uncultivated marine crenarchaeote Cenarchaeum symbiosum, Proc. Natl. Acad. Sci. USA, 103, 48, 18296–18301, https://doi.org/ 10.1073/pnas.0608549103, 2006.

Knapp, A. N., D. M. Sigman, and Lipschultz, F. : N isotopic composition of dissolved organic nitrogen and nitrate at the Bermuda Atlantic time-series study site, Global Biogeochem. Cycle, 19, https://doi.org/10.1029/2004gb002320, 2005.

Norton, J. M. Alzerreca, J. J. Suwa, Y. and Klotz, M. G. : Diversity of ammonia monooxygenase operon in autotrophic ammonia-oxidizing bacteria, Arch. Microbial., 177:139–149 https://doi.org/10.1007/s00203-001-0369-z, 2002.

Oksanen, J., Blanchet, F. G. Friendly, Kindt, M. R. Legendre, P. McGlinn, D. Minchin, P. R. O'Hara, R. B. Simpson, G. L. Solymos, P. M. Stevens, H. H. Szoecs, E. and Wagner, H.: vegan: Community Ecology Package, R package version 2.5-6. https://CRAN.R-project.org/package=vegan, 2019.

Pakulski, J. D., R. Benner, R. Amon, B. Eadie, and Whitledge, T. : Community metabolism and nutrient cycling in the Mississippi River Plume - Evidence for intense nitrification at intermediate salinities, Mar. Ecol. Prog. Ser., 117, 207–218, https://doi.org/10.3354/meps117207, 1995.

Sampou, P. and Kemp, W. N. :Factors regulating phytoplankton community respiration in Chesapeake Bay, Mar. Ecol. Prog. Ser., 110, 249–258, http://doi.org/10.3354/meps110249, 1994.

Sigman, D. M., K. L. Casciotti, M. Andreani, C. Barford, M. Galanter, and Bohlke, J. K. : A bacterial method for the nitrogen isotopic analysis of nitrate in seawater and freshwater, Anal. Chem., 73, 4145–4153, https://doi.org/10.1021/ac010088e, 2001.

Ward, B. B. : Nitrification and ammonification in aquatic systems, Life Support Biosph. Sci., 3, 25–29, 1996.

Wickham, H. : ggplot2: Elegant Graphics for Data Analysis. Springer-Verlag New York, 2016.

Section 2 List of relevant changes in the revised manuscript

2.1 List of relevant changes in the revised manuscript

List of relevant changes in manuscript

Line 23: "rate" is changed into "rate, which…"

Line 25: "15.30%" is changed into "12.18%"

Line 25: "unravel" is changed into "revealed"

Line 41: "as revealed by" is changed into "Based on the"

Line 41-45: The sentence is rephrased into "Based on the *amoA* gene (ammonia monooxygenase subunit A), the marine AOA was recognized to three major groups: water column A (WCA; shallow water ecotype dominating in epipelagic and upper mesopelagic water), water column B (WCB; deep water ecotype dominating in mesopelagic and bathypelagic water) and SCM1-like (affiliated to the first isolated AOA–*Nitrosopumilus maritimus* SCM1), corresponding to the group NP-Epsilon, NP-Alpha and NP-Gamma, respectively, in the global synthesis of Alves et al. 2018 (Alves 2018; Cheung et al. 2019)."

Line 59: We have changed "overlooked" into "underestimated the importance of some active groups in the natural environment"

Line 63: We added citation of Zhao et al. 2020

Line 72-73: The description of cruise design is rephrased into "In the first leg, 83 stations were designed within the 10-50m isobaths covering areas from the upper estuary to the continental shelf (Fig. S1)"

Line 79: We added citation of Zhao et al. 2020

Line 81: We have changed "bacterial" into "microbial".

Line 82-84: The description of flow cytometry(for microbial cell abundance) is rephrased into "Seawater for microbial abundance quantification was prefiltered through a 20 μm mesh, fixed with final concentration of 0.5 % seawater-buffed paraformaldehyde in cryotubes, and stored in liquid nitrogen until flow cytometric analysis (Liu et al. 2014).

Line 91: “less 10%” is changed into “less than 10%”

Line 89-102: We have elaborated the methodological detail of the rates measurement following the suggestions from reviewers. The current version is “Community respiration rates (CR) were estimated by measuring the oxygen consumption in triplicate 60ml BOD bottles without headspace after 24 h dark incubation submerged in seawater continuously pumped from sea surface. Nitrification were measured by incubating $^{15}NH_4^+$ amended (less than 10 % of ambient concentration) seawater in duplicate 200 ml HDPE bottles in dark for 6-12 h, with temperature controlled by running seawater. After incubation, filtrate (0.2 μm-syringe-filtered) was collected and stored in -20 ℃ for downstream $^{15}NO_x^-$ ($^{15}NO_3^-$+ $^{15}NO_2^-$) analysis (Sigman et al. 2001).

The nitrification rates were calculated using the following equation:

$$AO_b = \frac{(R_t NO_x^- \times [NO_x^-]_t) - (R_{t0} NO_x^- \times [NO_x^-]_{t0})}{t\text{-}t0} \times \frac{\left[{}^{14}_{NH_4^+}\right] + \left[{}^{15}_{NH_4^+}\right]}{\left[{}^{15}_{NH_4^+}\right]} \quad (1)$$

In equation 1, AO_b is the bulk nitrification rate. $R_{t0}\ NO_x^-$ and $R_t\ NO_x^-$ are the ratios (%) of ^{15}N in the NO_x^- pool measured at the initial (t_0) and termination (t) of the incubation. $[NO_x^-]_{t0}$ and $[NO_x^-]_t$ are the concentration of NO_x^- at the initial and termination of the incubation, respectively. $[^{14}NH_4^+]$ is the ambient NH_4^+ concentration. $[^{15}NH_4^+]$ is the final ammonium concentration after addition of the stable isotope tracer ($^{15}NH_4^+$). The NO_x^- was completely converted to N_2O by a single strain of denitrifying bacteria (*Pseudomonas aureofaciens,* ATCC#13985) which lack N_2O-reductase activity (Sigman et al. 2001). The converted N_2O was further analyzed using IRMS (Isotope Ration Mass Spectrometer, Thermo Scientific Delta V Plus) to calculate the isotopic composition of NO_x^- (Sigman et al. 2001; Casciotti et al. 2002; Knapp et al. 2005).”

Line 107: The equations are changed into “$NH_3 + 1.5O_2 \rightarrow NO_2^- + H_2O + H^+$ (2)”

Line 118: “transpired” is changed into “transferred”

Line 168-171: We added the method of new figure 8 (NMDS).

Line 250-255: We restructure the description of the spatial distribution of SCM1-like sublineages for clarity.

Line 268: “heterotrophic bacteria” is changed into “non-phototrophic prokaryotic cells”

Line 269-271: “Nutrient concentration showed an opposite pattern comparing with salinity…ammonia…” is changed into “In general, WCA sublineages were negatively correlated with nutrient concentration, while SCM1-like sublineages were positively correlated with nutrient concentration. Ammonium showed no significant correlation

with AOA sublineages”

Line 289: We deleted the repeated CR results.

Line 292: “in the Mississippi River plume” is added.

Line 302-305: We added the citation of Sampou and Kemp 1994.

Line 325: “substrate…” is changed into “substrate (ammonia) concentration requirement”

Line 323-325: "Though size-fractionated... were observed.” Is changed into “Moreover, size-fractionated study revealed that AOA were mainly distributed in the free-living fraction, while AOB were associated with the particles near upper estuary (Fig. 5 and Table S2), which may be explained by higher substrate (ammonia) concentration requirement of AOB than AOA (Martens-Habbena et al. 2009).”

Line 337-338: We added the citation of Happel et al 2018.

Line 382-384: We added the citation of Seyler 2014, 2018, 2019.

Line 388-389: “heterotrophic bacteria” is changed into “non-phototrophic prokaryotic cells”

Line 407-408: Small modification in Author contribution.

Line 417: We added accession number of the “Hong Kong Branch of Southern Marine Science & Engineering Guangdong Laboratory”

Line 482-483: We added the reference of Happel et al. 2018.

Line 529-531: We added the reference of Oksanen et al. for “vegan” package.

Line 560-561: We added the reference of Sampou and Kemp 1994.

Line 575-581: We added the reference of Seyler et al. 2014, 2018, 2019

Line 595: We added the reference of Wichham et al for “ggplot2”

Line 604-606: We added the reference of Zhao et al 2020.

Line 612-616: Figure 2 is changed. The current figure 2 displayed salinity, chl-a and DO at both surface and bottom layer. And a new figure (Figure S3) displayed nitrate,

nitrite and ammonia at both surface and bottom layer. These new figures is added according suggestions from reviewer 1.

Line 617-620: We updated the figure 3 according to Table S3. The NOD numbers in Table S3 are updated according to equation 2.

Line 621-624: We changed the scale of these figures according to suggestion from reviewer 1.

Line 629-637: We split the previous figure 6 based on sized-fraction community according to suggestion from reviewer 2. The new figure 6 displayed the particle-attached AOA communities and the new figure 7 displayed the free-living AOA communities.

Line 640-642: The previous figure 7 (NMDS) is replaced with figure 8(new) following the suggestion from reviewer 2.

Line 643-649: We modified Figure 9 (previous figure 8) following the suggestion from reviewer 2.

Line 650: The typo in figure 10 is corrected.

Line 654: "HB-heterotrophic bacteria" is changed into "NPC- non-phototrophic prokaryotic cells"

2.2 List of relevant changes in Supplementary information

Line 9-12: We added Figure S3. Figure S3 displayed the spatial distribution of nitrate, nitrite and ammonium.

Line 13-14: We added Figure S4. Figure S4 displayed the pattern of community respiration at the bottom layer.

Table S1: We added the citation of Horak et al. 2013 and Happel et al 2018.

Table S2: We added the sampling depth, temperature and standard deviation of qPCR results.

Table S3: We added the standard deviation of the rates measurement following the suggestion from reviewer 1. The NOD and NOD/CR% were recalculated according to equation 2.

Table S4: We added the standard deviation of qPCR results.

Table S5: We added the information of sample category at the bottom of the table.

Line 47-52: We added the reference of Happel et al. 2018 and Horak et al. 2013.

Section 3 Mark-up changes version of the revised manuscript

New Insight to Niche Partitioning and Ecological Function of Ammonia Oxidizing Archaea in Subtropical Estuarine Ecosystem

Yanhong Lu[1,2,†], Shunyan Cheung[2,†], Ling Chen[3], Shuh-Ji Kao[3], Xiaomin Xia[4], Jianping Gan[1], Minhan Dai[3], Hongbin Liu[2,5]

[1]SZU-HKUST Joint PhD Program in Marine Environmental Science, Shenzhen University, Shenzhen, China
[2]Department of Ocean Science, The Hong Kong University of Science and Technology, Hong Kong, China
[3]State Key Laboratory of Marine Environmental Science, Xiamen University, China
[4]Key Laboratory of Tropical Marine Bio-resources and Ecology, South China Sea Institute of Oceanology, Chinese Academy of Sciences, Guangzhou, China
[5]Hong Kong Branch of Southern Marine Science & Engineering Guangdong Laboratory, The Hong Kong University of Science and Technology, Hong Kong, China
†These authors shared equal contributions
Correspondence to: Hongbin Liu (liuhb@ust.hk)

Abstract. Nitrification plays a central role in estuarine nitrogen cycle. Previous studies in estuary mainly focused on the niche-partition between ammonia-oxidizing archaea (AOA) and bacteria (AOB), while the diversity, activity, biogeography and ecophysiology of different AOA groups remained unclear. Here, we first time reported niche partitioning as well as differentially distributed active populations among diverse AOA (inferred from *amoA* gene) in a typical subtropical estuary–Pearl River estuary (PRE). In the water column of PRE, the AOA communities mainly consisted of WCA and SCM1-like sublineages. Surprisingly, we observed a strong disagreement of AOA communities at DNA and RNA levels. In DNA samples, WCA generally dominated the AOA community, and the distributional pattern indicated that WCA I and WCA II sublineages preferred oceanic and coastal conditions, respectively. In contrast, diverse SCM1-like sublineages were identified and outnumbering WCA at RNA level, in which SCM1-like-III was limited to freshwater while the rest sublineages were widely distributed in the estuary. The SCM1-like sublineages strongly correlated with nitrification rate, which indicated their important contribution to ammonia oxidation. Furthermore, intense nitrification contributed significantly to hypoxia conditions (nitrification contributed averaged ~~15.30~~12.18 % of oxygen consumption) in the estuary. These results ~~unraveled~~ revealed different ammonia-oxidizing activities and niche partitioning among different AOA sublineages in estuarine water, which was unexplored in previous DNA and clone library-based studies. The ecological significance and functioning of the diverse AOA should be further explored in the marine ecosystem.

1 Introduction

Nitrification~~,~~ is a microbial mediated oxidation process of ammonia to nitrate, interconnects the source (N-fixation), and sink (N-loss) and plays a central role in the marine nitrogen cycling (Ward 1996). Particularly in the estuarine ecosystem, nitrification significantly impacts the N source for primary production and oxygen level in the water column (Yool et al. 2007; Erguder et al. 2009; Campbell et al. 2019). Regarding to the biogeochemical significance of ammonia oxidation (i.e. the first and rate-determining step of nitrification) in the estuarine ecosystem, the physiology and ecological function of ammonia oxidizers (i.e. ammonia-oxidizing archaea (AOA) and bacteria (AOB)) have been the major interest to understand the estuarine N transformation (Bernhard and Bollmann 2010). ~~The p~~Previous studies were mostly conducted in the sediment ~~compared to water columns in~~of estuarine ecosystems (summarized in Table S1) (Damashek et al. 2016). ~~Besides, those~~These studies ~~were~~ mainly ~~focusing~~ focused on the niche partition between AOA and AOB inferred from *amoA* genes abundance and collectively showed the AOA outnumbered AOB in the estuarine ecosystem (Caffrey et al. 2007; Abell et al. 2010; Bernhard et al. 2010). However, the biogeography, niche partition, and ecological function of different AOA groups were little analyzed (Table S1).

~~As revealed by~~Based on the *amoA* gene (ammonia monooxygenase subunit A), the marine AOA was ~~early~~ recognized ~~as~~ to three major groups~~,~~: ~~including~~ water column A (WCA; shallow water ecotype ~~dominant~~dominating in epipelagic and upper mesopelagic water)~~,~~ ~~and~~ water column B (WCB; deep water ecotype domina~~t~~ing~~nt~~ in ~~the~~ mesopelagic and bathypelagic water) and SCM1-like (affiliated to the first isolated AOA–*Nitrosopumilus maritimus* SCM1), corresponding to the group NP-Epsilon, NP-Alpha and NP-Gamma, respectively, in the global synthesis of Alves et al. 2018 (Alves 2018; Cheung et al. 2019). ~~in which t~~The distribution and abundance of WCA and WCB were much more studied than SCM1-like ecotype in the field observations (Francis et al. 2005; Hallam et al. 2006; Beman et al. 2008; Beman et al. 2012). ~~The WCA, WCB, and SCM1-like were corresponding to the group NP-Epsilon, NP-Alpha, and NP-Gamma respectively, in the global synthesis of Alves et al. 2018 (Alves 2018; Cheung et al. 2019). More r~~Recently, highly diverse sublineages of WCA and WCB were revealed in the global ocean, in which ~~the~~ sublineage within ~~the same~~each ecotype displayed varied distributional patterns and environmental determinants (Cheung et al. 2019). ~~On the other hand,~~Since most of ~~the~~ marine AOA remained uncultivated~~,~~ ~~which hinder~~ our understanding of the ecophysiology of most of AOA (especially WCA and WCB) in marine ecosystems relied heavily on field observations (Alves et al. 2018). ~~Therefore, the physiological understanding of marine AOA (especially WCA and WCB) heavily relied on field observations. Given that highly diverse uncultivated AOA sublineages have been recently defined, their ecophysiology and environmental determinants requir~~eed ~~further exploration in the environment.~~ For example, niche partitioning between WCB sublineages has been recently observed in the oxygen minimum zone off the Costa Rica Dome and potential anoxic adapted phylotypes were widely detected between the geographically distant OMZs (Lu et al. 2019).

As mentioned, population dynamics and ecological function of different AOA were rarely studied in the estuarine water comparing to the relatively well-characterized AOA populations in ~~the~~ oceanic waters, as well as sediment~~,~~ and soil

environments (Bernhard and Bollmann 2010; Damashek et al. 2016). ~~Besides, the p~~Previous studies of marine AOA ~~mostly~~ relied mainly on clone library analysis (summarized in Table S1), which were insufficient to recover the diversity and biogeography of AOA. Moreover, ~~previous~~ studies ~~largely~~ relied on DNA surveys do not provide information of ~~leaving the relatively~~ active AOA communities ~~at~~in the RNA level ~~unexplored~~. Recently, Wu et al. reported ~~the~~ differentially transcriptional activities of terrestrial AOA communities referred from DNA and RNA extracts, suggesting that ~~the overwhelming~~ studies ~~depended on~~using DNA may have underestimated the importance of some~~overlooked~~ active AOA groups in the natural environments (Wu et al. 2017). In this study, we have conducted a comprehensive study about ammonia oxidizers in a typical subtropical estuary-Pearl River estuary (PRE)~~-~~, characterized by its salt-wedge structure resulted from large amount of freshwater discharge during wet season ~~which is the second largest river in China in terms of freshwater discharge (Zhao 1990). During the wet season, Pearl River estuary is characterized by receiving 80 % of annual freshwater discharge forming a typical salt wedge estuary~~ (Harrison et al. 2008). Recently, the ~~reoccurring~~ recurrence of bottom water hypoxia ~~formation~~ at the lower estuary of PRE has received increasing concerns about its ecological impact on the estuarine ecosystem (Qian et al. 2018; Zhao et al. 2020). The steep natural gradients of salinity, nutrients, oxygen ~~concentration,~~ concentration and turbidity makes the Pearl River estuary ~~to be~~ an ideal environment to study the diversity and ecological function of ammonia oxidizers. ~~Together, b~~By revealing AOA community structure (dominant ammonia oxidizer) at DNA and RNA levels ~~by~~ using high throughput sequencing ~~Ion torrent sequencing~~ and fine-scale phylogenetic classification, along with quantification of AOA and AOB and nitrification rate measurement, we aim to 1) identify the major and active AOA in the estuarine ecosystem~~;~~, 2) ~~identify~~ reveal niche partitioning between different AOA sublineages based on ~~ecophysiology and~~ environmental determinants~~;~~, and 3) determine the potential contribution of nitrification to hypoxia formation in PRE.

2 Materials and methods

2.1 Sample collection

The cruise was conducted from July 11~~-~~ to August 1 in 2017 on ~~the~~ R/V Hai Ke 68. In the first leg, 83 stations were designed ~~along~~ within the 10-50m isobaths ~~of the 10-50m by 10m interval covered~~ covering areas from the upper estuary to the continental shelf (Fig. S1). Water samples were collected using ~~a~~ Niskin bottles equipped with CTD sensor (Sea-Bird SBE 917plus). Temperature, salinity, and depth data were acquired through the CTD sensor. The dissolved oxygen concentrations were measured on board using Winkler ~~Spectrophotometric~~ spectrophotometric and titration method~~, as described in~~ (Pai et al. 2001; Dai et al. 2006; Zhao et al. 2020). Dissolved inorganic nutrient samples were filtered through ~~the~~ pre-acid washed cellulose acetate fiber membranes and stored in -20 ℃ until analysis in a land-based laboratory in Xiamen University (Qian et al. 2018). Ammonium~~a~~ concentration was ~~determined~~ measured on board using the indophenol blue spectrophotometric method (Pai et al. 2001). Chlorophyll-*a* samples (250 to 500ml) were filter onto GF/F (Whatman, USA) and ~~soon~~ stored in foil bags in liquid nitrogen. The c~~C~~hlorophyll-*a* concentration was measured with~~on~~ a Turner Fluorometer (Welschmeyer 1994) after being extracted with 90 % acetone for 14 h at -20 ℃. The ~~bacterial~~ microbial abundances were quantified by a~~the~~ Becton-

Dickson FACSCalibur flow cytometer (Vaulot et al. 1989). Sea-water for microbial abundance quantification was prefiltered by through a 20 μm mesh and, fixed by with final concentration of 0.5 % seawater seawater-buffed paraformaldehyde in cryotubes, and stored in liquid nitrogen until flow cytometric analysis (Liu et al. 2014). At each sampling depth, 0.5-2 L of sea water were sequentially filtrated onto 3 μm and 0.2 μm polycarbonate membranes (GVS, USA) for particle-attached community and 0.2 μm polycarbonate membranes for the and free-living communitymicrobes. DNA/RNA samples were immersed in 500 μl RNAlater (Ambion, Austin, TX, USA) before stored in liquid nitrogen.

2.2 Rates measurement

Community respiration rates (CR) were measured estimated by measuaring the oxygen consumption in triplicate 60ml BOD bottles without headspacethrough the dissolved oxygen variance before and after 24 h dark incubation submerged in running seawater continuously pumped from sea surface. Nitrification were measured by incubating $^{15}NH_4^+$ amended (less than 10 % of ambient concentration) seawater in duplicate 200 ml HDPE bottles in dark for 6-12 h, with temperature controlled by running seawater.rates were After incubation, filtrate (0.2 μm-syringe-filtered) was collected and stored in -20 ℃ for downstream $^{15}NO_x^-$ ($^{15}NO_3^-$+ $^{15}NO_2^-$) analysis (Sigman et al. 2001).

The nitrification rates were calculated using the following equation:

$$AO_b = \frac{(R_t NO_x^- \times [NO_x^-]_t) - (R_{t0} NO_x^- \times [NO_x^-]_{t0})}{t\text{-}t0} \times \frac{\left[{}^{14}NH_4^+\right] + \left[{}^{15}NH_4^+\right]}{\left[{}^{15}NH_4^+\right]} \quad (1)$$

In equation 1, AO_b is the bulk nitrification rate. R_{t0} NO_x^- and R_t NO_x^- are the ratios (%) of ^{15}N in the NO_x^- pool measured at the initial (t_0) and termination time (t) of the incubation. $[NO_x^-]_{t0}$ and $[NO_x^-]_t$ areis the concentration of NO_x^- at the initial and termination of the incubationtime points, respectively. $[^{14}NH_4^+]$ is the ambient NH_4^+ concentration. $[^{15}NH_4^+]$ is the final ammonium concentration after addition of the stable isotope tracer ($^{15}NH_4^+$). The NO_x^- was completely converted to N_2O by a single strain of denitrifying bacteria (*Pseudomonas aureofaciens*, ATCC#13985) which lack N_2O-reductase activity (Sigman et al. 2001). The converted N_2O was further analyzed using IRMS (Isotope Ration Mass Spectrometer, Thermo Scientific Delta V Plus) to calculate the isotopic composition of NO_x^- (Sigman et al. 2001; Casciotti et al. 2002; Knapp et al. 2005).The dissolved oxygen concentration was determined by the Winkler titration method (Oudot et al. 1988). Nitrification was measured through 6-12 h dark incubations conducted in a 200ml HDPE bottle added with ^{15}NH (less 10 % of ambient concentration) in running seawater. The $\delta^{15}N$ in NO the product of nitrification, was determined using the denitrifier method (Sigman et al. 2001; Casciotti et al. 2002; Knapp et al. 2005). Nitrification rate is adopted from another study conducted during the same cruise (L. Chen et al. in review). We analyzed the correlation between nitrification rates and AOA sublineages. Equation 1 2 and 2 waswere generally considered as the sequential oxidation of ammonia to nitratenitrite. Inferred from the nitrification rates, we estimated the nitrification oxygen demand (NOD) based on equations 12 and 2. Inferred from the nitrification rates, we estimated the nitrification oxygen demand (NOD) based on equation 23 coupling with carbon

assimilation (Dai et al. 2006; Dai et al. 2008). We used NOD/CR ratio (percentage) to evaluate the potential the contribution of nitrification to total oxygen consumption in the field.

$NH_3 + 1.5O_2 \longrightarrow NO_2^- + H_2O + H^+$ (1)

$NO_2^- + H_2O \longrightarrow NO_3^- + 2H^+ + 2e^-$ (2)

$NH_4^+ + 1.89O_2 + 1.98HCO_3^- \longrightarrow 0.984NO_3^- + 0.016C_5H_7O_2N + 1.90CO_2 + 2.93H_2O$ (3)

2.3 DNA and RNA extraction and cDNA synthesis

The sample filters immersed in RNAlater were thawed on ice. RNAlater was removed following the procedure described in Xu et al. 2013 (Xu et al. 2013). For DNA extraction, filters were cut into pieces and carefully collected into the 2ml Lysing Matrix E tubes with the addition of 978 µl sodium phosphate buffer and 122 µl MT buffer provided in FastDNA™ SPIN Kit for Soil (MP Biomedical, Solon, OH, USA). The lysing matrix was homogenized by Mini-Beadbeater-24 (Biospec Product, Bartlesville, OK, USA), at 3500 oscl/min for 60 seconds. The subsequent procedures of DNA extraction were performed according to FastDNA Spin kit for soil manufacture's instruction and preserved at -80 ℃. For RNA extraction, sample filters were incubated in 1 ml TRIzol for 5 min at room temperature in 2ml sterile microcentrifuge tubes. After the incubation, 200 µl chloroform was added into the tubes and mixed vigorously by hand until the membrane fully dissolved. After 3 min room temperature incubation for 3 min, the samples were centrifuged at 12000 × g and at 4 ℃ for 15 min. The supernatant was carefully transpired transferred into a new 2ml microcentrifuge and mixed with an equal volume of 70 % ethanol. The purification and elution procedures were performed according to the manufacture's instruction of the PureLink RNA Mini Kit (Life Technologies, Carlsbad, CA, USA). RNA samples were immediately treated with DNase at 37 ℃ for 30 min using the TURBO DNA-free Kit to eliminate DNA contamination. After incubation, the DNase was inactivated following the manufacturer's instruction. The DNA-free RNA samples were reversely transcribed into cDNA with random primers using the SuperScript III First-Strand Synthesis System (Life Technologies, Carlsbad, CA, USA). The synthesized cDNA was further treated with RNase H at 37 ℃ for 20 min to remove the residual RNA.

2.4 PCR amplification and high throughput sequencing

The DNA and cDNA were used as templates in PCR amplification. The archaeal *amoA* gene fragments were as amplified using the barcoded primers Arch-amoAF (5'-adaptor+barcode+GAT+STAATGGTCTGGCTTAGACG-3') and Arch-amoAR (5'-adaptor+barcode+GAT+GCGGCCATCCATCTGTATGT-3') (Francis et al. 2005). Triplicated PCR reactions were performed in 12.5 µl mixture contained 1×PCR buffer, 2 mM $MgCl_2$, 0.2 mM dNTP mix, 0.4 µM of respective primers, and 2 U Invitrogen Platinum Taq DNA polymerase (Life Technologies, Carlsbad, CA, USA) and 1 µl template. The PCR thermal cycle consisted of 5 min initial denaturation at 95 ℃ and followed by 33 cycles of 95 ℃ for 30s, 53 ℃ for 45s, and 72 ℃ for 60s and 10 min of final extension step at 72 ℃. The triplicated PCR products of each sample were pooled together and sequenced on the Ion GeneStudio S5 system (Thermo Fisher Scientific, USA) which could generate around 600 bp high quality reads.

2.5 Standard curve construction and Quantitative PCR

The *amoA* gene of AOA and β-AOB *amoA* was amplified by the primer pair Arch-amoAF-amoAR (Francis et al. 2005) and amoA-1F and amo-2R (Rotthauwe et al. 1997) respectively, using the DNA mixture from A-transect samples. The PCR products were purified using the illustra GFX PCR DNA and Gel band purification kit (GE Healthcare, UK) and ligated into T-vector pMD 19 at 4 ℃ for 12 h (Takara, Japan). The ligated vectors solution was mixed with freshly prepared *E. coli* BL21 competent cell and incubated on ice for 30 min. Heat-shock treatment at 42 ℃ were performed for the mixture for 90 s and incubated on ice for 5 min. After 5min incubation, 200 μl of liquid lysogeny broth was added and incubated at 37 ℃ for 1h in incubator shaker (250 rpm/min). The culture was soon spread on to ampicillin (100 mg·L^{-1}) containing plates and incubated at 37 ℃ for 12 h. White clone was selected and confirmed with respective PCR amplification. The clones were expanded with ampicillin (100 mg·L^{-1}) lysogeny broth and sequenced in BGI Tech (BGI, Shenzhen, China). The sequence of the selected plasmid was confirmed as an archaeal *amoA* gene by blast against the NCBI database. The plasmid of the selected clone was extracted and purified by the TIANprep Mini Plasmid Kit (TIANGEN, China). The extracted plasmid was linearized by EcoRI (New England Biolabs) at 37 ℃ for 12 h and purified by electrophoresis on 1.2 % agarose gel. The linearized plasmid DNA concentration was determined via dsDNA HS assay on the Qubit fluorometer v3.0 (Thermo Fisher Scientific, Singapore). Series dilution of the linearized plasmids was amplified as standard curves together with the field samples on the 384-well plates on Roche LightCycler 480.

Triplicated quantitative PCR (qPCR) was performed in 10 μl mixture contained 1 × LightCycler® 480 SYBR® Green I Master, 0.5 μM primers pairs and DNA templates. The thermal cycle of the quantitative qPCR that targeted archaeal *amoA* gene consisted of a 5 min denaturation at 95 ℃, followed by 45 cycles each at 95 ℃ for 30s, 53 ℃ (60 ℃ for β-AOB) for 45s, 72 ℃ for 60s with single signal acquisition at the end of each cycle. Amplification specificity was confirmed via the melting curve and gel electrophoresis. In both Both particle particle-attached (> 3 μm) and free-living (0.2-3 μm) from DNA (and RNA), the (using cDNA as a template) AOA and β-AOB ammonia-oxidizing archaea and ammonia-oxidizing β-proteobacteria abundance were quantified based on the *amoA* gene abundance through quantitative polymerase chain reactionthe qPCR (Table S2).

2.6 Bioinformatic analysis

ThIn total, 76 sample e archaeal *amoA* gene sequencing data of 76 samples (contained 2523 reads per samplefile) files were quality control and analyzed using the microbial ecology community software program Mothur (Schloss et al. 2009). The sequencing output was split according to corresponding barcode sequences in the forward primer. Quality control was performed by discarding the reads with low-quality (average quality score < 20), , or reads with incorrect length (no shorter than 300 bp and no longer than 630 bp), or reads, containing any ambiguous base or , or reads containing homopolymers longer than 8 bp. The chimeric sequences were identified and discarded by the *Chimera.uchime* in Mothur package. The remaining high-quality archaeal *amoA* sequences were aligned withthrough alignment of the reference *amoA* sequences from the NCBI database using Mothur (Agarwala et al. 2018) and. The remaining high-quality sequences were clustered into operational

taxonomic units (OTUs) at 95 % DNA similarity. The singletons and doubletons were discarded from the OTUs table before downstream analysis. The representative sequences of the top OTUs were randomly selected through *getotu.rep* in Mothur and searchedblast against the NCBI database using Blastn. (The top OTUs were selected based on relative abundance ≥ 0.1 % (Logares et al. 2014). The Maximum Likelihood phylogenetic tree was constructed in MEGAega 7 with the recommended model (T92+G+I) after the best model selection. The ML-tree wasere further edited with iTOL (Letunic and Bork 2016). The Bray-Curtis community dissimilaritiesy among the AOA communities wereas calculated within R by "*vegdist*" function ofin the "*vegan*" package in R. Nonmetric multidimensional scaling (NMDS) analysis was performed based on the Bray-Curtis dissimilarities withusing the "*vegan*" package and visualized withby "*ggplot2*" package in R (Oksanen, et al. 2019; Wickham, 2016).

Considering the strong stratification and steep variation of environmental factors that associated with the freshwater discharge in the PRE, SSpearman correlation analysis wasas performed by separating theto determine the relationship between the AOA sublineages and environmental factors community retrieved from in sSurface DNA,; sSurface RNA,; bBottom DNA, and; bBottom RNA, samples, respectively. Besides, ; and corresponding environmental factors, respectively, regarding strong stratification and steep variation of environmental factors that associated with the freshwater discharge in the PRE. Spearman correlation analysis was performed between nitrification rates and *amoA* gene (AOA and β-AOB) abundances retrieved from particle particle-attached (> 3 μm) and free-living (3-0.2 μm) samples.

3 Results

3.1 Hydrographic characteristics of Pearl River estuary

The Pearl River estuary consists of three major sub-estuaries, namely Lingdingyang, Modaomen, and Huangmaohai (Fig. 1), which contributed to 55 %, 28 %, and 13 % of the annual mean of freshwater discharge by 55 %, 28 %, and 13 %, respectively (Zhao 1990). This investigatione observation was conducted in the wet season when the high freshwater dischargeed formed a large plume extending southwestward (Fig. 2a and d) into Pearl River estuary can reach 80 % of the annual river discharge (Zhao 1990). The studied area covered a full range of salinity from 0.1 to 34.7, and a huge freshwater plume extended southwestward (Fig. 2a). Associated with the plume area, an excessive phytoplankton bloom was observed in the lower estuary with the chlorophyll-*a* concentration peaked (28.4 μg·L^{-1}) at station F202 (Fig. 2b and e). Furthermore, wide-spread bottom water hypoxia (DO < 2 mg·L^{-1}) was observed in the lower reach of Pearl River estuary extending from Huangmaohai to the southern water of Hong Kong island (Fig. 2f). Our study area covered a full range of salinity from 0.1 to 34.7. The variation of spatial pattern of nitrate concentration was associated with that offollowed salinity gradient (Fig. 2cS3a and d). The hHigh concentrations of nitrate wereas detected in low salinity waters near the outlets of sub-estuaries, and the nitrate concentrationwith the highest value (over ≥ 115 μmol·L^{-1}) observedpeaked in the surface water of Lingdingyang (station A01-03). Similar to nitrate, the concentrations of nitrite concentration at in the surface layer was were also higher near the estuary outlets and peaked atin station A01 with (9.5 μmol·L^{-1}), while but relatively constant (< 2 μmol·L^{-1}) in the bottom layer,

~~nitrite displayed relatively constant concentration (< 2 μmol·L^{-1}), spreading southeastward~~ (Fig. S3c and ~~f~~2e). The ammonium concentration displayed a different spatial pattern compared to nitrate and nitrite, with maximum concentration occurred at A06 (2.5 μmol·L^{-1} and 3.2 μmol·L^{-1} in surface and bottom layer, respectively) possibly influenced by ~~which was probably because of~~ local sewage discharges~~. The ammonium concentration peaked at A06 at both surface and bottom layer with 2.5 μmol·L^{-1} and 3.2 μmol·L^{-1} respectively during the cruise period~~. A patch of relatively high ammonium ~~replete~~ water (~~over~~ ≥ 1 μmol·L^{-1}) was observed in the southern water of Hong Kong, spreading eastward at the stations along the south ~~border line~~borderline of Hong Kong water (Fig. S3c~~2d~~).

3.2 The spatial pattern of nitrification rates and their oxygen consumption

The nitrification rates ~~were~~~~as~~ generally higher in bottom water than in surface water, except station A01 and F601 (Fig. 3). At the surface layer, ~~a~~ high nitrification rates ~~were~~~~as~~ detected in the outlet of Humen and Modaomen (station A01 and F301) and the southern water of Hong Kong (station F601 and F701) (Table S2). At the bottom layer, ~~a~~ high nitrification rates ~~were~~~~as~~ detected in the Humen outlet and the lower estuary from Huangmaohai to the southern water of Hong Kong (Fig. 3a). Based on equation 2, t~~T~~he ~~oxygen demand of nitrification (~~NOD~~)~~ were estimated ranging~~ranged~~ from 0.0001 to ~~0.1376~~0.1092 mg $O_2 \cdot L^{-1} \cdot d^{-1}$ (Fig. 3). The ~~community respiration rate~~CR ~~(total oxygen consumption rate, CR)~~ was higher at the surface layer than the corresponding bottom layer in all stations (Fig. 3, Table S3). The ~~community respiration rate~~CR at surface layer ranged from 0.22 to 1.68 mg $O_2 \cdot L^{-1} \cdot d^{-1}$, and that at bottom layer ranged from 0.002 to 0.82 mg $O_2 \cdot L^{-1} \cdot d^{-1}$ (Fig. S4). Based on the ratio between NOD and CR, nitrification contributed 0.01-17.82~~22.45~~ % and ~~0.01~~0.009-~~229.21~~181.91 % of total oxygen consumption at the surface and bottom layer, respectively (Fig. 3). It is noteworthy that nitrification contributed substantially to the total oxygen consumption in the upper estuary and bottom hypoxic water. For the upper estuary in Lingdingyang, nitrification potentially contributed ~~7.78~~6.18 % and ~~11.90~~9.45 % of the total oxygen consumption at station A01 and A05, respectively. As for the bottom hypoxic water, nitrification accounted for ~~35.45~~28.14 % at F101, ~~14.22~~11.28 % at F301, ~~10.27~~8.15 % at F303, ~~5.44~~4.53 % at A09, ~~81.77~~64.89 % at F305 and ~~229.21~~181.91 % at F701 of the total oxygen consumption.

3.3 Spatial patterns of the abundance of AOA and β-AOB

As inferred from the *amoA* gene copy number, AOA ~~showed a~~were 2-3 orders of magnitude more abundant than β-AOB (Fig. 4, Table S2). The archaeal *amoA* gene was more abundant at the bottom layer than at the surface layer (Fig. 5). The abundance of archaeal *amoA* gene ranged from 6.27×10^4 to 3.63×10^7 copy·L^{-1} at surface layer and 3.59×10^5 to 4.98×10^8 copy·L^{-1} at the bottom layer, ~~in which the~~ with maximum abundance ~~peaked~~ occurred at the bottom layer of station F405. The archaeal *amoA* gene abundance showed a general decreasing trend from the upper estuary to the continental shelf at the surface layer (Fig. 4 and 5, Table S2). It is noteworthy that archaeal *amoA* gene was highly abundant in the hypoxic water located in the lower reach of the estuary. The abundance of β-proteobacteria *amoA* gene at surface layer ranged from 2.03×10^2 to 1.07×10^5 copy·L^{-1}, while ~~at the bottom layer, the abundance of β-proteobacteria *amoA*~~it ranged from 1.91×10^3 to 2.44×10^5

copy·L^{-1} at the bottom layer (Fig. 5, Table S2). The β-proteobacteria *amoA* gene abundance peaked at the surface layer of station A01 in the upper estuary of Lingdingyang with 1.07 × 10^5 copy·L^{-1} while the lowest abundance was detected at the surface layer of station A12 with 2.03 × 10^2 copy·L^{-1}. ~~The~~ In general, the spatial pattern of β-proteobacteria *amoA* gene at the surface layer was more abundant at the upper estuary of Lingdingyang (~~at~~ station A01 ~~and~~, ~~&~~A05 and ~~F303 at~~ Modaomen (station F303), while the abundance decreased seaward at the bottom layer. Overall, the AOA showed higher abundance in the free-living fraction while AOB was more abundant in the particle attached fraction (Fig. 5, Table S2). ~~Quantification of *amoA* from cDNA (template for RNA level from 13 selected stations)~~ At RNA level, ~~showed~~ archaeal *amoA* gene ranged from 6.03 × 10^2 to 3.21 × 10^6 copy·L^{-1} while β-proteobacteria *amoA* gene were under detection limit (Table S4). Nitrification rate~~s~~ showed a ~~moderate~~positive correlation with the total abundance of β-AOB (r_s= 0.38, P < 0.05) at DNA level. At the particle attached fraction, n~~N~~itrification rate~~s~~ displayed ~~moderate~~ positive correlations with the abundance of AOA (r_s= 0.38, P < 0.05) and β-AOB (r_s= 0.33, P < 0.05) ~~at particle attached fraction~~, respectively.

3.4 Phylogenetic diversity of AOA

Given that the AOA were~~was~~ the dominant ammonia oxidizers throughout the estuary, we further investigated the phylogenetic diversity of AOA at DNA and RNA levels in 13 stations covering from the upper estuarine to ~~oceanic~~ shelf environments (Fig. 6, 7 and 8). In total, 191,748 high-quality *amoA* sequences were retrieved from 76 samples in the 13 stations (Table S5). ~~and o~~Operational ~~taxonomic units (~~OTUs~~)~~ were detected at 95 % DNA similarity after removal of singletons and doubletons. Top OTUs (OTUs with mean relative abundance ≥ 0.1 % among all samples) were focused in this study. The Maximum likelihood (ML) phylogenetic tree showed that the top 85 OTUs ~~(OTUs with mean relative abundance ≥ 0.1 % among samples)~~ affiliated to WCA sublineages and SCM1-like clade according to the reference sequences in Jing et al. 2017 and Cheung et al. 2019 (Jing et al. 2017; Cheung et al. 2019~~; Jing et al. 2017~~). More than ~~Half~~ half of the top OTUs were affiliated to the two WCA sublineages, WCA I (13 OTUs) and WCA II (32 OTUs). Besides, diverse ~~phylotypes~~ OTUs that affiliated to the SCM1-like clade, which showed > 90 % DNA similarity with the *amoA* sequences of *Nitrosopumilis maritimus* SCM1, were recovered. These SCM1-like OTUs were grouped into four sublineages according to the topology of the ML tree, includes SCM1-like-I (10 OTUs), SCM1-like-II (16 OTUs), SCM1-like-III (6 OTUs) and SCM-like-IV ~~clade~~ (8 OTUs) (Fig. 6 and 7). The SCM1-like ~~-~~III were also phylogenetically close to *Nitrosoarchaeum limnia* (Fig. 6, 7 and S2)

3.5 Differential distribution of AOA sublineages at DNA and RNA level

As revealed by the ~~Non-metric multidimensional scaling (~~NMDS plot~~)~~ ~~analysis~~, a strong dissimilarity between DNA and RNA communities were observed (Fig. 8~~7~~). ~~On the other hand, d~~Different AOA sublineages showed distinct distributional patterns (Fig. 6, 7 and 8). WCA I was mainly distributed in bottom layers except for the upper reach of Lingdingyang. At the surface layer, ~~the~~ WCA I was generally a minor component ~~in~~ of the AOA community, ~~while~~ though it was dominant occasionally in the plume area with ~~median~~ intermediate salinity. At RNA level, WCA I showed low~~er~~ relative abundance in the surface layer

with~~of at~~ ~~in median~~ mid salinity ~~at the surface layer~~ and ~~showed~~ an increasing ~~relative abundance~~trend seaward (Fig. 6, 7 and 8).

The AOA community at DNA level was dominated by WCA II which showed a ubiquitous distribution ~~for~~ across the whole salinity range of 0.1-34.~~5~~7. Exceptionally, WCA II was outnumbered by SCM1-like-III at the surface layer at station F301 near the Modaomen and Huangmaohai ~~which is~~ close to freshwater discharge. At RNA level, WCA II showed similar distributional patterns and relative abundance with WCA I~~; and contributed~~ sharing an increasing proportion of the active AOA community from the upper estuary to the continental shelf (Fig. 6, 7 and 8).

~~However, the~~ SCM1-like sublineages were surprisingly dominating the active AOA communities at RNA level expect SCM1-like III, which was dominating at stations near river outlets. Among SCM1-like sublineages, the SCM1-like-III was the most abundant at DNA level. Their distribution was limited to surface water of the Pearl River and freshwater plume (salinity < 14) (Fig. 6, 7 and 8). The distribution of SCM1-like-III at RNA level was limited to the freshwater regions (Fig. 6, 7), similar to its distribution pattern showed at DNA level. In addition, SCM1-like-III was the least abundant among the SCM1-like sublineages at RNA level. SCM1-like-I ~~mainly~~ distributed mainly at the lower reach of the estuary~~; and SCM1-like-I and II were outnumbered by other AOA phylotypes at DNA level~~. ~~Among SCM1-like sublineages, the SCM1-like-III was the most abundant at DNA level. Their distribution was limited to surface water of the Pearl River and freshwater plume (salinity < 14) (Fig. 6 and 8). However, the SCM1-like sublineages were surprisingly dominating the active AOA communities at RNA level.~~ The SCM1-like-II dominated the active AOA communities in the Pearl River and its lower reach at the bottom layer, while ~~at the surface layer,~~ the SCM1-like-IV ~~was~~ showed high relative abundance at the surface layer ~~at RNA level~~ (Fig. 8). ~~Besides,~~ ~~t~~The SCM1-like-I was less abundant than SCM1-like-II at RNA level at the bottom layer, and its spatial pattern was similar to SCM1-like-II. ~~In addition, SCM1-like-III was the least abundant among the SCM1-like sublineages at RNA level. The distribution of SCM1-like-III at RNA level was still limited to the freshwater regions (Fig. 6), similar to its spatial pattern showed at DNA level.~~

3.6 Correlation between AOA sublineages and environmental factors

To reveal the connections between ~~genetic diversity~~the relative abund~~a~~ance of AOA sublineages and environmental factors, ~~the~~ correlations between different sublineages and environmental factors were examined using Spearman correlation coefficients. The AOA communities were separated into 4 parts: surface DNA~~,~~; surface RNA~~,~~; bottom DNA~~,~~; and bottom RNA levels~~,~~, and were analyzed with the corresponding environmental factors. Generally, the relative abundance of AOA sublineages showed a more significant correlation with environmental factors both at DNA and RNA levels at the bottom layer compared to surface layer (Fig. 10~~9~~). Among 9 environmental factors, salinity ~~showed~~ was the most significant ~~correlation~~ factor affecting the distribution of~~with~~ AOA sublineage ~~distribution~~.

The sublineages of WCA ~~sublineages~~ showed a strong positive correlation with salinity while SCM1-like sublineages showed a negative correlation with salinity. At RNA level in the bottom layer, SCM1-like-I and IV were positively correlated with nutrient concentration and ~~heterotrophic bacteria~~non-phototropic prokaryotic cell abundance while negatively correlated

with salinity and dissolved oxygen concentration. SCM1-like-III showed a strong negative correlation with salinity at both surface and bottom layers. In general, WCA sublineages were negatively correlated with nutrient concentration, while SCM1-like sublineages were positively correlated with nutrient concentration. Nutrient concentration showed an opposite pattern comparing with salinity which was regarded as an association of nutrients with freshwater discharge. Ammonium, as the substrate for nitrification, showed no significant correlation with AOA sublineage distribution which may be introduced by the large variance of the ammonia concentration in the dynamic estuarine ecosystem.Ammonium showed no significant correlation with AOA sublineages.

The Spearman correlation between nitrification rates (NR) and the relative abundance of AOA sublineages in RNA based communities wereas also revealed intested (Fig. 109). SCM1-like-III showed a positive correlation (r_s= 0.72, P < 0.05) with nitrification rate at surface water at RNA level, while SCM1-like-I (r_s= 0.81, P < 0.05) and SCM1-like-IV sublineages (r_s= 0.73, P < 0.05) sublineages showed a positive correlations with nitrification rates at the bottom layer at RNA level. Besides, WCA I showed a positive correlation with nitrification rates (r_s= 0.75, P < 0.05) only at the surface layer ,at RNA level wWhile WCA II showed a negative correlation (r_s= -0.73, P < 0.05) with nitrification rates at the bottom layer.

4 Discussion

4.1 Nitrification and its oxygen consumption in the hypoxia zone

We observed a wide-spread hypoxia-zone at the lower estuary of Pearl River, extending from Huangmaohai to South south of Hong Kong which was in favor bya result of both physical and biogeochemical conditions (Fig. 2f-F). During the 2017 summer cruise, we observed intensive river discharge inferred fromwas high as indicated by the salinity at the surface layer (Fig. 2-Aa), which is the typical wet season pattern of Pearl River estuary (Harrison et al. 2008). The continuous river discharge sustained strong water column stratification at the lower estuary which blocked prevents the efficient supply of the air-sea oxygen exchange to the bottom water. Furthermore, a high concentration of nutrients associated with the freshwater from three sub-estuaries sustained high phytoplankton biomass in the lower reach of the estuary (Fig. 2b-B). The massive locally generated and riverine organic matter sunk down to the bottom layer and they were rapidly degraded by heterotrophic bacteriaprokaryotes, leading toresulting in high oxygen consumption (Harrison et al. 2008; Lu et al. 2018).

In the Pearl River estuary, we foundOur results suggest that nitrification could contribute a large proportion of oxygen consumption in the hypoxia zone (Table S3) in which nitrification potentially accounted for 35.35 % at F101, 14.22 % at F301, 10.27 % at F303, 5.14% at A09 and 81.77 % at F305 and 229.21 % at F701. Despite limited data with large variation, our estimate falls in general the ranges of previous reports. In the eutrophic Delaware River estuary, nitrification accounted for over 20 % of the oxygen consumption river downstream (Lipschultz et al. 1986). Intensive nitrification was observed at intermediate salinities, and which it accounted for 20 to over 50 % of oxygen consumption in the Mississippi River plume (Pakulski et al. 1995). In the downstream of Pearl River (from Guangzhou to Humen), It has been reported that nitrification could contribute to one-third of total oxygen consumption in the upper (from Guangzhou to Humen) Pearl River estuary (Dai

et al. 2008) ~~which suggested active nitrification could substantially draw down oxygen concentration leading to hypoxia formation~~. In our study, h~~H~~igh community respiration rates as well as nitrification rates were observed at lower reach of the Pearl River estuary corresponding to the hypoxia zone at the bottom layer (Fig. 2f). ~~highly~~ ~~Respiration and nitrification are both important and coupled oxygen-consuming processes.~~ It is well-known that ammonia, the substrate of nitrification, was produced during the organic matter degradation (respiration) (Ward, 1996). Thus, high rate of nitrification was ~~not only~~ supported not only by riverine ammonia but also ~~supported~~ by rapid organic matter degradation ~~in the Pearl River estuary~~. We observed the high nitrification rate associated with the upper estuary and ~~the~~ hypoxia zone (Fig. 3) ~~where the corresponding community respiration rates were high as well in the bottom layer~~. Respiration and nitrification are both important and coupled oxygen-consuming processes. Comparing with the community respiration, we found that nitrification ~~substantially~~ contributed a substantial proportion (averaged 12.18 %, excluding the unusual number of 181.91 % from F701) to total oxygen consumption at the bottom layer ~~by 15.30 % (excluding 229.21 % from F701) on average (ranged from 0.01 to 229.21 %)~~. We found that the NOD exceeded CR at the bottom layer of station F701, which~~Although it~~ might be caused ~~introduced~~ by the underestimation of CR in~~under~~ ~~low~~ oxygen depleted condition using the traditional incubation and titration method. ~~We~~ we ~~found one data of NOD exceeding CR from our entire cruise observed at F701.~~ Sampou and Kemp have found that oxygen concentration i~~as~~ one of the limiting factors of~~on community respiration rates~~CR. In their study, CR ~~. Community respiration rates~~ ~~was~~ere found to decrease when DO was lower than 0.8 mg·L^{-1} (Sampou and Kemp 1994). ~~In 2014 in~~Besides, ~~Changjiang estuary, Hsiao et al. also found the potential nitrification oxygen consumption exceeded the total oxygen consumption~~ ~~in the Changjiang estuary~~ and ~~they~~ ~~speculated the other oxidants (Fe and Mn) could potentially oxidize~~ed ammonia ~~(Hsiao et al. 2014). Oxygen might be considered as limiting factors to nitrifying activity as oxygen concentration were much lower under hypoxic condition (< 2mg·L^{-1}).~~ In contrast to the CR, ~~However,~~ nitrification can remain~~ed~~ active under nanomolar range of oxygen (< 10 nM) (Bristow et al. 2016). During the cruise, the lowest oxygen concentration wa~~i~~s 0.54 mg·L^{-1} (16.88 μM) ~~that~~which would ~~the oxygen concentration did~~ not limit the~~was not limiting for~~ nitrification activities (Bristow et al. 2016). Hence, in the Pearl River Estuary, nitrification could substantially draw down oxygen concentration ~~favored by physicochemical and biogeochemical conditions, sustaining~~and sustain hypoxia formation at the lower estuary. It should be mentioned that exceedance of potential ~~nitrificatioin oxygen consumption~~ NOD over the total oxygen consumption was also found in the Changjiang estuary by Hsiao et al. (2014), and they speculated that other oxidants (Fe and Mn) could oxidize ammonia.

4.2 Relative distribution of AOA and AOB in Pearl River Estuary

Both AOA and AOB are present in ~~the~~ estuarine environment, however, their corresponding contribution to ~~the~~ nitrification activities remained under ~~exploration~~explored. ~~The abundance of the AOA and AOB in the pelagic ocean~~ It has been well identified ~~with~~ that AOA outnumber AOB by orders of magnitude in pelagic waters, ~~while~~ whereas in the estuarine environment~~s~~, the ratio~~s~~ of AOA and AOB were rather variable. B~~Estimated b~~ased on ~~quantitative PCR (qq~~PCR~~)~~ of *amoA* gene, AOB were ~~relatively~~ more abundant than AOA ~~the~~ in many coastal and estuarine sediments (Caffrey et al. 2007; Mosier

and Francis 2008; Santoro et al. 2008; Magalhaes et al. 2009; Wankel et al. 2011). while AOA were orders of magnitude more abundant than AOB in other estuaries and coastal environments (Caffrey et al. 2007; Moin et al. 2009; Abell et al. 2010; Bernhard et al. 2010; Mosier and Francis 2011). The variance and relative ~~distribution~~ importance of AOA and AOB, as well as the nitrification rates in estuarine environments were ~~have been~~ shown being related to ~~various~~ physicochemical parameters such as salinity, dissolved oxygen, ammonia and~~,~~ pH~~, etc. in the various estuarine environments~~ (Bernhard and Bollmann 2010; Mosier and Francis 2011). Comparing to the previous estuarine studies based on DNA survey, we conducted ~~a~~ comprehensive quantification of AOA and β-AOB abundance at both DNA and RNA levels, ~~as well as~~in association with in situ~~the~~ nitrification rates measurements in the Pearl River estuary. In Pearl River estuary, AOA ~~outnumbers~~ outnumbered AOB throughout the estuarine at DNA level. ~~Furthermore,~~ At RNA level, AOA was detectable, ~~in RNA level while~~ but AOB was ~~lower than the detection limit~~not, ~~which suggested~~ suggesting that AOA were the active ammonia oxidizers in the Pearl River estuary. ~~Though~~ Moreover, size-fractionated study revealed that ~~nitrifiers abundance, the differential distribution of these two group ammonia oxidizers were observed. We found~~ AOA wereas mainly distributed in the free-living fraction, while AOB were associated with the particles near upper estuary (Fig. 5 and Table S2), which may be explained by higher substrate (ammonia) concentration requirement of AOB than AOA (Martens-Habbena et al. 2009).

4.3 Unneglectable disagreement of the AOA community at DNA and RNA level

In our study, the positive correlations between ~~-~~nitrification rates and different AOA sublineages suggested the divergence of nitrification activities among the AOA ~~population~~ community in the dynamic estuarine ecosystems (Fig. 10~~9~~). Given that AOA plays a central role in the nitrogen cycle, the physiological characteristics of the highly diverse AOA are an essential basis for understanding the nitrogen cycle in the current and future ocean. With the limitation of underrepresented cultures and genomes, numerous AOA related studies in the ocean were based on amplicon sequencing and qPCR targeting archaeal *amoA* (Beman et al. 2008; Bernhard and Bollmann 2010; Peng et al. 2013; Santoro et al. 2017; Alves et al. 2018). However, it should be noted that almost all these studies were based on DNA samples. In our study, the obvious disagreement between the AOA communities at DNA and RNA levels (Fig. 8) indicated that different AOA sublineages may have functional differences. Coincidentally, a similar phenomenon has also been recently reported in the terrestrial ecosystem, in which *Nitrososphaera* and its sister groups were more active than *Nitrosotalea* in acidic forest soils (Wu et al. 2017). In Baltic Sea, a distinct AOA community were retrieved from RNA level and a few phylotypes related to *Nitrosomarinus* showed widespread expression in the coastal region (Happel et al. 2018). As reported in a previous study in the Pacific Ocean, the *amoA* gene abundance of WCA and WCB have no correlation with nitrification rates throughout the water column indicated the active functional group of AOA might be ~~neglected~~ underrepresented in~~at~~ DNA based studies~~y~~ (Smith et al. 2016). In the light of our finding, the abundant AOA sublineages (WCA) can be much less active ammonia oxidizers than the rare sublineages (SCM1-like) (Fig. 8~~7~~ and 8~~9~~), which suggested that the DNA-based observations were insufficient to unravel the major ammonia oxidizers in the ocean. Furthermore, given that highly diverse sublineages of WCA and WCB have recently been reported in the oceanic waters

(Cheung et al. 2019; Lu et al. 2019), the nitrification activity of different AOA sublineages should be further verified in ~~the~~ future field studies.

4.4 AOA sublineages and their potential niche in the estuarine ecosystem

The ammonia-oxidizing archaea in the estuarine water were less studied compared to ~~the populations~~those in~~from~~ estuarine sediments, oceanic waters, and soils since the discovery of AOA (Damashek et al. 2016). In the sediment ~~from~~ of San Francisco Bay, Mosier and Francis (2008) had proposed a cluster of AOA phylotypes potentially adapted to ~~a~~ the low salinity environment (Mosier and Francis 2008). However, these phylotypes were then also observed in a salt marsh (Moin et al. 2009) which leads to questionable the low-salinity adaption assumption (Bernhard and Bollmann 2010). On the other hand, exploration of diversity and biogeography of different AOA were limited by low-coverage clone library method as well as the underrepresented~~neglected~~ active population at RNA level. Furthermore, in most cases, relatively weak or no correlations were found between nitrification rates and archaeal *amoA* gene abundances (Bernhard and Bollmann 2010) indicating~~ed~~ diverse ~~the~~ physiological ~~differences~~ characteristics among ~~of~~ ammonia oxidizers. The above-mentioned scenarios ~~indicated that it is necessary to~~raise the necessity to study key and active ammonia oxidizers ~~among the population~~in the community to understand their contribution in nitrification activities in the field.

In our study, we found ~~the differential~~ niche partitioning ~~of~~ among AOA sublineages in the dynamic PRE ecosystem in which the AOA community is mainly consisted of WCA and SCM1-like sublineages, while WCB is~~were~~ not detected. This pattern is~~was~~ consistent with the previous studies that show WCA and SCM1-like are mainly distributed in surface water and WCB is~~was~~ limited to deep mesopelagic waters (Francis et al. 2005; Beman et al. 2008). In a recent study based on the Tara *Oceans* dataset, WCA I dominated the surface water AOA communities throughout the global oceans (Cheung et al. 2019). In this study, WCA I was generally minor in the estuary except for the high salinity bottom water ~~that~~ intruded from the South China Sea (Fig. 8), which indicated that WCA I prefer the conditions of oceanic waters. As revealed by the genomic and proteomic information of its representative culture (*Candidatus Nitrosopelagicus brevis* CN25), the WCA I have a streamlined genome with high coding density and are ubiquitously distributed in oligotrophic surface ocean (Santoro et al. 2015). In contrast, WCA II was dominant in the AOA communities throughout ~~the~~ our studied region at DNA level (Fig. 8), which agrees with the previous study that its relative abundance was generally higher in marginal seas (the Gulf of Mexico, the Red Sea, and the Arabian Sea) than in oceanic waters (Cheung et al. 2019). The present study showed that WCA II outnumbered WCA I in the estuarine ecosystem, which strongly indicated ~~the~~ a niche partitioning between WCA I (oceanic water preferred) and WCA II (coastal water preferred). Nevertheless, these two WCA sublineages only contributed a small portion of the archaeal *amoA* gene transcripts and did not show a significant correlation with nitrification rate (Fig. 10~~9~~), which indicated that they were not the major ammonia oxidizers in the estuarine ecosystem. Hence, the ecological function of these abundant WCA sublineages in the estuarine ecosystem should be further explored in future studies.

Regarding the active populations in RNA level, highly diverse SCM1-like OTUs that are highly similar to *amoA* gene of Nitrosopumilus maritimus SCM1 were recovered in this study~~, which was highly similar to the *amoA* gene of *Nitrosopumilus*~~

maritimus SCM-1 (Fig. 6 and 7) (Konneke et al. 2005). In particular, the 4 SCM1-like sublineages defined in this study displayed distinct distributional patterns: SCM1-like-I and II mainly distributed in the lower reach of the river; SCM1-like-IV was mainly active at the surface layer in the estuary; SCM1-like-III was limited to freshwater, implied implying distinct niche partitioning of the SCM1-like sublineages (Fig. 8). As inferred from RNA communities and the correlation analysis result, SCM1-like-I was the major active ammonia oxidizer in the PRE water column. The earlier view presumed that the AOA are chemolithoautotrophs that largely rely on ammonia oxidation for energy acquisition. However, increasing evidence suggested that marine AOA (i.e. *N. maritimus* strains) can utilize organic nitrogen (i.e. urea and cyanate) as the substrates of nitrification, or utilize organic nutrient (Qin et al. 2014; Kitzinger et al. 2019). Using the stable isotope probing technology, the utilization of organic matter provided evidences of heterotrophy of AOAThaumarcheota in the salt marsh sediment and oceanic environment (Seyler, et al. 2014; Seyler et al. 2018; Seyler et al. 2019). Hence, it may explain that the high nitrification activities of the SCM1-like sublineages were facilitated by the enriched and diverse nitrogen sources in estuarine water. Recent culture-based studies found the physiology of *N. maritimus* was not significantly influenced by salinity changes in the growth medium (Elling et al. 2015, Qian et al. 2015), which indicated SCM1-like can tolerant to wide salinity range. Furthermore, SCM1-like-I showed a positive correlation with non-phototropic prokaryotic cellheterotrophic bacteria abundance, which, at RNA level together with a high abundances of AOA and non-phototropic prokaryotic cellheterotrophic bacteria in the hypoxic zone, suggestindicating potential interaction and coupling between organic matter degradation and nitrification activities. On the other hand, SCM1-like-I and II were the major ammonia oxidizers in the hypoxic waters (Fig. 109), where nitrification contributed significantly to the total oxygen consumption (Fig. 4). Consistently, *N. maritimus* can was actively oxidize ammonianitrifying and grew under low oxygen conditions (Qin et al. 2017).

The spatial distribution of SCM1-like-III as well as the negative correlation with salinity indicated thate SCM1-like-III is associated with freshwater discharge. The SCM1-like-III was closely related to the *amoA* gene fragment of *Nitrosoarchaeum limnia* which was is a low-salinity adapted species (Fig. S2). The functional potential of low-salinity adaptation of *N. limnia* was further evidenced by genomic information from an enrichment culture (estuarine sediment from San Francisco Bay) (Blainey et al. 2011). The genome of *N. limnia* SFB1 possessed numerous motility- and chemotaxis-associated genes that might facilitate their adaptation to the fluctuating estuarine environment (Blainey et al. 2011). Further genomic and metabolic studies were needed to understand the ecological role of SCM1-like-III in the freshwater discharge. In summary, our study provides the first evidence of the niche partition and different activities of different AOA sublineages in estuarine water, suggesting that more efforts are needed for a comprehensive understanding of the ecological role of AOA in various ecosystems.

5 Data availability

The *amoA* gene abundance at DNA level from 23 station along with nitrification rates were listed in Table S2. Nitrification and community respiration and nitrification oxygen demand were listed in Table S3. The *amoA* abundance at RNA (cDNA)

level from 13 stations were listed in Table S4. The complete sequencing dataset was available at NCBI under the Bioproject number PRJNA610708. Data will be released once the paper is published. –The information of the sequencing samples was listed in Table S5.

6 Author Contributions:

HBL conceived the project and revised the manuscript. YHL performed experiments, analyzed the dataed. ~~and~~ interpreted the data and wrote the manuscript. ~~YHL and~~ SYC interpreted the data and wrote the manuscript. XMX edited the manuscript. LC and SJK provided nitrification rates data. JPG provided physical profiles of the project. MHD provided nutrient and dissolved oxygen profiles of the project. All the authors provided critical feedback and help shape the research, analysis and manuscript.

7 Competing interests:

The authors declare that they have no conflict of interest.

8 Acknowledgments

This work was supported by the Research Grants Council (Hong Kong RGC) Theme-Based Research Scheme (T21-602/16-R), the RGC-NSFC Joint Research Scheme (N_HKUST609/15), and the GRF grants (16128416, 16101318). This study was also supported by the Hong Kong Branch of Southern Marine Science & Engineering Guangdong Laboratory (Guangzhou) (SMSEGL20SC01).

9 References

Abell, G. C. J., A. T. Revill, C. Smith, A. P. Bissett, J. K. Volkman, and Robert, S. S. : Archaeal ammonia oxidizers and *nirS*-type denitrifiers dominate sediment nitrifying and denitrifying populations in a subtropical macrotidal estuary, ISME J., 4, 286–300, https://doi.org/10.1038/ismej.2009.105, 2010.

Agarwala, R. Barrett, T. Beck, J. Benson, D. A. Bollin, C. Bolton, E. Bourexis, D. Brister, J. R. Bryant, S. H. Canese, K. Cavanaugh, M. Charowhas, C. Clark, K. Dondoshansky, I. Feolo, M. Fitzpatrick, L. Funk, K. Geer, L. Y. Gorelenkov, V. Graeff, A. Hlavina, W. Holmes, B. Johnson, M. Kattman, B. Khotomlianski, V. Kimchi, A. Kimelman, M. Kimura, M. Kitts, P. Klimke, W. Kotliarov, A. Krasnov, S. Kuznetsov, A. Landrum, M. J. Landsman, D. Lathrop, S. Lee, J. M. Leubsdorf, C. Lu, Z. Y. Madden, T. L. Marchler-Bauer, A. Malheiro, A. Meric, P. Karsch-Mizrachi, I. Mnev, A. Murphy, T. Orris, R. Ostell,

J. O'Sullivan, C. Palanigobu, V. Panchenko, A. R. Phan, L. Pierov, B. Pruitt, K. D. Rodarmer, K. Sayers, E. W. Schneider, V. Schoch, C. L. Schuler, G. D. Sherry, S. T. Siyan, K. Soboleva, A. Soussov, V. Starchenko, G. Tatusova, T. A. Thibaud-Nissen, F. Todorov, K. Trawick, B. W. Vakatov, D. Ward, M. Yaschenko, E. Zasypkin, A. and Zbicz, K. : Database resources of the National Center for Biotechnology Information, Nucleic Acids Res. 46**:** D8–D13. https://doi.org/10.1093/nar/gkx1095, 2018.

Alves, R. J. E., B. Q. Minh, T. Urich, A. von Haeseler, and Schleper, C. : Unifying the global phylogeny and environmental distribution of ammonia-oxidising archaea based on *amoA* genes. Nat. Commun., 9, https://doi.org/10.1038/s41467-018-03861-1, 2018.

Beman, J. M., B. N. Popp, and Alford, S. E. : Quantification of ammonia oxidation rates and ammonia-oxidizing archaea and bacteria at high resolution in the Gulf of California and eastern tropical North Pacific Ocean, Limnol. Oceanogr., 57, 711–726, https://doi.org/10.4319/lo.2012.57.3.0711, 2012.

Beman, J. M., B. N. Popp, and Francis, C. A. : Molecular and biogeochemical evidence for ammonia oxidation by marine Crenarchaeota in the Gulf of California, ISME J., 2, 429–441, https://doi.org/10.1038/ismej.2007.118, 2008.

Bernhard, A. E., and Bollmann, A. : Estuarine nitrifiers: New players, patterns and processes, Estuar. Coast. Shelf Sci. 88, 1–11, https://doi.org/10.1016/j.ecss.2010.01.023, 2010.

Bernhard, A. E., Z. C. Landry, A. Blevins, J. R. de la Torre, A. E. Giblin, and Stahl, D. A. : Abundance of ammonia-oxidizing archaea and bacteria along an estuarine salinity gradient in relation to potential nitrification rates, Appl. Environ. Microbiol. 76, 1285–1289, https://doi.org/10.1128/Aem.02018-09, 2010.

Blainey, P. C., A. C. Mosier, A. Potanina, C. A. Francis, and Quake, S. R. : Genome of a Low-salinity ammonia-oxidizing archaeon determined by single-cell and metagenomic analysis, PLoS One, 6, https://doi.org/10.1371/journal.pone.0016626, 2011.

Bristow, L. A. Dalsgaard, T. Tiano, L. Mills, D. B. Bertagnolli, A. D. Wright, J. J. Hallam, S. J. Ulloa, O. Canfield, D. E. Revsbech, N. P. Thamdrup, B. : Ammonium and nitrite oxidation at nanomolar oxygen concentrations in oxygen minimum zone waters, Proc. Natl. Acad. Sci. USA 113, 10601–10606, https://doi.org/10.1073/pnas.1600359113, 2016.

Caffrey, J. M., N. Bano, K. Kalanetra, and Hollibaugh, J. T. : Ammonia oxidation and ammonia-oxidizing bacteria and archaea from estuaries with differing histories of hypoxia, ISME J., 1, 660–662, https://doi.org/10.1038/ismej.2007.79, 2007.

Campbell, L. G., J. C. Thrash, N. N. Rabalais, and Mason, O. U. : Extent of the annual Gulf of Mexico hypoxic zone influences microbial community structure, PLoS One, 14, https://doi.org/10.1371/journal.pone.0209055, 2019.

Casciotti, K. L., D. M. Sigman, M. G. Hastings, J. K. Bohlke, and Hilkert, A. : Measurement of the oxygen isotopic composition of nitrate in seawater and freshwater using the denitrifier method., Anal. Chem., 74, 4905–4912, https://doi.org/10.1021/ac020113w, 2002.

Chen, L., Zhang, X., Lai, Y., Liu, J., Lu, Y. H., Liu, H. B., Dai, M. H., Gan, J. P. and Kao, S. J. : Dark ammonium transformations in the Pearl River Estuary during summer (in review)

Cheung, S., W. Mak, X. M. Xia, Y. H. Lu, Y. Y. Cheung, and Liu, H. B. : Overlooked genetic diversity of ammonia oxidizing archaea lineages in the global oceans., J. Geophys. Res. Biogeo., 124, 1799–1811, https://doi.org/10.1029/2018jg004636, 2019.

D. Kahle and Wickham, H. : ggmap: Spatial Visualization with ggplot2. The R J., 51, 144-161, URL http://journal.r-project.org/archive/2013-1/kahle-wickham.pdf, 2013.

Dai, M. H. Guo, X. G. Zhai, W. D. Yuan, L. Y. Wang, B. W. Wang, L. F. Cai, P. H. Tang, T. T. and Cai, W. J. : Oxygen depletion in the upper reach of the Pearl River estuary during a winter drought, Mar. Chem., 102, 159–169, https://doi.org/10.1016/j.marchem.2005.09.020, 2006.

Dai, M. Wang, L. Guo, X. Zhai, W. Li, Q. He, B. and Kao, S. J. : Nitrification and inorganic nitrogen distribution in a large perturbed river/estuarine system: the Pearl River Estuary, China, Biogeosciences, 5, 1227–1244. https://doi.org/10.5194/bg-5-1227-2008, 2008.

Damashek, J., K. L. Casciotti, and Francis, C. A. : Variable nitrification rates across environmental gradients in turbid, nutrient-rich estuary waters of San Francisco Bay, Estuar. Coast., 39, 1050–1071, https://doi.org/10.1007/s12237-016-0071-7, 2016.

Elling, F. J., M. Konneke, M. Mussmann, A. Greve, and Hinrichs,K. U. : Influence of temperature, pH, and salinity on membrane lipid composition and TEX86 of marine planktonic thaumarchaeal isolates, Geochim. Cosmochim. Ac., 171, 238–255, https://doi.org/10.1016/j.gca.2015.09.004, 2015.

Erguder, T. H., N. Boon, L. Wittebolle, M. Marzorati, and Verstraete, W. : Environmental factors shaping the ecological niches of ammonia-oxidizing archaea, FEMS Microbiol Rev., 33, 855–869, https://doi.org/10.1111/j.1574-6976.2009.00179.x, 2009.

Francis, C. A., K. J. Roberts, J. M. Beman, A. E. Santoro, and Oakley, B. B. : Ubiquity and diversity of ammonia-oxidizing archaea in water columns and sediments of the ocean, Proc. Natl. Acad. Sci. USA, 102, 14683–14688, https://doi.org/10.1073/pnas.0506625102, 2005.

Hallam, S. J. Mincer, T. J. Schleper, C. Preston, C. M. Roberts, K. Richardson, P. M. and DeLong, E. F. : Pathways of carbon assimilation and ammonia oxidation suggested by environmental genomic analyses of marine Crenarchaeota, PLoS Biol., 4, 520–536, https://doi.org/10.1371/journal.pbio.0040095, 2006.

Happel, E. I. Bartl, M. Voss, and Riemann, L. : Extensive nitrification and active ammonia oxidizers in two contrasting coastal systems of the Baltic Sea, Environ. Microbiol., 20 (8), 2913–2926, https://doi.org/10.1111/1462-2920.14293, 2018.

Harrison, P. J., K. D. Yin, J. H. W. Lee, J. P. Gan, and Liu, H. B. : Physical-biological coupling in the Pearl River Estuary. Cont. Shelf Res., 28, 1405–1415, https://doi.org/ 10.1016/j.csr.2007.02.011, 2008.

Hsiao, S. S. Y. Hsu, T. C. Liu, J. W. Xie, X. Zhang, Y. Lin, J. Wang, H. Yang, J. Y. T. Hsu, S. C. Dai, M. and Kao, S. J. : Nitrification and its oxygen consumption along the turbid Chang Jiang River plume, Biogeosciences, 11, 2083–2098, https://doi.org/10.5194/bg-11-2083-2014, 2014.

Jing, H. M., S. Y. Cheung, X. M. Xia, K. Suzuki, J. Nishioka, and Liu, H. B. : Geographic distribution of ammonia-oxidizing archaea along the Kuril Islands in the western subarctic Pacific, Front. Microbiol., 8, https://doi.org/10.3389/fmicb.2017.01247, 2017.

Kitzinger, K. Padilla, C. C. Marchant, H. K. Hach, P. F. Herbold, C. W. Kidane, A. T. Konneke, M. Littmann, S. Mooshammer, M. Niggemann, J. Petrov, S. Richter, A. Stewart, F. Wagner, M. Kuypers, M. M. M. and Bristow, L. A. : Cyanate and urea are substrates for nitrification by Thaumarchaeota in the marine environment. Nat. Microbiol., 4, 234–243, https://doi.org/10.1038/s41564-018-0316-2, 2019.

Knapp, A. N., D. M. Sigman, and Lipschultz, F. : N isotopic composition of dissolved organic nitrogen and nitrate at the Bermuda Atlantic time-series study site, Global Biogeochem. Cycle, 19, https://doi.org/10.1029/2004gb002320, 2005.

Konneke, M., A. E. Bernhard, J. R. de la Torre, C. B. Walker, J. B. Waterbury, and D. A. Stahl. : Isolation of an autotrophic ammonia-oxidizing marine archaeon, Nature 437, 543–546, https://doi.org/10.1038/nature03911, 2005.

Letunic, I., and Bork, P. : Interactive tree of life (iTOL) v3: an online tool for the display and annotation of phylogenetic and other trees, Nucleic Acids Res., 44, W242–W245, https://doi.org/10.1093/nar/gkw290, 2016.

Lipschultz, F., S. C. Wofsy, and Fox, L. E. : Nitrogen-metabolism of the eutrophic Delaware River ecosystem, Limnol. Oceanogr., 31, 701–716, https://doi.org/10.4319/lo.1986.31.4.0701, 1986.

Liu, H. B., H. M. Jing, T. H. C. Wong, and Chen, B. Z. : Co-occurrence of phycocyanin- and phycoerythrin-rich *Synechococcus* in subtropical estuarine and coastal waters of Hong Kong. Environ. Microbiol. Rep., 6, 90–99, https://doi.org/10.1111/1758-2229.12111, 2014.

Logares, R. Audic, S. Bass, D. Bittner, L. Boutte, C. Christen, R. Claverie, J. M. Decelle, J. Dolan, J. R. Dunthorn, M. Edvardsen, B. Gobet, A. Kooistra, W. H. C. F. Mahe, F. Not, F. Ogata, H. Pawlowski, J. Pernice, M. C. Romac, S. Shalchian-Tabrizi, K. Simon, N. Stoeck, T. Santini, S. Siano, R. Wincker, P. Zingone, A. Richards, T. A. de Vargas, C. and Massana, R. : Patterns of rare and abundant marine microbial eukaryotes, Curr. Biol., 24, 813–821, https://doi.org/10.1016/j.cub.2014.02.050, 2014.

Lu, Y. H., X. M. Xia, S. Y. Cheung, H. M. Jing, and Liu, H. B. : Differential distribution and determinants of ammonia oxidizing archaea sublineages in the oxygen minimum zone off Costa Rica, Microorganisms, 7, https://doi.org/10.3390/microorganisms7100453, 2019.

588 Lu, Z. M., J. P. Gan, M. H. Dai, H. B. Liu, and Zhao, X. Z. : Joint effects of extrinsic biophysical fluxes and intrinsic
589 hydrodynamics on the formation of hypoxia west off the Pearl River Estuary. J. Geophys. Res. Ocean, 123, 6241–6259,
590 https://doi.org/10.1029/2018jc014199, 2018.

591 Magalhaes, C. M., A. Machado, and Bordalo, A. A. : Temporal variability in the abundance of ammonia-oxidizing bacteria vs.
592 archaea in sandy sediments of the Douro River estuary, Portugal, Aquat. Microb. Ecol., 56, 13–23,
593 https://doi.org/10.3354/ame01313, 2009.

594 Martens-Habbena, W., P. M. Berube, H. Urakawa, J. R. de la Torre, and Stahl, D. A. : Ammonia oxidation kinetics determine
595 niche separation of nitrifying Archaea and Bacteria, Nature 461, 976–U234, https://doi.org/10.1038/nature08465, 2009.

596 Moin, N. S., K. A. Nelson, A. Bush, and Bernhard, A. E. : Distribution and diversity of archaeal and bacterial ammonia
597 oxidizers in salt marsh sediments, Appl. Environ. Microbiol., 75, 7461–7468, https://doi.org/10.1128/Aem.01001-09, 2009.

598 Mosier, A. C., and Francis, C. A. : Relative abundance and diversity of ammonia-oxidizing archaea and bacteria in the San
599 Francisco Bay estuary, Environ. Microbiol., 10, 3002–3016, https://doi.org/10.1111/j.1462-2920.2008.01764.x, 2008.

600 Mosier, A. C., and Francis C. A. : Determining the distribution of marine and coastal ammonia-oxidizing archaea and bacteria
601 using a quantitative approach, Meth. Enzymol., 486, 205–221, https://doi.org/10.1016/S0076-6879(11)86009-X, 2011.

602 Oksanen, J., Blanchet, F. G. Friendly, Kindt, M. R. Legendre, P. McGlinn, D. Minchin, P. R. O'Hara, R. B. Simpson, G. L.
603 Solymos, P. M. Stevens, H. H. Szoecs E. and Wagner, H.: vegan: Community Ecology Package, R package version 2.5-6.
604 https://CRAN.R-project.org/package=vegan, 2019.

605 Oudot, C., R. Gerard, P. Morin, and Gningue, I. : Precise shipboard determination of dissolved-oxygen (Winkler Procedure)
606 for productivity studies with a commercial system, Limnol. Oceanogr., 33, 146–150, https://doi.org/10.4319/lo.1988.33.1.0146,
607 1988.

608 Pai, S. C., Y. J. Tsau, and Yang, T. I. : pH and buffering capacity problems involved in the determination of ammonia in saline
609 water using the indophenol blue spectrophotometric method, Anal. Chim. Ac., 434, 209–216, https://doi.org/10.1016/S0003-
610 2670(01)00851-0, 2001.

611 Pakulski, J. D., R. Benner, R. Amon, B. Eadie, and Whitledge, T. : Community metabolism and nutrient cycling in the
612 Mississippi River Plume - Evidence for intense nitrification at intermediate salinities, Mar. Ecol. Prog. Ser., 117, 207–218,
613 https://doi.org/10.3354/meps117207, 1995.

614 Peng, X. F., A. Jayakumar, and Ward, B. B. : Community composition of ammonia-oxidizing archaea from surface and anoxic
615 depths of oceanic oxygen minimum zones, Front. Microbiol., 4, https://doi.org/ 10.3389/fmicb.2013.00177, 2013.

Qian, W. Gan, J. P. Liu, J. W. He, B. Y. Lu, Z. M. Guo, X. H. Wang, D. L. Guo, L. G. Huang, T. and Dai, M. H. : Current status of emerging hypoxia in a eutrophic estuary: The lower reach of the Pearl River Estuary, China, Estuar. Coast. Shelf S., 205, 58–67, https://doi.org/10.1016/j.ecss.2018.03.004, 2018.

Qin, W. Amin, S. A. Martens-Habbena, W. Walker, C. B. Urakawa, H. Devol, A. H. Ingalls, A. E. Moffett, J. W. Armbrust, E. V. and Stahl, D. A. : Marine ammonia-oxidizing archaeal isolates display obligate mixotrophy and wide ecotypic variation, Proc. Natl. Acad. Sci. USA, 111, 12504–12509. https://doi.org/10.1073/pnas.1324115111, 2014.

Qin, W. Carlson, L. T. Armbrust, E. V. Devol, A. H. Moffett, J. W. Stahl, D. A. and Ingalls, A. E. : Confounding effects of oxygen and temperature on the TEX86 signature of marine Thaumarchaeota, Proc. Natl. Acad. Sci. USA, 112, 10979–10984, https://doi.org/10.1073/pnas.1501568112, 2015.

Qin, W. Meinhardt, K. A. Moffett, J. W. Devol, A. H. Armbrust, E. V. Ingalls, A. E. and Stahl, D. A. Influence of oxygen availability on the activities of ammonia-oxidizing archaea, Environ. Microbiol. Rep., 9, 250–256, https://doi.org/10.1111/1758-2229.12525, 2017.

Reji, L., B. B. Tolar, J. M. Smith, F. P. Chavez, and Francis, C. A. : Differential co-occurrence relationships shaping ecotype diversification within Thaumarchaeota populations in the coastal ocean water column, ISME J., 13, 1144-1158, https://doi.org/10.1038/s41396-018-0311-x, 2019.

Rotthauwe, J. H., K. P. Witzel, and Liesack, W. : The ammonia monooxygenase structural gene *amoA* as a functional marker: Molecular fine-scale analysis of natural ammonia-oxidizing populations, Appl. Environ. Microbiol., 63, 4704–4712, 1997.

Sampou, P. and Kemp, W. N. : Factors regulating phytoplankton community respiration in Chesapeake Bay, Mar. Ecol. Prog. Ser., 110, 249–258, http://doi.org/10.3354/meps110249, 1994.

Santoro, A. E., C. A. Francis, N. R. de Sieyes, and Boehm, A. B. : Shifts in the relative abundance of ammonia-oxidizing bacteria and archaea across physicochemical gradients in a subterranean estuary, Environ. Microbiol., 10, 1068–1079, https://doi.org/10.1111/j.1462-2920.2007.01547.x, 2008.

Santoro, A. E. Dupont, C. L. Richter, R. A. Craig, M. T. Carini, P. McIlvin, M. R. Yang, Y. Orsi, W. D. Moran, D. M. and Saito, M. A. : Genomic and proteomic characterization of "*Candidatus Nitrosopelagicus brevis*": An ammonia-oxidizing archaeon from the open ocean. Proc. Natl. Acad. Sci. USA, 112, 1173–1178, https://doi.org/10.1073/pnas.1416223112, 2015.

Santoro, A. E., M. A. Saito, T. J. Goepfert, C. H. Lamborg, C. L. Dupont, and DiTullio, G. R., Thaumarchaeal ecotype distributions across the equatorial Pacific Ocean and their potential roles in nitrification and sinking flux attenuation. Limnol. Oceanogr., 62, 1984–2003, https://doi.org/10.1002/lno.10547, 2017.

Schloss, P. D. Westcott, S. L. Ryabin, T. Hall, J. R. Hartmann, M. Hollister, E. B. Lesniewski, R. A. Oakley, B. B. Parks, D. H. Robinson, C. J. Sahl, J. W. Stres, B. Thallinger, G. G. Van Horn, D. J. and Weber, C. F. Introducing mothur: Open-Source,

Platform-Independent, Community-Supported Software for describing and comparing microbial communities, Appl. Environ. Microbiol., 75, 7537–7541, https://doi.org/10.1128/Aem.01541-09, 2009.

Seyler, L. M., L. M. McGuinness, and Kerkhof, L. J. : Crenarchaeal heterotrophy in salt marsh sediments, ISME J., 8, 1534–1543, http://doi.org/10.1038/ismej.2014.15, 2014.

Seyler, L. M., L. R. McGuinness, J. A. Gilbert, J. F. Biddle, D. L. Gong, and Kerkhof, L. J. Discerning autotrophy, mixotrophy and heterotrophy in marine TACK archaea from the North Atlantic, FEMS Microbiol. Ecol., 94, https://doi.org/10.1093/femsec/fiy014, 2018.

Seyler, L. M., S. Tuorto, L. R. McGuinness, D. L. Gong, and Kerkhof, L. J. Bacterial and archaeal specific-predation in the North Atlantic Basin, Front. Mar. Sci., 6, 555, https://doi.org/10.3389/fmars.2019.00555, 2019.

Sigman, D. M., K. L. Casciotti, M. Andreani, C. Barford, M. Galanter, and Bohlke, J. K. : A bacterial method for the nitrogen isotopic analysis of nitrate in seawater and freshwater, Anal. Chem., 73, 4145–4153, https://doi.org/10.1021/ac010088e, 2001.

Smith, J. M., J. Damashek, F. P. Chavez, and Francis, C. A. : Factors influencing nitrification rates and the abundance and transcriptional activity of ammonia-oxidizing microorganisms in the dark northeast Pacific Ocean, Limnol. Oceanogr., 61, 596–609, https://doi.org/10.1002/lno.10235, 2016.

Vaulot, D., C. Courties, and Partensky, F. : A simple method to preserve oceanic phytoplankton for Flow Cytometric Analyses, Cytometry, 10: 629–635, https://doi.org/10.1002/cyto.990100519, 1989.

Wankel, S. D., A. C. Mosier, C. M. Hansel, A. Paytan, and Francis, C. A. : Spatial variability in nitrification rates and ammonia-oxidizing microbial communities in the agriculturally impacted Elkhorn Slough Estuary, California, Appl. Environ. Microbiol., 77, 269–280, https://doi.org/10.1128/Aem.01318-10, 2011.

Ward, B. B. : Nitrification and ammonification in aquatic systems, Life Support Biosph. Sci., 3, 25–29, 1996.

Welschmeyer, N. A. : Fluorometric analysis of Chlorophyll-a in the presence of Chlorophyll-B and pheopigments, Limnol. Oceanogr., 39, 1985–1992, https://doi.org/10.4319/lo.1994.39.8.1985, 1994.

Wickham, H. : ggplot2: Elegant graphics for data analysis, Springer-Verlag New York, 2016.

Wu, R. N., H. Meng, Y. F. Wang, W. S. Lan, and Gu, J. D. : A more comprehensive community of ammonia-oxidizing archaea (AOA) revealed by genomic DNA and RNA analyses of *amoA* gene in subtropical acidic Forest Soils, Microbiol. Ecol., 74, 910–922, https://doi.org/10.1007/s00248-017-1045-4, 2017.

Xu, J., H. M. Jing, L. L. Kong, M. M. Sun, P. J. Harrison, and Liu, H. B. : Effect of seawater-sewage cross-transplants on bacterial metabolism and diversity. Microbiol. Ecol. 66: 60–72. https://doi.org/10.1007/s00248-013-0207-2, 2013.

674 Yool, A., A. P. Martin, C. Fernandez, and Clark, D. R. : The significance of nitrification for oceanic new production. Nature,
675 447, 999–1002, https://doi.org/ 10.1038/nature05885, 2007.

676 Zhao, H.T. : Evolution of the Pearl River Estuary, China Ocean Press, Beijing, 1–357, (in Chinese), 1990

677 Zhao, Y. Y., Liu, J., Uthaipan, K., Song, X., Xu, Y., He, B. Y., Liu, H., B. Gan, J. P. and Dai, M. H. : Dynamics of inorganic
678 carbon and pH in a large subtropical continental shelf system: Interaction between eutrophication, hypoxia, and ocean
679 acidification Limnol. Oceanogr. 9999, 1-21, https:/.doi.org/ 10.1002/lmo.11393, 2020

680 **10 Figures**

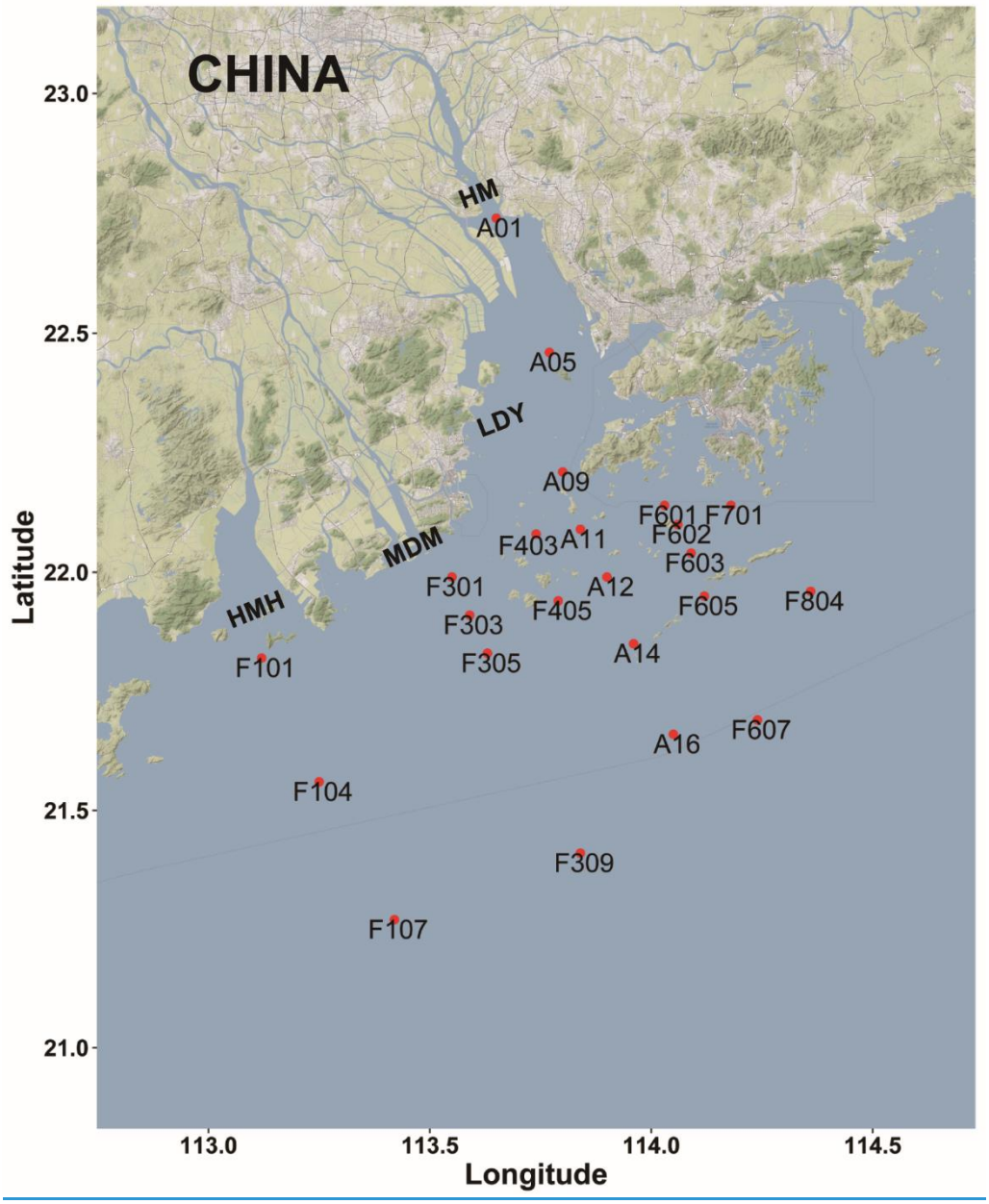

681

682 **Figure 1. Sampling and rates measurement location during the Pearl River estuary cruise in 2017 summer (HMH-**
683 **Huangmaohai; MDM-Modaomen; HM-Humen; LDY-Lingdingyang). The sampling location information was overlaid**
684 **on Google Maps (© Google Maps) image using "ggmap" with "ggplot2" in R (D. Kahle and H. Wickham, 2013)**

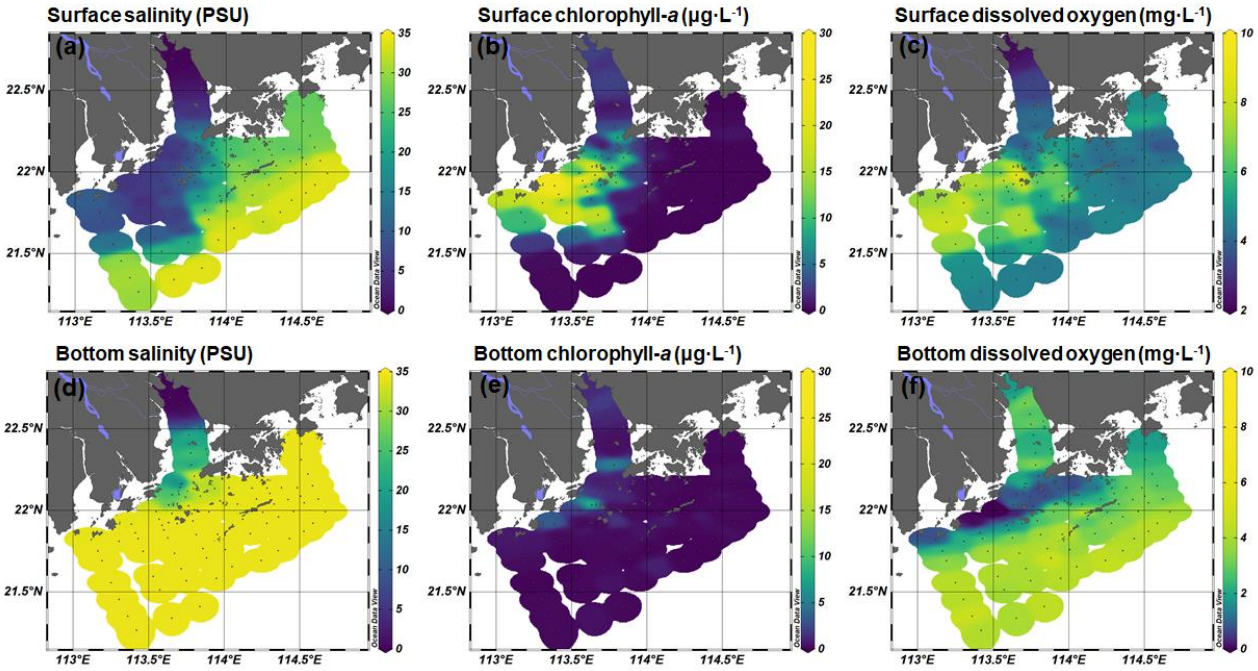

Figure 2. Spatial distribution of (a & d) salinity, (b & e) chlorophyll-*a*, ~~(c) nitrate, (d) ammonium at the surface layer, (e) nitrite,~~ and (c & f) dissolved oxygen concentration at surface and bottom layer during the 2017 summer cruise in Pearl River estuary. These figures were generated using Ocean Data View v. 5.0.0 (http://odv.awi.de).

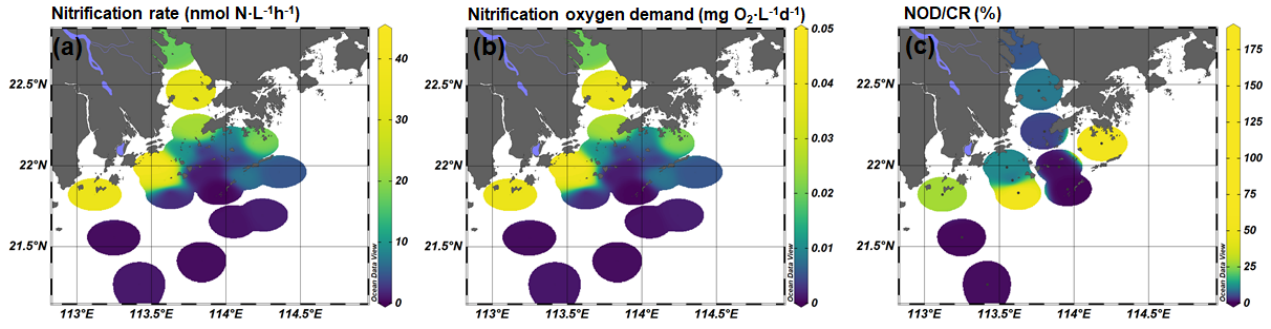

Figure 3. (a) Nitrification rates (nmol N·L^{-1} h^{-1}), (b) nitrification oxygen demand (NOD) (mg O2·L^{-1}·d^{-1}) and, (c) nitrification oxygen demand/-community respiration (NOD/CR) ratio (%) at the bottom layer (Data from F305 and F701 are not displayed).

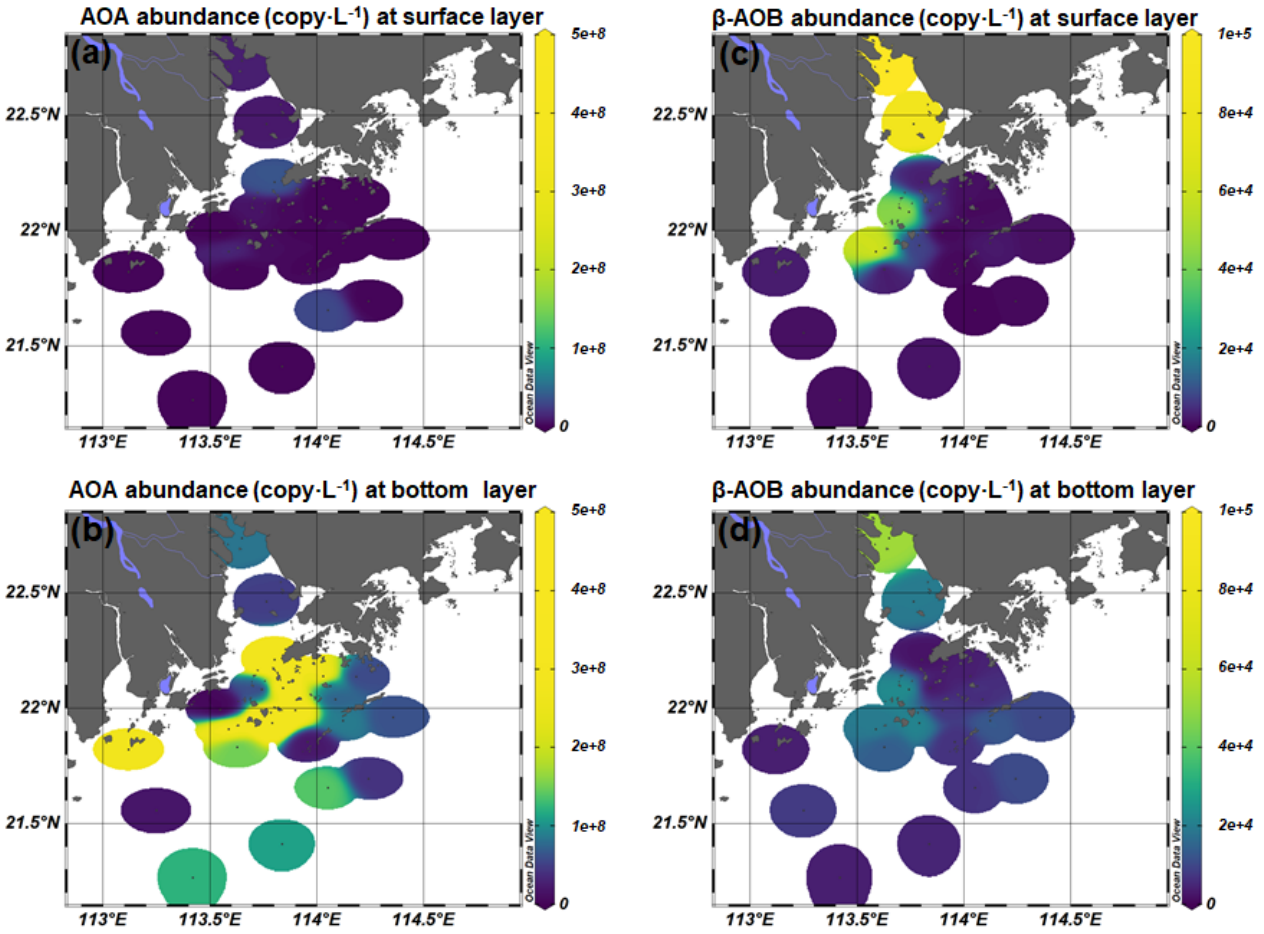

Figure 4. Spatial distribution of (a & b) AOA and (c & d) β-AOB abundance at the surface and the bottom layer at DNA level.

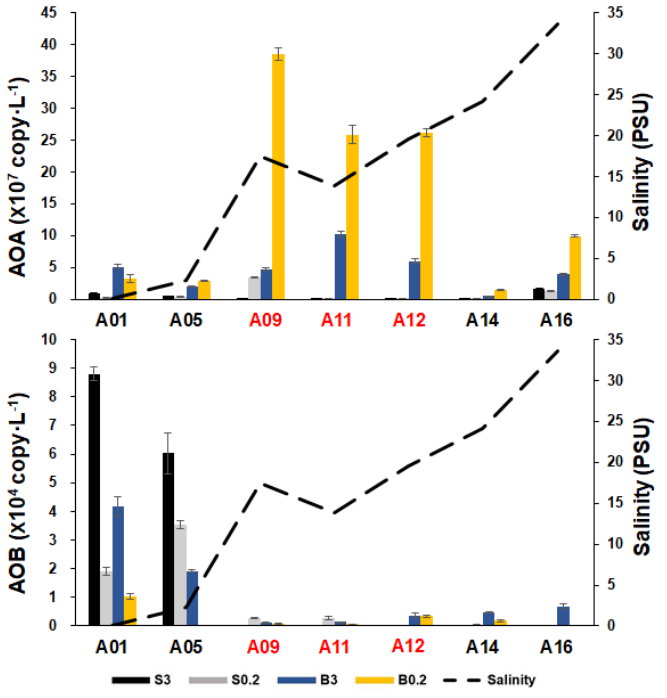

Figure 5. The abundance of AOA and β-AOB at DNA level estimated~~quantified~~ by qPCR of *amoA* gene along the salinity gradient of the A-transect in the Pearl River estuary. Size fractionation wais performed with 3 μm (particle-attached) and 0.2 μm (free-living), and the hypoxic stations (bottom DO < 2 mg·L^{-1}) are labelled in red color.

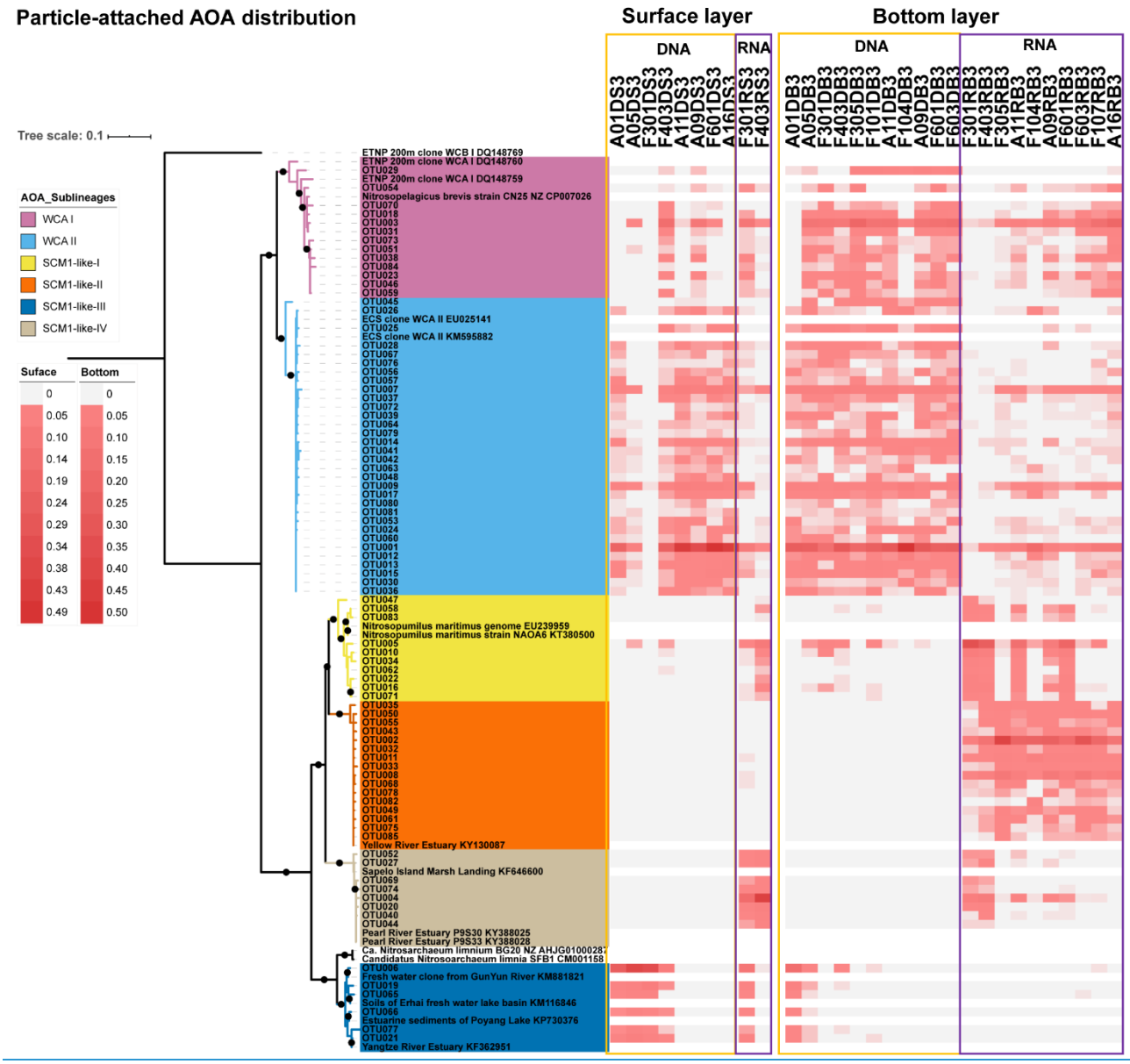

~~Figure 6. Maximum likelihood phylogenetic tree of top 85 OTUs based on *amoA* gene sequences using T92+G+I model with 1000 bootstrap. The associated heat map is generated based on the relative abundance of top OTUs. Samples are listed from left to right along the ascending salinity gradient.~~Figure 6. Maximum likelihood phylogenetic tree of top 85 OTUs based on amoA gene sequences using T92+G+I model with 1000 bootstrap. The associated heat map is generated based on the relative abundance of top OTUs in the particle-attached samples. Samples are listed from left to right along the ascending salinity gradient.

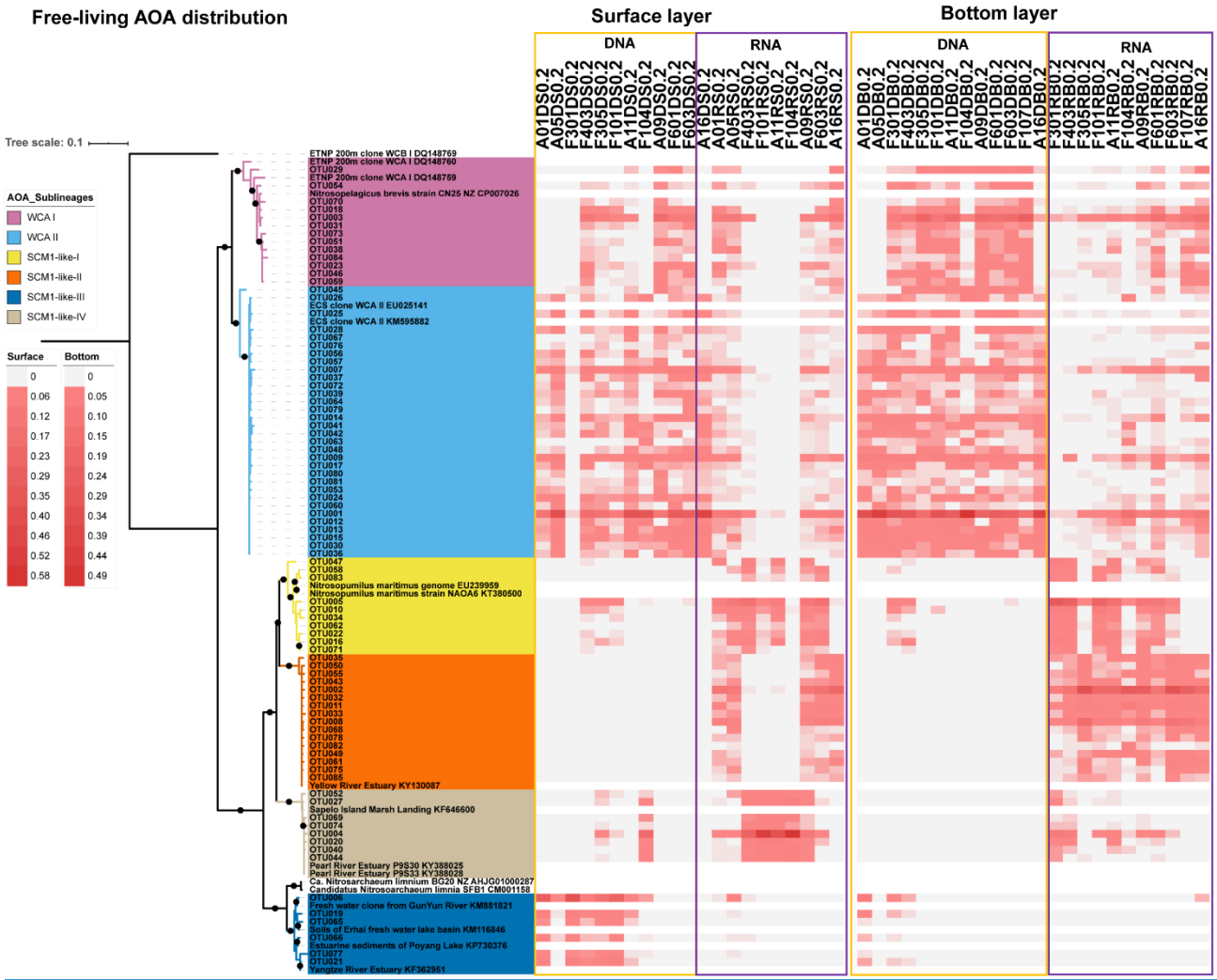

Figure 7. Maximum likelihood phylogenetic tree of top 85 OTUs based on amoA gene sequences using T92+G+I model with 1000 bootstrap. The associated heat map is generated based on the relative abundance of top OTUs in the free-living samples. Samples are listed from left to right along the ascending salinity gradient.

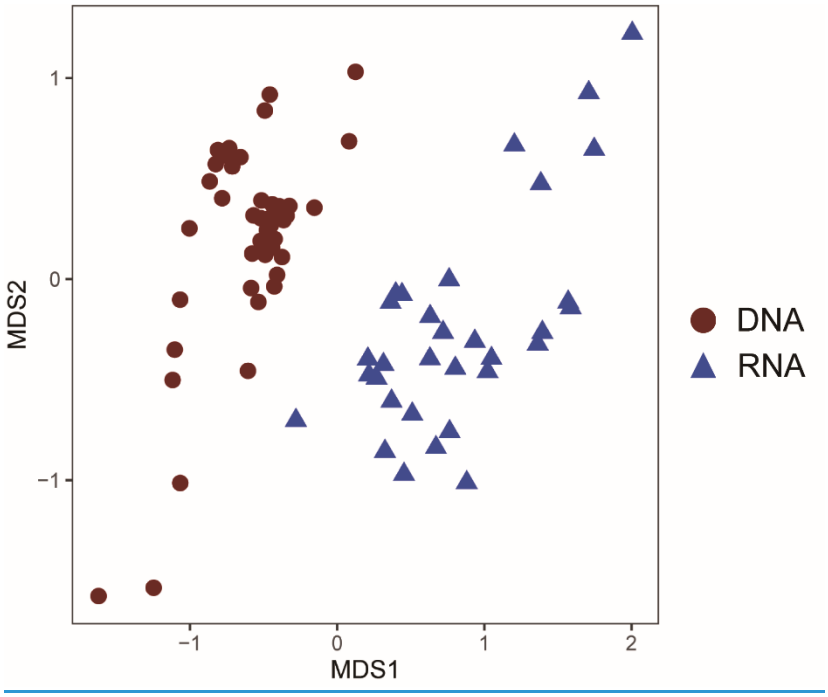

Figure 78. Nonmetric multidimensional scaling (NMDS) plot of AOA community similarity at DNA and RNA level.

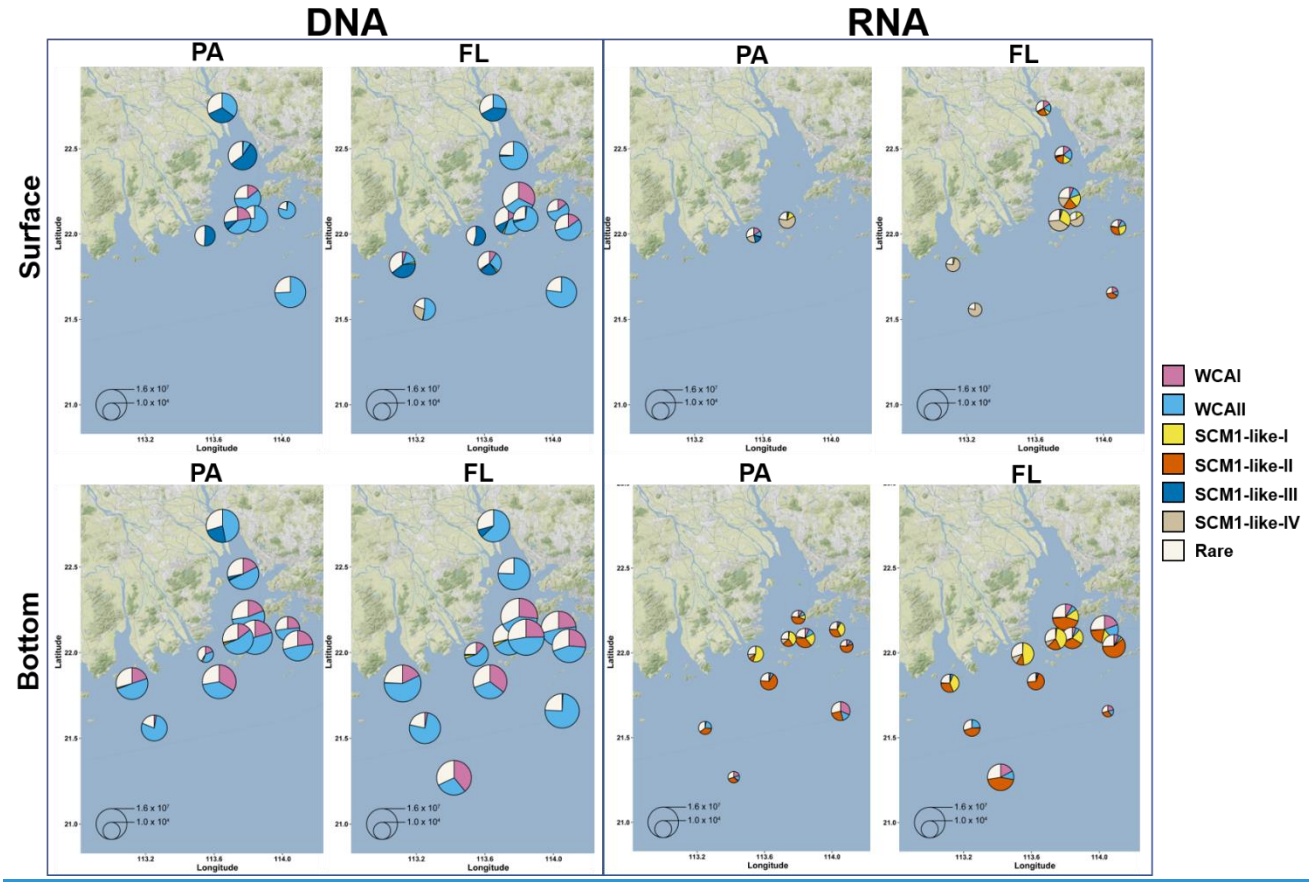

Figure ~~8~~9. Free-living (FL) and particle-attached (PA) AOA community composition and distribution in the Pearl River estuary. The size of the pie charts represents the archaeal *amoA* gene abundance quantified by qPCR. For a clear display of the AOA community composition, the minimum size of the pie charts is set as ~~100~~ 500 copies·L^{-1}. The charts were overlaid on Google Maps (© Google Maps) images using "ggmap" with "ggplot2" in R (D. Kahle and H. Wickham, 2013)

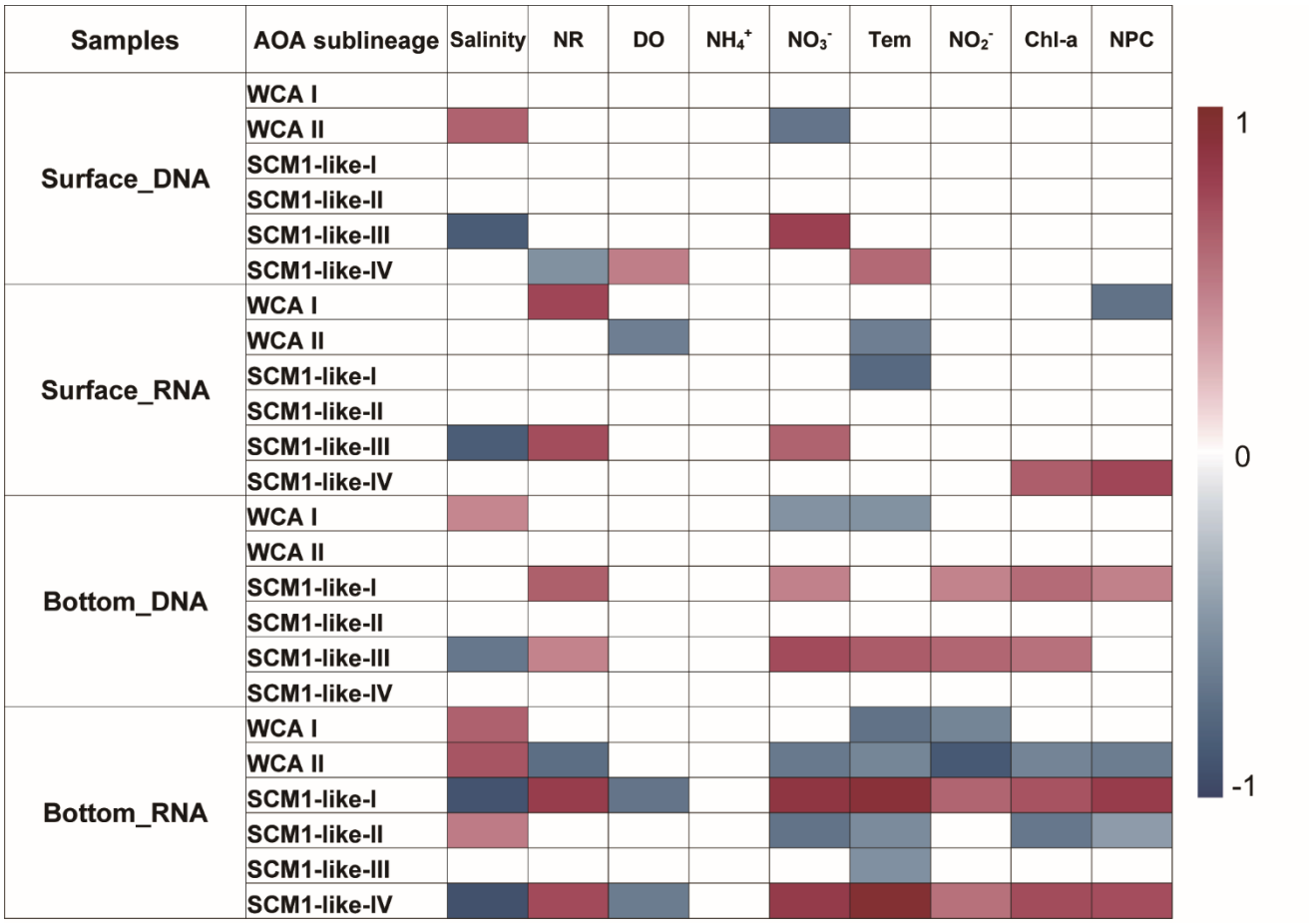

Figure ~~9~~10. Spearman correlation between AOA sublineages (relative abundance at DNA and RNA levels) and environmental factors in the surface and bottom layers of the water column~~s~~ in the Pearl River estuary during summer 2017. Only the significant correlations (P<0.05) are displayed (NR-nitrification rates; DO-dissolved oxygen; Tem-Temperature; ~~HB~~NPC-~~heterotrophic bacteria abundance~~non-phototrophic prokaryotic cells).